To the Graduate Council:

I am submitting herewith a thesis written by John W. Young entitled "Digital Windowing of Transient Signals for Fourier Spectrum Enhancement". I have examined the final copy of this thesis for form and content and recommend that it be accepted in partial fulfillment of the requirements for the degree of Master of Engineering, with a major in Electrical Engineering.

Robert E. Bodenheimer

R. E. Bodenheimer, Major Professor

We have read this thesis
and recommend its acceptance:

Donald W. Bouldin

James N. Rochelle

Accepted for the Council:

C W Minkel

Vice Provost
and Dean of The Graduate School

STATEMENT OF PERMISSION TO USE

In presenting this thesis in partial fulfillment of the requirements for a Master's degree at the University of Tennessee, Knoxville, I agree that the Library shall make it available to borrowers under rules of the Library. Brief quotations from this thesis are allowable without special permission, provided that accurate acknowledgment of the source is made.

Permission for extensive quotation from or reproduction of this thesis may be granted by my major professor, or in his absence, by the Head of Interlibrary Services when, in the opinion of either, the proposed use of the material is for scholarly purposes. Any copying or use of the material in this thesis for financial gain shall not be allowed without my written permission.

Signature John W. Young

Date Feb. 4, 1987

DIGITAL WINDOWING OF TRANSIENT SIGNALS FOR FOURIER SPECTRUM ENHANCEMENT

A Thesis

Presented for the

Master of Engineering

Degree

The University of Tennessee, Knoxville

John W. Young

March 1987

ACKNOWLEDGEMENTS

I am grateful for the help and support of the Electrical Engineering Department at the University of Tennessee and especially to Professor Robert Bodenheimer who is my major professor and who suggested the topic for the thesis as well as provided direction and encouragement for its completion. I also acknowledge that the information in Chapter V is a direct result of a suggestion by Professor Jim Rochelle and his help and encouragement are also deeply appreciated.

The research for the thesis was performed under a research contract for the National Institute of Justice. The equipment used, mainly a Texas Instruments Business-Pro computer and a HP3561A Dynamic Signal Analyzer, was purchased by the project and the use of the instruments made the investigation of the material contained in the thesis possible. Also, the Interactive Library Science software program aided in the investigation of signal processing and was invaluable in the generation of most of the figures contained in the thesis.

ABSTRACT

This thesis was written from the experience gained on digital processing. The purpose of the thesis is to investigate the effects of different windows on transient data. Several common windows are used to reduce the leakage effects in the Discrete Fourier Transform (DFT) of data acquisition. These windows have been investigated in detail and their effect on the Fourier spectrum of digital data is well known. However, these windows are not all the possible windows and may not be the most effective window for transient data. Several different exponential windows were analyzed to determine their effects on the DFT of transient data, especially in the presence of noise.

TABLE OF CONTENTS

LIST OF TABLES

LIST OF FIGURES

FIGURE		PAGE

FIGURES PAGE

FIGURE PAGE

CHAPTER I

INTRODUCTION

Advances in digital technology have influenced the increased use of digital signal processing. In recent years computation speeds of digital systems have increased by a factor of a thousand or more while the cost of digital systems continually decreases. With increased memory capacity of digital computers and advances in LSI and VLSI circuity, dedicated systems are being built to preform specialized data acquistion that offers several advanges over analog techniques. Digital signal processing offers stable preformance and greater flexibility over similiar analog systems. Small integrated circuit implementation and time sharing of major operations also reduces the cost and size of digital systems (Oppenheim, 1983).

Although digital data acquistion does have several advantages over analog systems, some limitations do exist in digital systems. One of the greatest limitations of digital signal processing is the limit on the complexity of an operation that a digital system can preform and still be able to run the system "real time". That is, being able to analyze the data as fast as the data is being received. If the process does not require on-line computations then the acquired data can be easily stored and analyzed at a later time. Another limitation of a digital system is due to the fact that numbers have a finite resolution when expressed as a finite length binary number. Therefore, even though a digital system is very stable, small errors are introduced in the system due to quantization of the input data and of the constants used in the computations. In addition, improper scaling and overflow oscillations must be avoided when using digital systems.

A digital system acquires data using an analog to digital converter and a sample and hold circuit to convert the analog input signal into a binary number. Operations are then performed on the data by a digital system and a result calculated. This result can then be used either in the digital form or in the analog form by reconverting the result into an analog signal using a digital to analog converter (Stearns, 1975). A block diagram of a digital signal acquisition system is shown in Figure I-1.

The sampling rate of the analog to digital converter is an important parameter in a digital acquisition system. According to the Nyquist criterian, the sampling rate must be at least twice the highest frequency of interest to avoid aliasing (Childers, 1975). However, as the sampling rate increases, the digital system has less time to preform operations on the input data before the next input data point is sampled. Therefore, in order to preform a

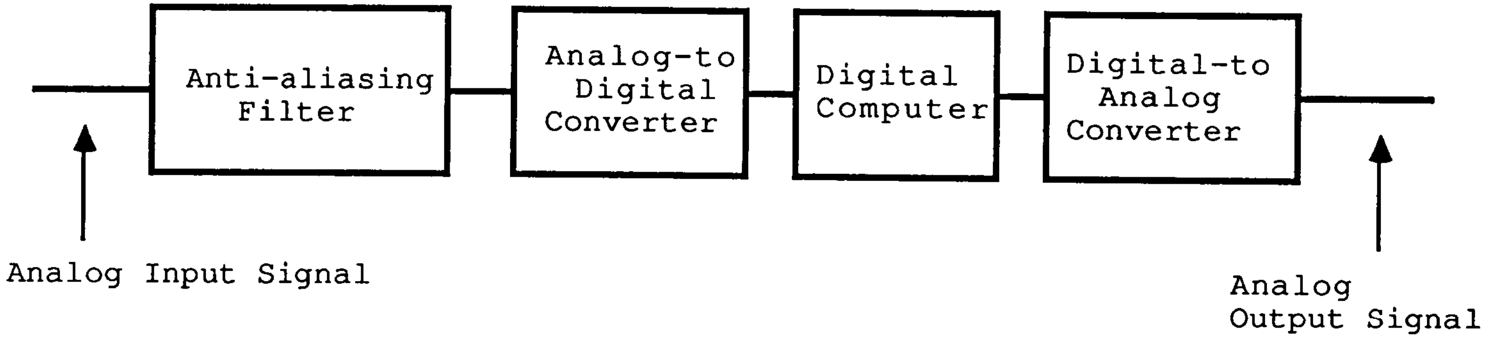

Figure I-1. Block diagram of a digital data acquisition system.

task in "real time", a lower sampling rate is desirable even though this sampling rate limits the highest frequency that is not aliased. To avoid aliasing of input data, a lowpass prefilter is needed to block-out frequencies above the Nyquist rate (Chen, 1979). As digital systems continue to increase in speed, the sampling rate in which digital systems will be able to operate in real time will continue to increase giving digital systems greater applications in signal processing.

CHAPTER II

THE DISCRETE FOURIER TRANSFORM

Any real signal may be expressed as a Fourier transform. Therefore, observing the frequency content of acquired data is equivalent to analyzing the time sequence of the data, but the frequency spectrum often presents the data in a more useful form. When acquiring data by digital means, the Discrete Fourier Transform (DFT) is used to determine the frequency spectrum of the data. The value obtained for each frequency component corresponds to the magnitude of the Fourier series coefficients. Therefore, one must have an understanding of the Fourier series in order to interpret the results of a discrete Fourier transform correctly.

In order for a signal to be represented by a Fourier series it must meet certain conditions. The Fourier series representation of a signal is applicable only to periodic signals. Therefore, to use the discrete Fourier transform the input data is assumed to be periodic. In addition, the input must satisify the Dirichlet conditions. That is, the data must have a finite number of discontinuities in any period, a finite number of maxima and minima in any period, and the input data must be absolutely integrable in any period (Ramirez, 1985). The Dirichlet conditions are met for any real signal.

A periodic signal with a period of 2Π that satisfies the Dirichlet conditions can be expressed as the Fourier series

$$f(x) = a_0 + \sum_{n=1}^{\infty} [a_n \cos(nx) + b_n \sin(nx)] \qquad (1)$$

where f(x) is the signal. By integrating both sides of equation (1) over the interval $-\Pi$ to Π, the coefficient a_0 can be determined as follows:

$$\int_{-\Pi}^{\Pi} f(x)\, dx = a_0 \int_{-\Pi}^{\Pi} dx + \sum_{n=1}^{\infty} [a_n \int_{-\Pi}^{\Pi} \cos(nx)\, dx + b_n \int_{-\Pi}^{\Pi} \sin(nx)\, dx)] \qquad (2)$$

which implies

$$a_0 = 1/2\Pi \int_{-\Pi}^{\Pi} f(x)\, dx \qquad (3)$$

since

$$\int_{-\Pi}^{\Pi} dx = 2\Pi \qquad (4)$$

and the other integrals on the right side of equation (2) equal zero.

The coefficients a_n can be determined by multiplying equation (1) by cos(mx) and again integrating from $-\Pi$ to Π resulting in

$$\int_{-\Pi}^{\Pi} f(x)\ \cos(mx)\ dx = \int_{-\Pi}^{\Pi} [a_0 + \sum_{n=1}^{\infty} (a_n \cos(nx) + b_n \sin(nx)]\ \cos(mx)\ dx \quad (5)$$

Now, integrating the right side of the equation results in

$$a_0 \int_{-\Pi}^{\Pi} \cos(nx)\ dx + \sum_{n=1}^{\infty} [a_n \int_{-\Pi}^{\Pi} \cos(nx)\ \cos(mx)\ dx + b_n \int_{-\Pi}^{\Pi} \sin(nx)\ \cos(mx)\ dx] \quad (6)$$

Since the sine and cosine functions are orthogonal over the interval of 2Π,

$$\int_{-\Pi}^{\Pi} \sin(nx)\ \cos(mx)\ dx = 0 \qquad \text{for all n and m} \quad (7)$$

Also, the following relations are true:

$$\int_{-\Pi}^{\Pi} \cos(nx)\ \cos(mx)\ dx = 0 \qquad \text{for all } n \text{ and } m \quad (n \neq m) \tag{8}$$

$$\int_{-\Pi}^{\Pi} \cos(nx)\ dx = 0 \tag{9}$$

and
$$\int_{-\Pi}^{\Pi} \cos\ (nx)dx = \Pi \tag{10}$$

Therefore, the coefficients a_n can be determined using

$$a_n = 1/\Pi \int_{-\Pi}^{\Pi} f(x)\ \cos(nx)\ dx \tag{11}$$

Similiarly, by multiplying equation (1) by sin(mx), the same procedure can be used to determine an equation for calculating the coefficients b_n. The result is

$$b_n = 1/\Pi \int_{-\Pi}^{\Pi} f(x)\ \sin(nx)\ dx \tag{12}$$

Equations (3), (11) and (12) are known as Euler's formulas (Kreyszig,1983).

The Fourier series formula may be extended to represent a function of an arbitrary period T, by setting

$$t = (T * x)/2 \tag{13}$$

so that

$$x = (2\Pi t)/T \tag{14}$$

Therefore, the Fourier series can now be expressed as

$$f(t)=f({}^{tT}/_{2\Pi})=a_0+\sum_{n=1}^{\infty} [a_n \cos({}^{tT}/_{2\Pi})+b_n \sin({}^{tT}/_{2\Pi})] \tag{15}$$

where Euler's equations become

$$a_0 = 1/T \int_{-T/2}^{T/2} f(t)\ dt \tag{16}$$

$$a_n = 2/T \int_{-T/2}^{T/2} f(t)\ \cos({}^{tT}/_{2\Pi})\ dt \tag{17}$$

and

$$b_n = 2/T \int_{-T/2}^{T/2} f(t)\ \sin({}^{tT}/_{2\Pi})\ dt \tag{18}$$

By using Euler's identies

$$\sin(x) = 1/2j\ (e^{jx} - e^{-jx}) \tag{19}$$

and

$$\cos(x) = 1/2\ (e^{jx} + e^{-jx}) \tag{20}$$

the Fourier series can be expressed in exponential form as

$$f(t) = \sum_{n=-\infty}^{\infty} c_n\ e^{jn\omega t} \tag{21}$$

where c_n is determined by

$$c_n = 1/T \int_{-T/2}^{T/2} f(t)\ e^{-jn\omega t}\ dt \tag{22}$$

The Fourier series can now be extended once again for signals which are not periodic by letting the period of the signal go to infinity. As the period approaches infinity, the summation in the Fourier series becomes an integral and equation (21) and (22) become

$$f(t) = 1/2\Pi \int_{-\infty}^{\infty} F(\omega)\ e^{j\omega t}\ d\omega \tag{23}$$

and $$F(\omega) = \int_{-\infty}^{\infty} f(t)\ e^{-j\omega t}\ dt \tag{24}$$

respectively. These two equations are known as the Fourier transform pair (Cheng, 1959). When using a digital system, the discrete Fourier transform is a discrete approximation to the Fourier integral (Ramirez, 1985).

As an example of the Fourier transform, consider a sine wave that is assumed to have started at minus infinity and continues to plus infinity. The Fourier transform of the sine wave is determined by substituting $f(t)=A\ \sin(\omega_c t)$ into equation (24) as follows:

$$F(\omega) = \int_{-\infty}^{\infty} A\ \sin(\omega_c t)\ e^{-j\omega t}\ dt \tag{25}$$

Using Euler's idenity

$$\sin(\omega_c t) = A/2j\ (e^{j\omega_c t} - e^{-j\omega_c t}) \tag{26}$$

equation (25) becomes

$$F(\omega) = \int_{-\infty}^{\infty} A/2j\ (e^{j\omega_c t} - e^{-j\omega_c t})\ e^{-j\omega t}\ dt$$

$$= A/2j \left(\int_{-\infty}^{\infty} e^{jt(\omega_c-\omega)}\, dt - \int_{-\infty}^{\infty} e^{-jt(\omega_c-\omega)}\, dt \right.$$

$$= A/2j\ [\delta(-\omega_c) - \delta(\omega_c)] \tag{27}$$

Therefore, the Fourier transform of an infinite sine wave consists of two impulses, one of one-half the amplitude of the sine wave at $\omega=(-\omega_c)$ and the other with negative the same weight at $\omega=\omega_c$, as shown in Figure II-1. (The frequency of the sine wave is ω_c=15.625 hertz).

For real-valued signals the negative frequency components of the Fourier transform are exact duplicates of the positive frequency components. That is, the magnitude frequency plot of the Fourier transform for real-valued signals is symmetric about the zero frequency or dc point. Therefore, since only the real-valued signals are considered in this thesis, only the positive frequencies will be shown when the Fourier transform is taken of an input signal or window function.

Now consider the transform of a rectangular pulse as shown in Figure II-2. The Fourier transform of this signal can be determined by again appling equation (24)

(a)

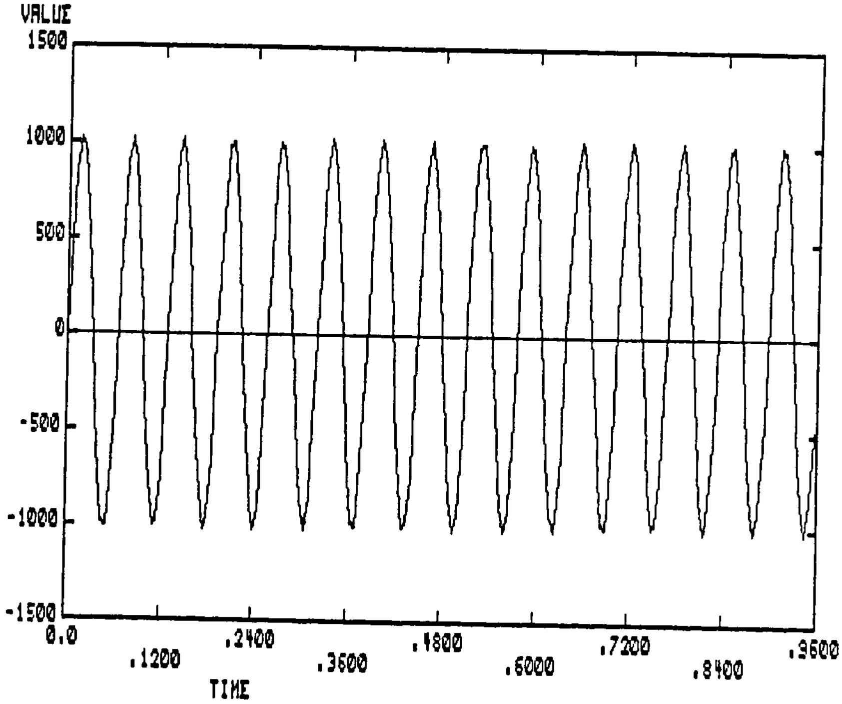

(b)

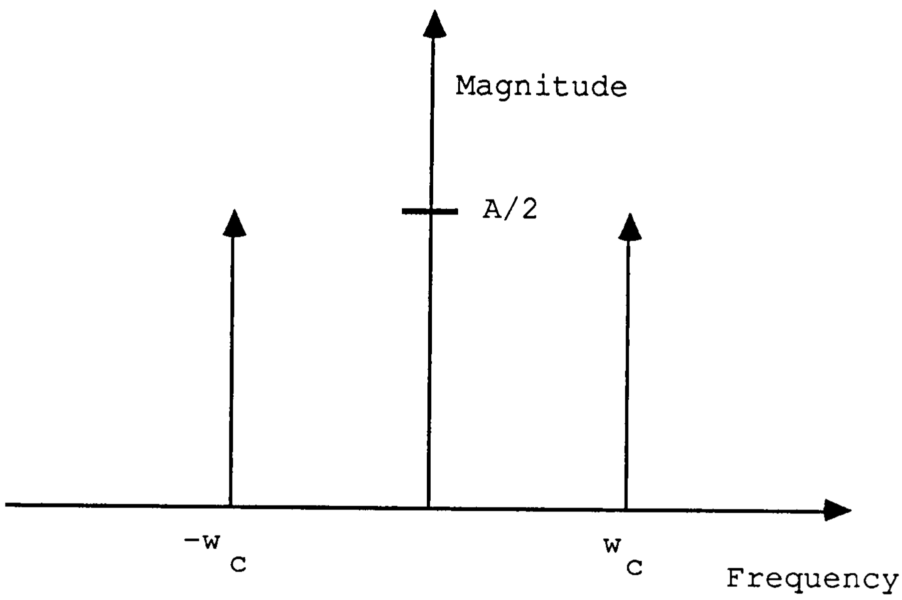

Figure II-1. Infinite duration sine wave with frequency w_c (a) and the Fourier transform of the sine wave (b).

(a)

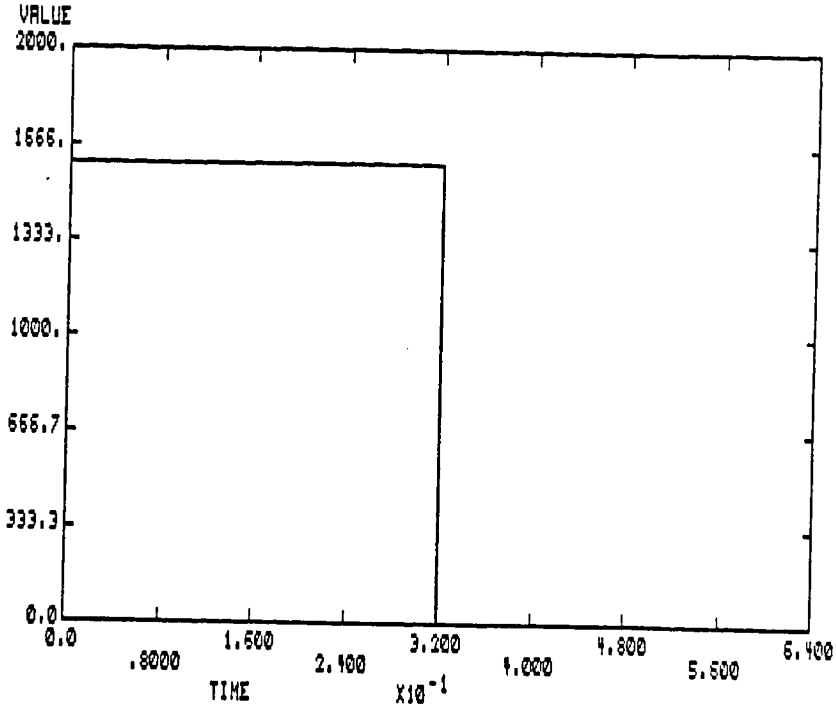

(b)

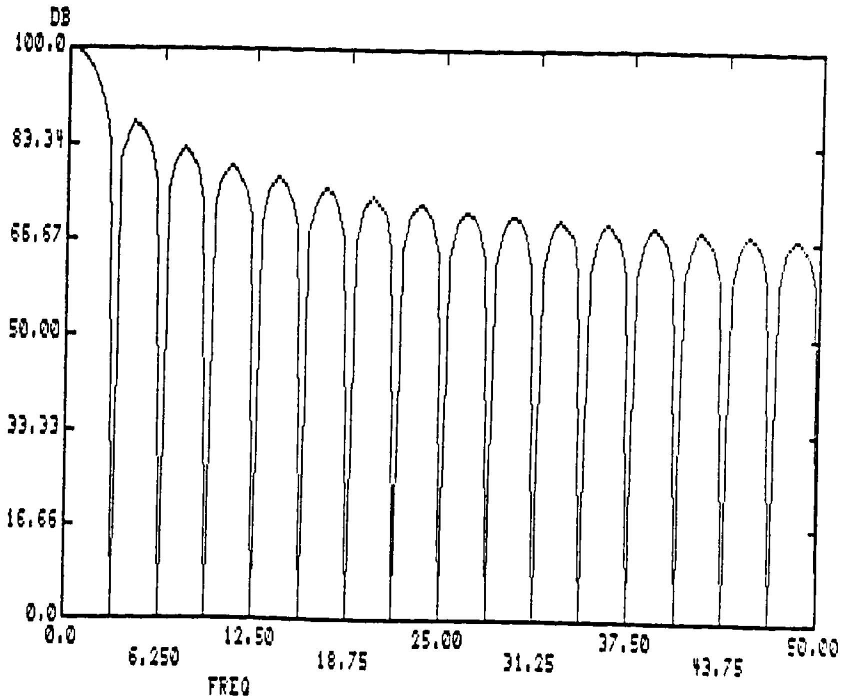

Figure II-2. Rectangular pulse of duration T=0.32 seconds (a) and the Fourier transform of the pulse (b).

with f(t)=u(t+T)-u(t-T) as follows:

$$F(\omega) = \int_{-\infty}^{\infty} f(t)\ e^{-j\omega t}\ dt = \int_{-T}^{T} e^{-j\omega t}\ dt \qquad (28)$$

Using Euler's idenity

$$F(\omega) = \int_{-\infty}^{\infty} [1/2\ (\cos(\omega t) - j \sin(\omega t)]\ dt$$

$$= 1/2 \int_{-T}^{T} \cos(\omega t)\ dt - j/2 \int_{-T}^{T} \sin(\omega t)\ dt$$

$$= 1/2\omega\ \sin(\omega t)\Big|_{-T}^{T} + j/2\omega\ \cos(\omega t)\Big|_{-T}^{T}$$

$$= 1/2\omega\ \{[\sin(\omega T) - \sin(-\omega T)]$$

$$+ j[\cos(\omega T) - \cos(-\omega T)]\}$$

$$= \sin(\omega T)/\omega \qquad (29)$$

The Fourier transform of the rectangular pulse is also shown in Figure II-2.

One of the important properties of the Fourier transform is multiplication in the time domain results in convolution in the frequency domain. Therefore, if the sine wave in Figure II-1 and the rectangular pulse in

Figure II-2 are multiplied together, the resultant time and frequency functions as shown in Figure II-3 results.

The side lobes of the Fourier transform shown in Figure II-3 are not of equal magnitude on each side of the main lobe as might be expected from the convolution. The side lobes are greater at lower frequencies due to the addition of the side lobes of the negative frequency components (not shown). Or, in terms of the convolution, both the impulses of Figure II-1 contribute to the magnitude of the Fourier transform. If the impulses in Figure II-1 were seperated by a greater distance (i.e. greater frequency spread), the side lobes shown in Figure II-3 would be of equal magnitude.

If the sine wave in Figure II-1 is sampled using a discrete system starting at t=0 and ending at t=0.32 seconds and the spectrum obtained using a DFT, the frequency spectrum consist of a single impulse at the proper frequency as would be expected for an infinite duration sine wave. This transform is due to the fact that the DFT approximated the Fourier transform by sampling the transform at the points indicated on Figure II-4. (The heavy dots represent the discrete Fourier transform frequencies and the continuous line represents the continuous Fourier transform of the wave form). This spectrum is obtained due to the fact that the DFT assumes that the input data is periodic. Therefore, the input

(a)

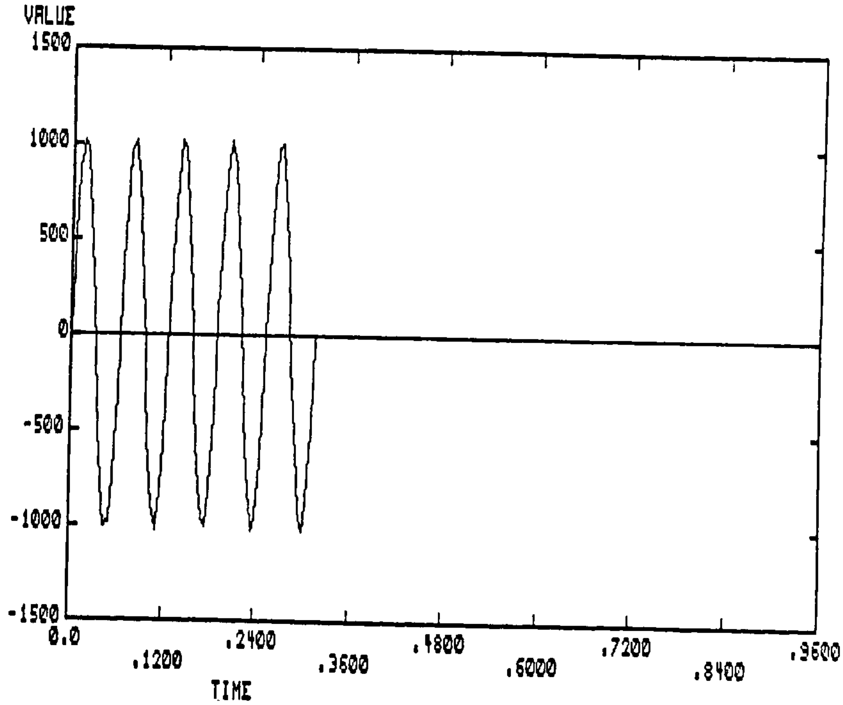

(b)

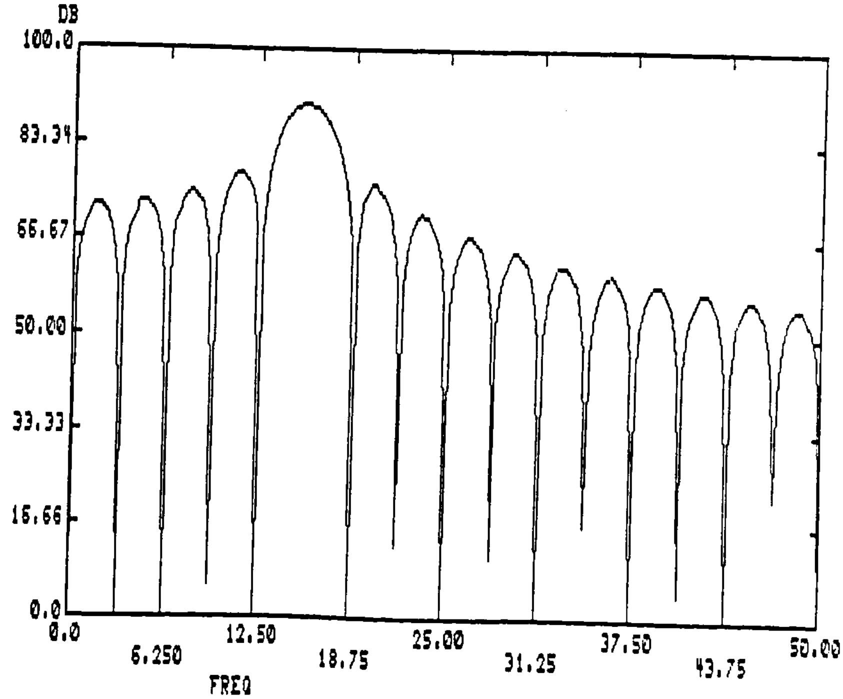

Figure II-3. Time wave form (a) and Fourier transform (b) of an infinite duration sine wave multiplied by a rectangular pulse (Same as the convolution of the Fourier transforms of the two signals).

(a)

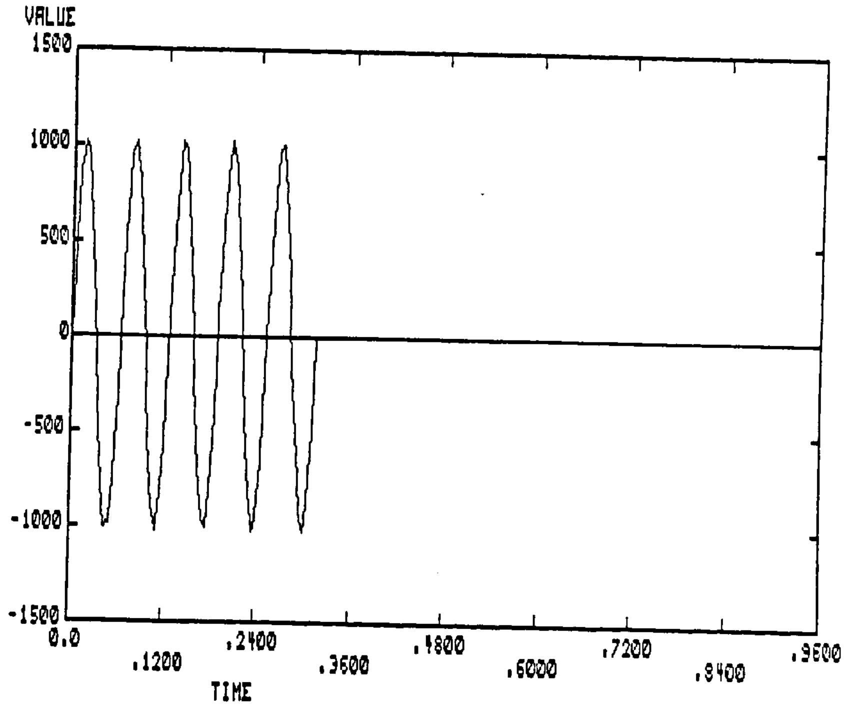

(b)

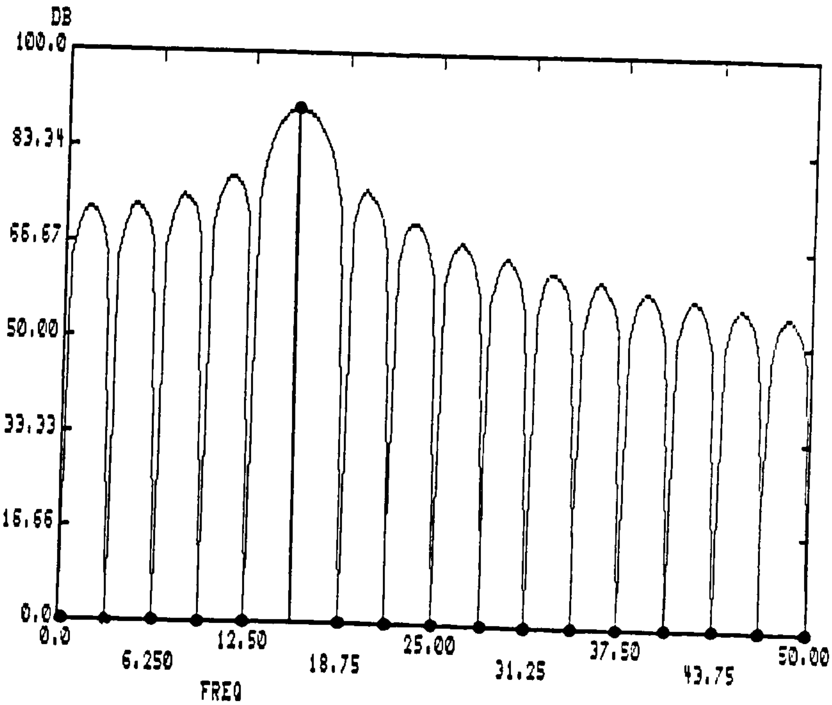

Figure II-4. Time wave form (a) and the discrete Fourier transform (b) of the sine wave of Figure II-1 with the period from t=0 to t=0.32 seconds. (i.e. Even number of cycles in the time window).

data would result in an infinite duration sine wave. In general, using a rectangular window, the discrete Fourier transform of a sine or cosine wave form that has an even number of cycles in the time window is an impulse. The transform is independent of the phase shift since the phase shift does not create a discontinuity when the input of the Fourier transform is assumed to be periodic. An even number of cycles in the sine wave corresponds to a spectral line in the discrete Fourier transform. The amplitude of the impulse is equal to the amplitude of the sine wave times one half the number of points in the time record. If a sine wave does not contain an even number of cycles, then the frequency of the input data does not correspond to one of the spectral lines in the DFT, and the transform is spread out over a range of frequencies. This spreading is due to taking the transform of a finite duration signal and is known as leakage. The amount of leakage that results in the Fourier transform is influenced by the length of the time window, but is not a result of sampling the input signal (Harris, 1978). For example, if the sine wave in Figure II-1 (p.13.) is the input data to a system and is observed from time t=0 to t=0.352 seconds, the frequency spectrum has a transform as shown in Figure II-5. As can be seen in Figure II-5, this spreading is due to the Fourier transform of a rectangular windowed sine wave being approximated by

(a)

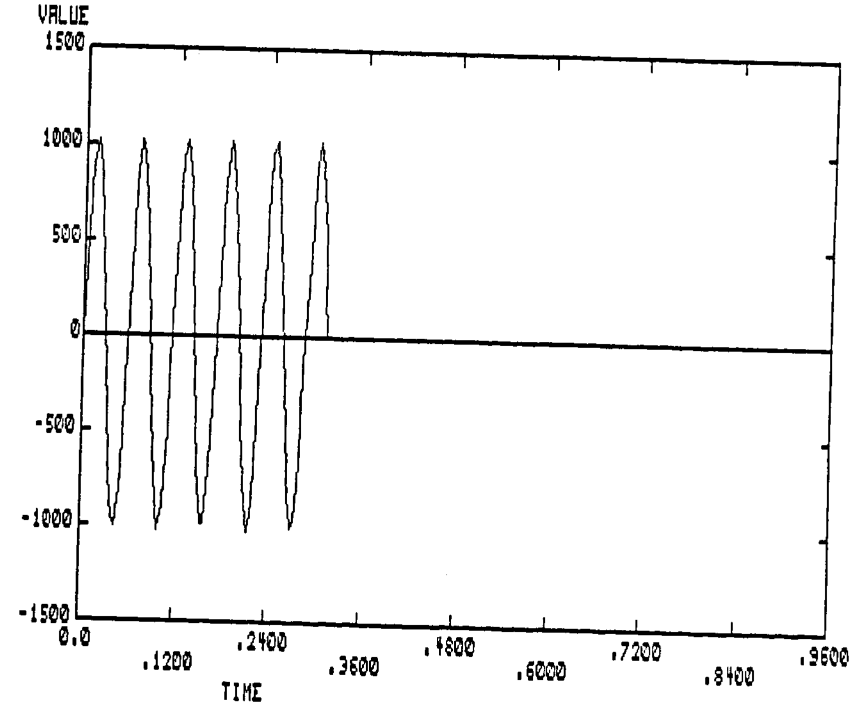

(b)

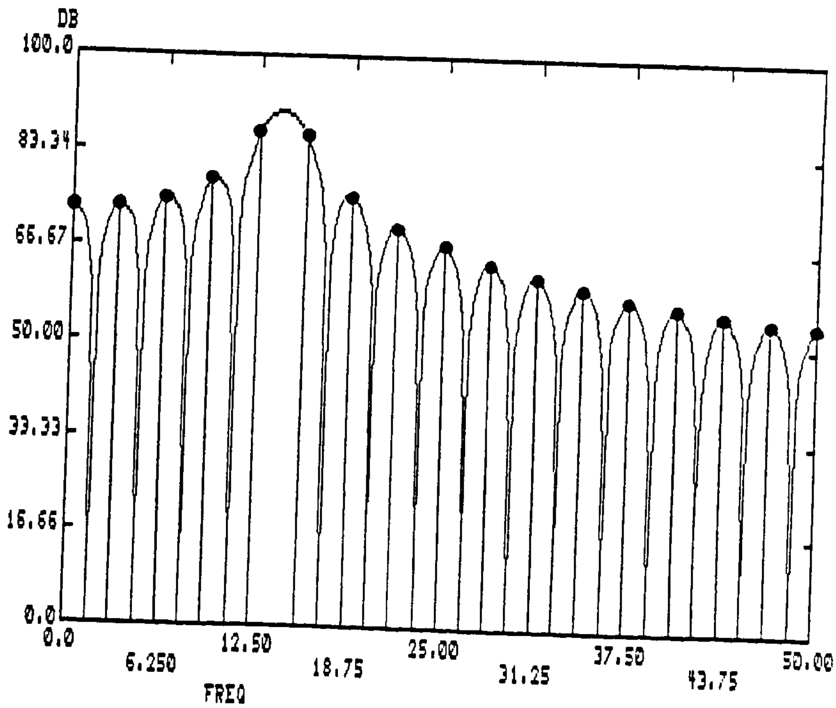

Figure II-5. Time wave form (a) and the discrete Fourier transform (b) of the sine wave of Figure II-1 with the period from t=0 to t=0.352 seconds. (i.e. Uneven number of cycles in the time window).

sampling the continuous Fourier transform at points of some finite amplitude besides at the null points in the sidebands as in Figure II-4. If discontinunities exist between the first data point and the last data point, then the Fourier spectrum shows distortion from the desired spectrum.

A damped sine wave (independent of phase shift) cannot be represented by a single impulse (i.e. a single spectral line) in the Fourier transform. This can be shown by once again appling equation (24) with

$$f(t) = e^{-at} \sin(bt)\, e^{-j\omega t} \tag{30}$$

Therefore,

$$F(\omega) = \int_0^\infty e^{-at} \sin(bt)\, e^{-j\omega t}\, dt$$

$$= \int_0^\infty e^{-t(a+j\omega)}\, 1/2j\, [e^{jbt} - e^{-jbt}]\, dt$$

$$= 1/2j \int_0^\infty e^{-t[a+j(\omega-b)]}\, dt$$

$$- 1/2j \int_0^\infty e^{-t[a+j(\omega+b)]}\, dt$$

$$= 1/2j\ [{}^{1}/_{(a+j(\omega-b)} - {}^{1}/_{(a+j(\omega+b)}]$$

$$= 1/2j\ \{{}^{[a-j(\omega-b)]}/_{[a2+(\omega-b)2]}$$

$$- {}^{[a-j(\omega+b)]}/_{[a2+(\omega+b)2]}\} \qquad (31)$$

The Fourier transform of the damped sine wave is shown in Figure II-6.

As the damping constant is increased the transform of the data spreads out over a larger range of spectral lines. Changing the phase shift of the damped data does not cause a significant increase in spectral leakage even though the phase shift now causes a discontinuity in the input data. The effects of the damping of the data are greater than the effects of the discontinuity in the Fourier Transform. Changing the input frequency to a frequency that is not one of the discrete spectral lines in the Fourier spectrum causes slightly more leakage, but not a significant amount for moderately damped data.

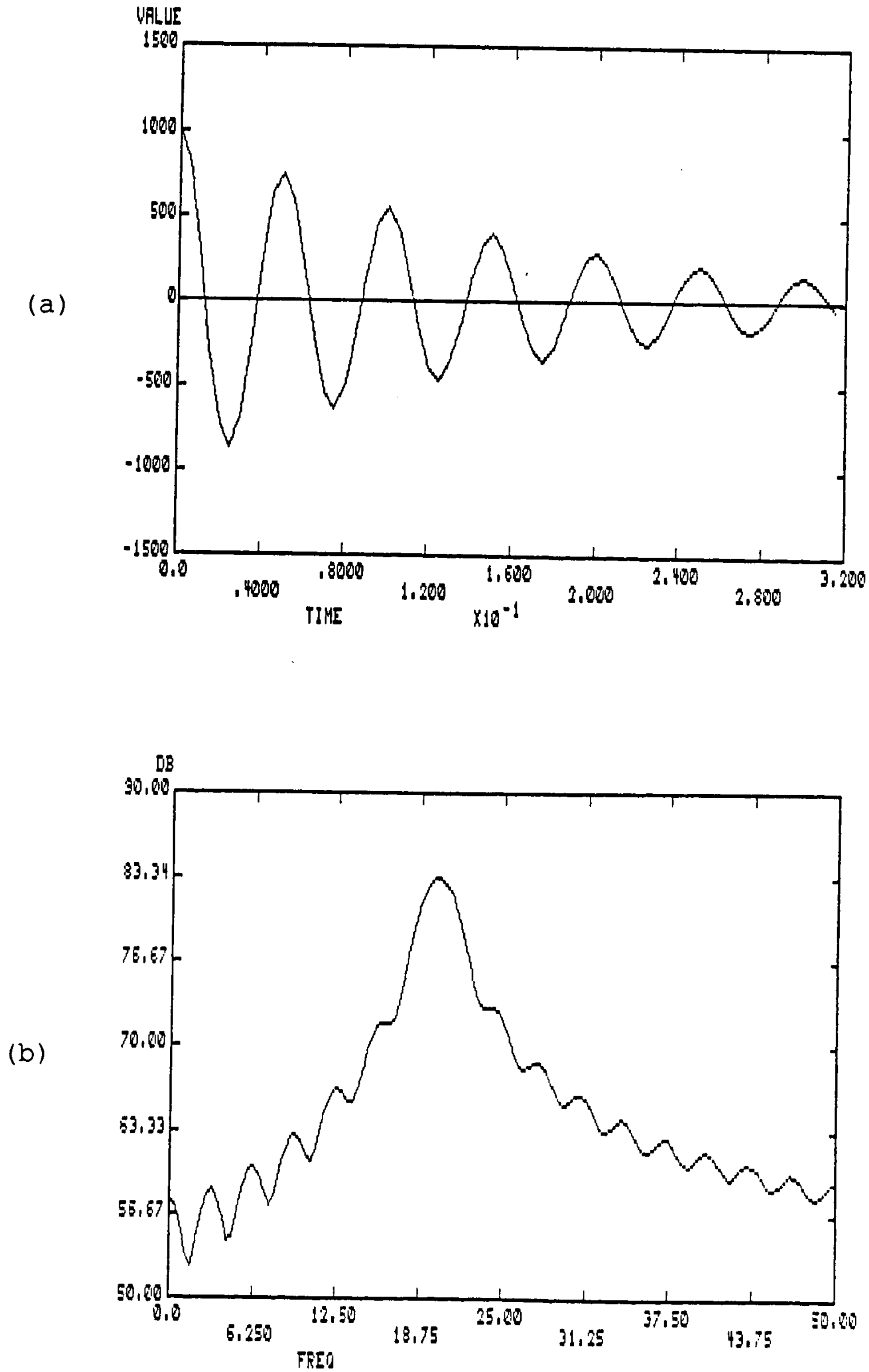

Figure II-6. Time wave form of an exponentially damped sine wave (a) along with its Fourier transform (b) [$f(t)=1000 \sin(20t)\ e^{-2t}$].

CHAPTER III

WINDOWING

Any realizable system that acquires data uses a window function. The most common window is the rectangular window which corresponds to the time period that the data is taken. The rectangular window simply truncates an infinite wave form to a wave form of finite length. Truncation of the wave form, however, causes a spreading of each frequency in the Fourier transform to adjacent frequencies (Childers, 1975).

Leakage is noticable in the discrete Fourier transform for any signal with frequency components that do not correspond to one of the frequency bins in the DFT. Each frequency spectra of the DFT is actually a measure of the correlation of the input signal with a cosine wave for the real part and with a sine wave for the imaginary part. The first spectral line corresponds to a sine (or cosine) wave of exactly one period with the same sampling frequency and time window as the input data. Likewise, the second spectral line corresponds to a sine wave with exactly two periods, the third to a sine wave of three periods, and so on (see Figure III-1 a, b and c). The last spectral line corresponds to a sine wave that has an even number of cycles in the time window and has a frequency just below the Nyquist frequency. The sine wave

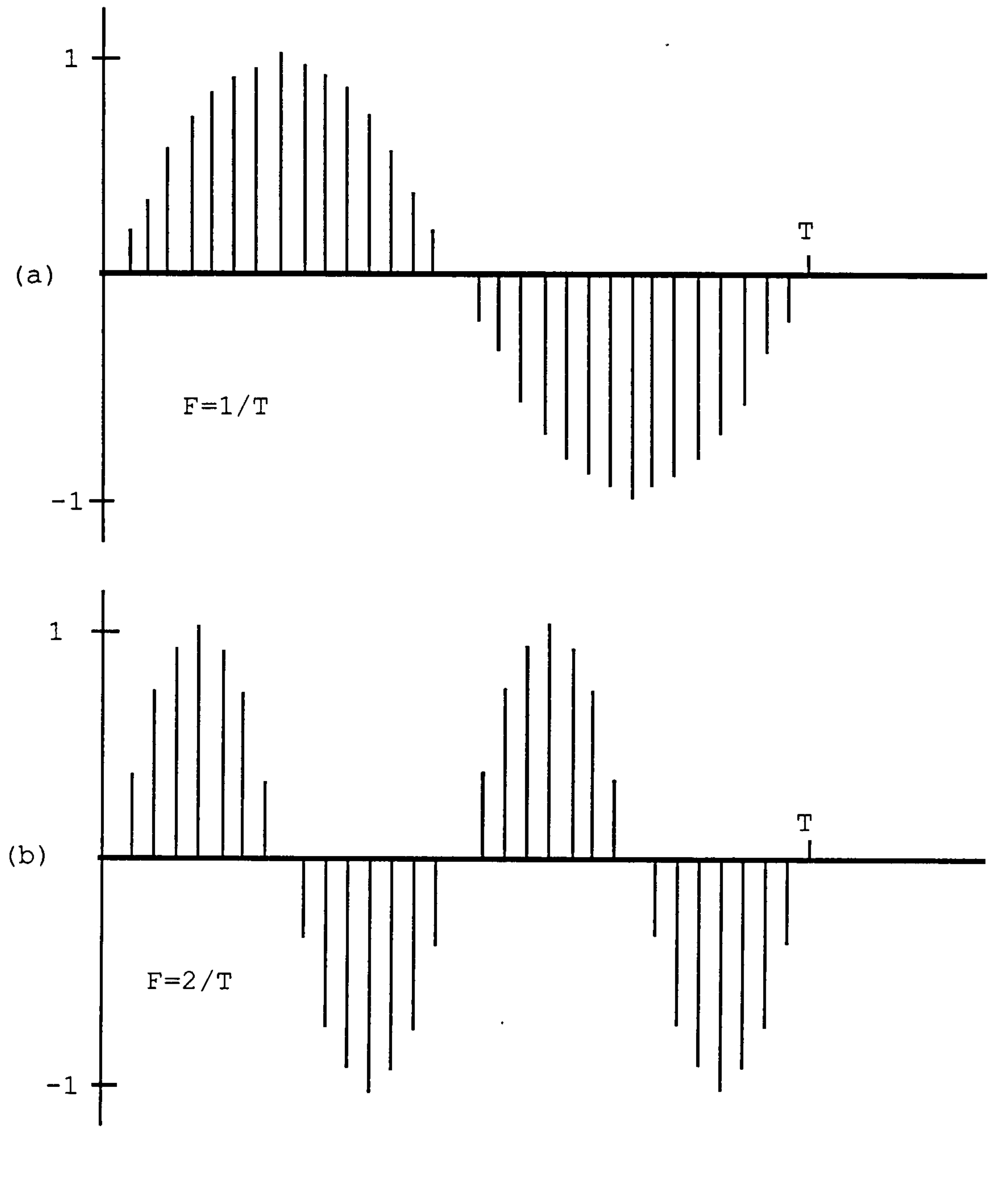

Figure III-1. Correlation sine waves of the DFT.

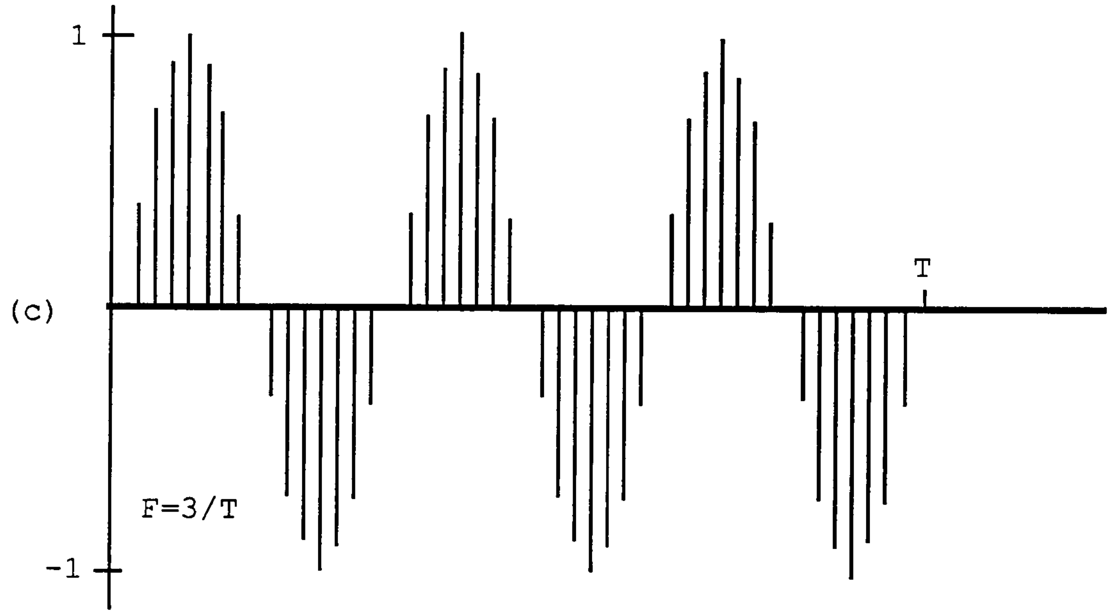

Figure III-1. (Continued).

at the Nyquist frequency produces the same result as the first spectral line. The magnitude of the transform is then obtained by taking the square root of the sum of the squares of the real and imaginary parts.

The DFT merely determines how correlated the input signal is to a set of sine and cosine functions of given discrete frequencies. The sine and cosine functions form the othorgonal basis of the Fourier transform. If the input signal consist of a sine wave of a frequency that corresponds to one of the frequency bins of the DFT, then its correlation is maximum at that frequency. In addition, its correlation is zero at all the other frequencies of the DFT. However, if the input signal contains a sine wave of a frequency which does not correspond to any frequency of the DFT, then the correlations of the transform never produce a maximum value which corresponds to a correlation of a sine wave of the same frequency. However, all the frequencies of the DFT have some correlation with the input data so the frequency spectrum appears to spread out. This spreading of the transform is known as leakage.

By viewing the DFT as a set of correlation functions, the amount of a certain frequency component in a wave form is easily determined by preforming the correlation. For example, to determine the frequency component of a certain frequency w1, the input wave form is correlated with a sine wave and a cosine wave each with a frequency of w1. The results of each of these correlations are then squared and summed. The square root of this summation is refered to the spectral line of the DFT at the frequency w1. However, the frequency w1 must result in sine and cosine functions with an even number of cycles in the time window in which the data was taken. If the desired frequency spectra does not correspond to a sine wave with an even number of cycles, the time record must be shortened or extended to an integer multiple of 2Π times that frequency. Since the first frequency spectra corresponds to a sine wave of a single cycle, the length of the time window along with the sampling frequency determines the lowest frequency component as well as the frequency resolution of the DFT.

As stated previously, the highest frequency component that can be analyzed is determined by the sampling rate. Trying to calculate the frequency component of a wave form above the Nyquist frequency produces the same result as one of the frequency spectra below the Nyquist frequency. To see this, consider the sine wave in Figure III-2 with a frequency w1. If w1 is greater than the Nyquist frequency, then the DFT not only produces an impulse at w1, but also at w2 which is the aliased wave form of the sine wave. Because of the aliasing effects of sampling, a DFT only contains information for frequencies

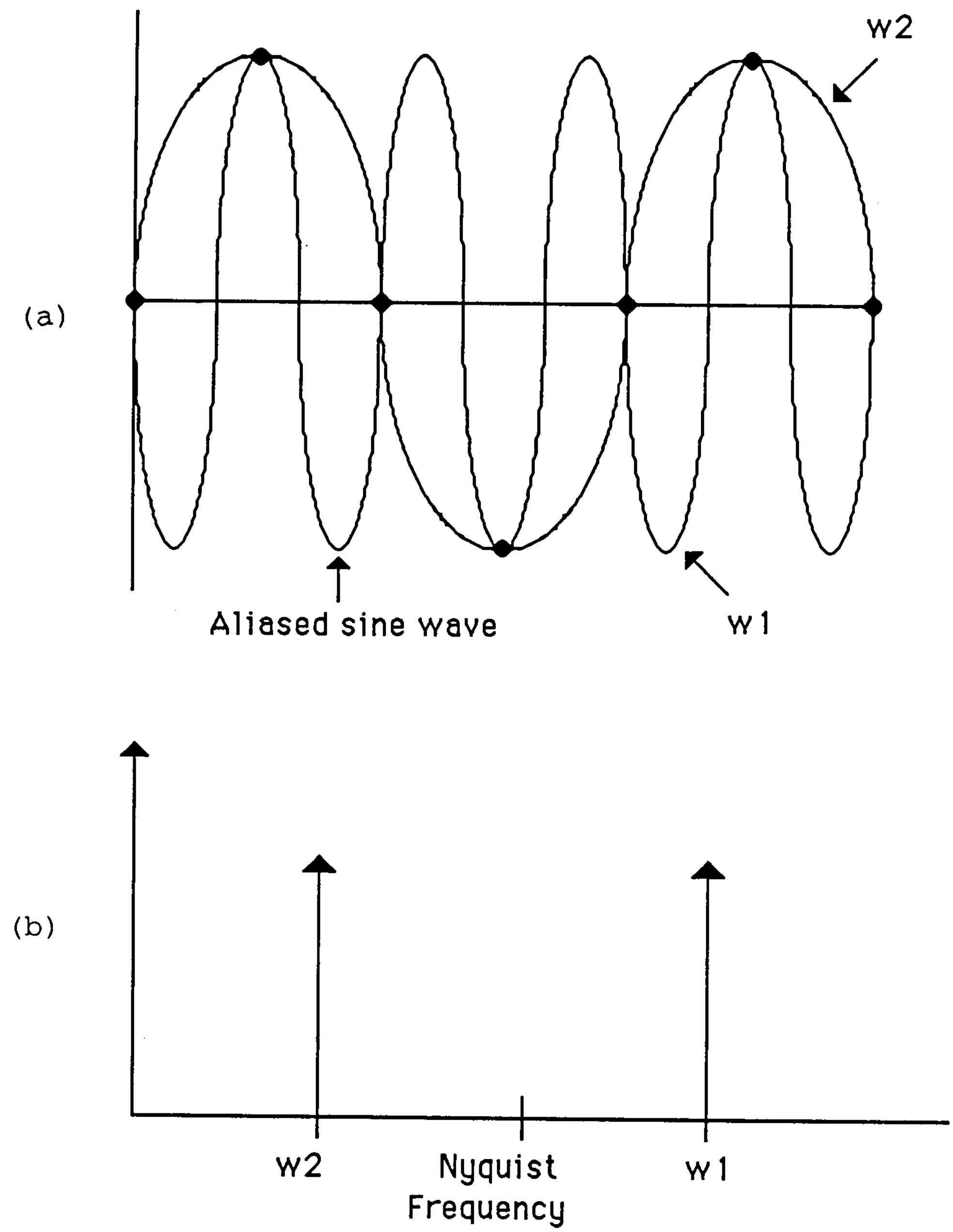

Figure III-2. Time trace of a sine wave with frequency w1 with w1 greater than the Nyquist frequency and the wave form with frequency w2 assumed by the DFT (a) and the Fourier spectrum of the sine wave (b).

below the Nyquist frequency. In addition, any frequencies that are greater than the Nyquist frequency are aliased and give a false representation of the Fourier transform of the signal. Therefore, all frequencies above the Nyquist frequency must be filtered out of the input signal before the DFT may be used.

Given the length of the time window and the sampling rate, the frequency resolution of the DFT may be determined as follows. Let

f_s = the sampling rate

L = the length of the time window

N = the number of points sampled.

These three variables are related by the equation given below. That is, the number of points sampled is determined by the length of the time window multiplied by the sampling rate

$$N = L * fs \quad \text{or} \quad L = N / f_s \tag{1}$$

The lowest frequency sine wave that can complete one period in time L determines the frequency resolution. Therefore, the frequency spacings between the DFT spectra lines can be determined by equating the argument of a sine wave to 2Π where Δf is the frequency resolution. The following equation must be satisified.

$$\sin(2\Pi \, \Delta f \, t) = 0 \qquad \text{(end of one period)} \qquad (2)$$

Since t must equal L -- the length of the time window -- equating the argument of the sine wave to 2Π gives

$$2\Pi \, \Delta f \, L = 2\Pi$$

$$\text{or} \qquad \Delta f \;\; L = 1 \qquad \text{which implies} \qquad \Delta f = 1 \,/\, L \qquad (3)$$

Substituting equation (1) into equation (3) yeilds

$$\Delta f = 1 \,/\, (N \,/\, f_s) \qquad \text{or} \qquad \Delta f = f_s \,/\, N \qquad (4)$$

Therefore, given the sampling rate and the time window, the frequency resolution of the DFT can be determined from equation (4).

The input of an arbitrary signal can be modified by multipling it by a window function to reduce the leakage in the frequency spectrum. Since the DFT assumes that the input data is periodic, an input sine wave that does not have the same frequency as one of the DFT frequencies contains a discontinuity between the first and last data point and/or a phase shift which cause the leakage in the input signal's frequency spectrum. For example, consider the sine wave in Figure III-3. Since the DFT assumes the input signal to be periodic, the assumed input by the DFT is shown in Figure III-4 along with its frequency spectrum. To reduce the leakage effects in Figure III-4, the input data can be multiplied by a window function. The triangular window along with its Fourier transform as shown in Figure III-5 reduces the leakage in the transform by forcing the beginning and end of the time window to zero in a smooth manner.

The windowed sine wave, the periodic extension of the windowed sine wave and the Fourier transform of the data are shown in Figure III-6. The effects of the discontinuities and the phase shift are reduced and as can be seen in Figure III-6 the Fourier transform has been altered. The leakage in the Fourier transform has been reduced by decreasing the magnitude of the side lobes with respect to the main lobe. The first side lobes of the unwindowed sine wave of Figure III-4 are only 13 dB down from the main lobe while the first side lobes of the windowed sine wave of Figure III-6 are 26 dB down from the main lobe. However, even though the leakage due to the side lobes is reduced by using the triangular window, the main lobe of Figure III-6 is approximately 50 percent wider than the main lobe of Figure III-4. Window

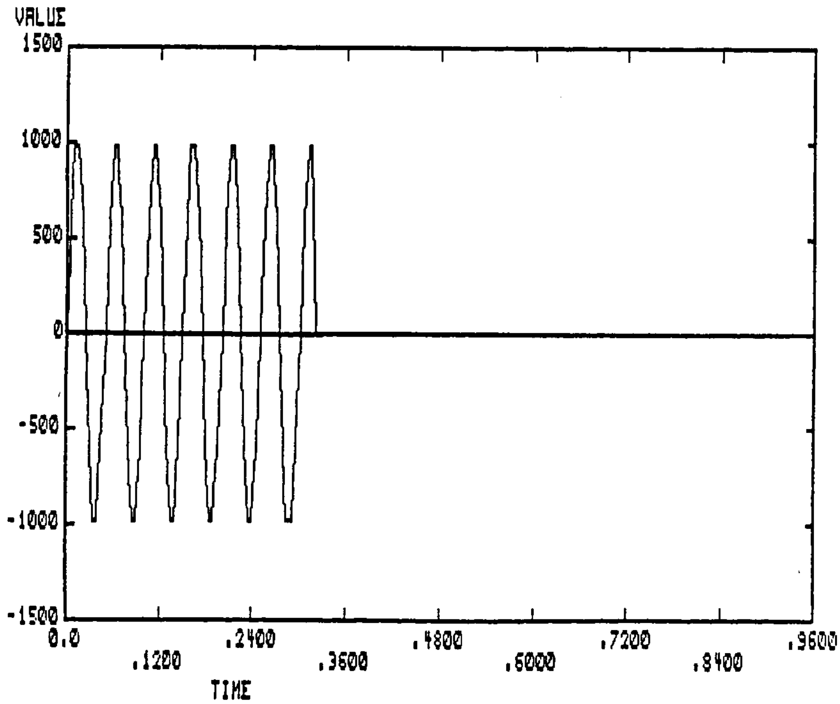

Figure III-3. Sine wave of an uneven period in the time window. [Frequency=20 KHz, length of time window=0.325 seconds].

(a)

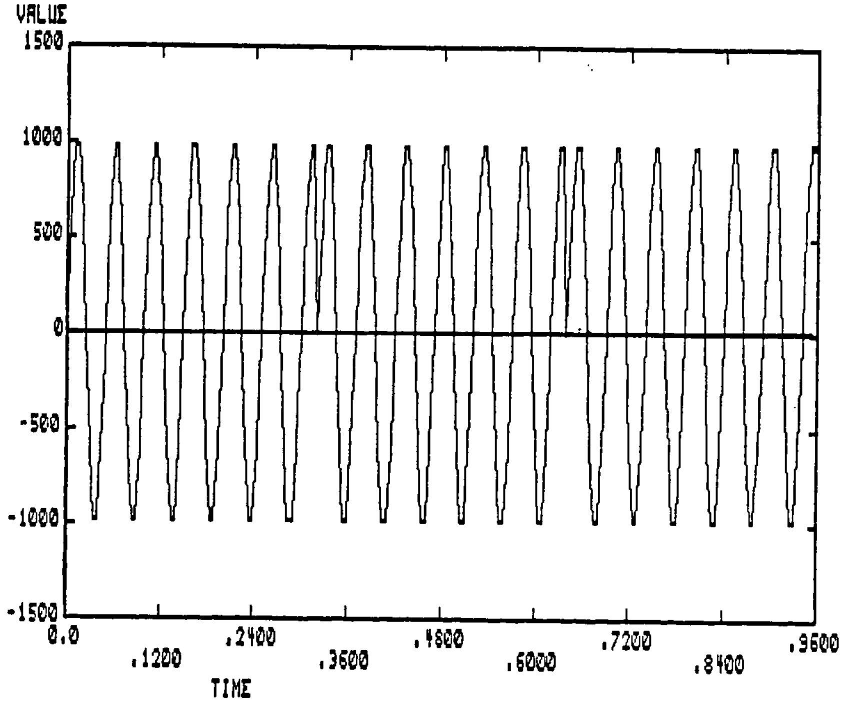

(b)

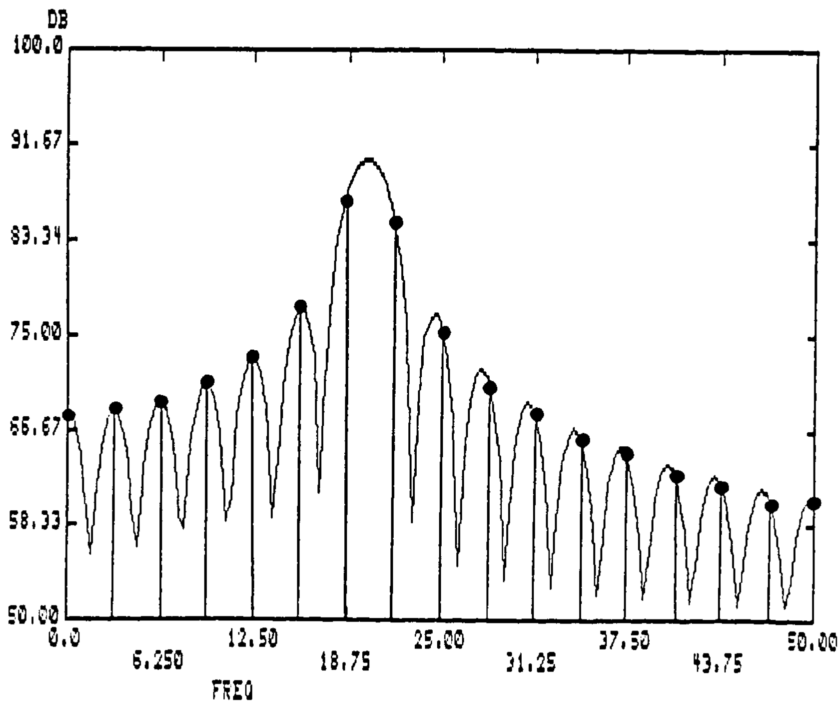

Figure III-4. Periodic extension of Figure III-3 (a) along with its discrete Fourier transform (b).

(a)

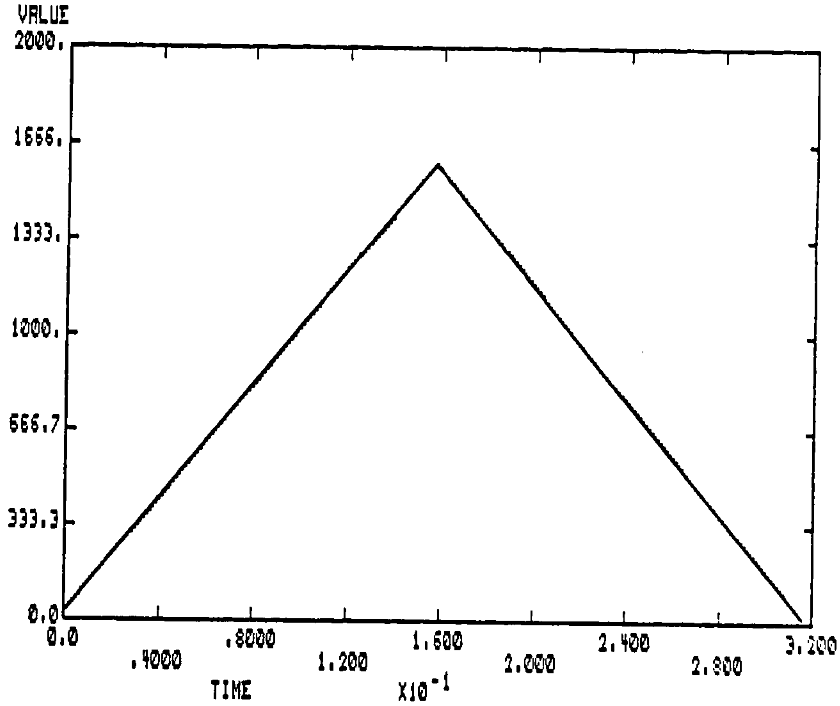

(b)

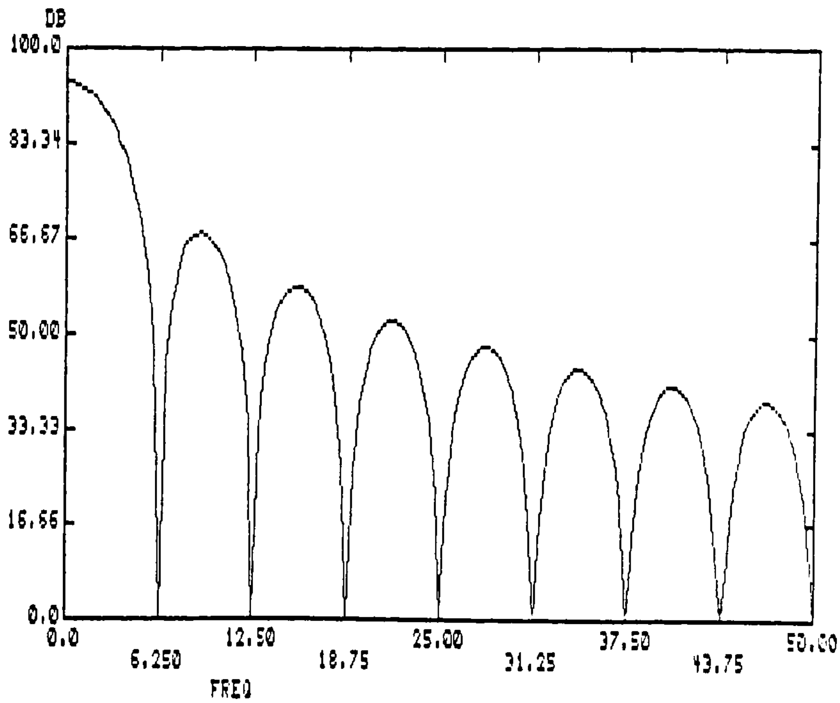

Figure III-5. Triangular window (a) along with its Fourier transform (b).

(a)

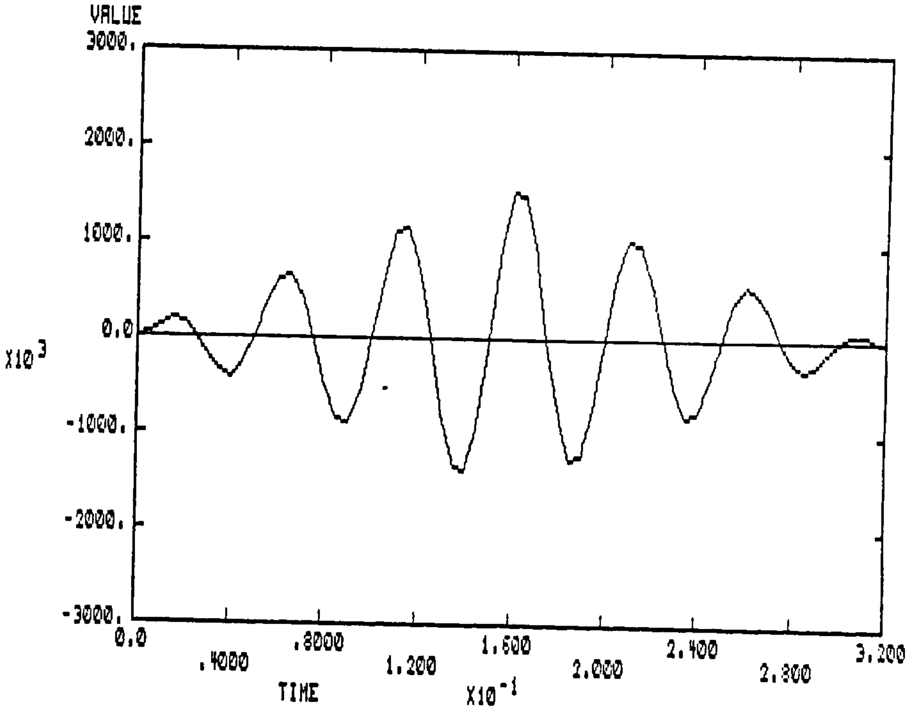

(b)

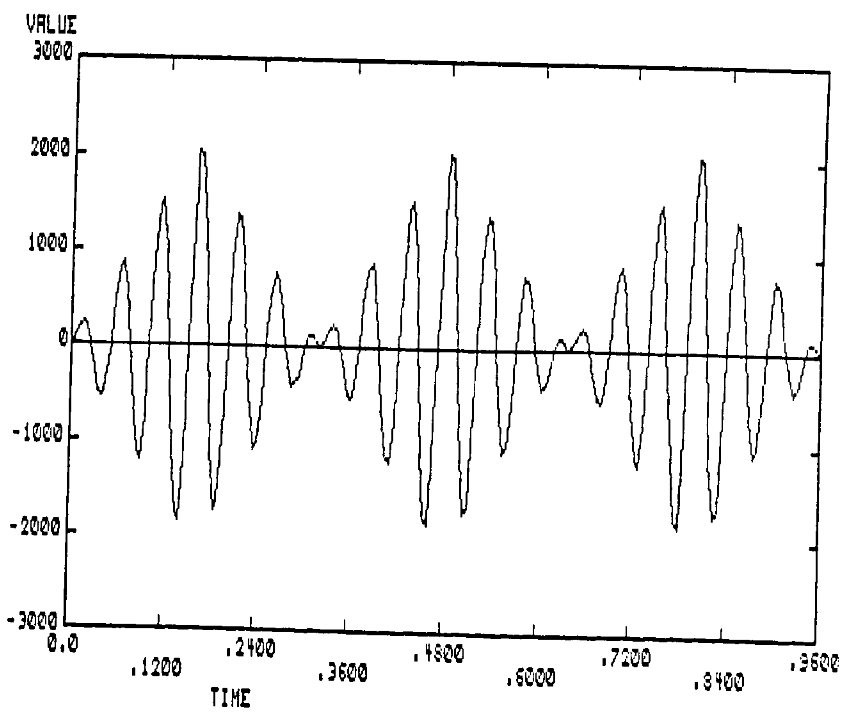

Figure III-6. Triangular windowed sine wave of Figure III-3 (a) along with the periodic extension of the signal (b) and its Fourier transform (c).

(c)

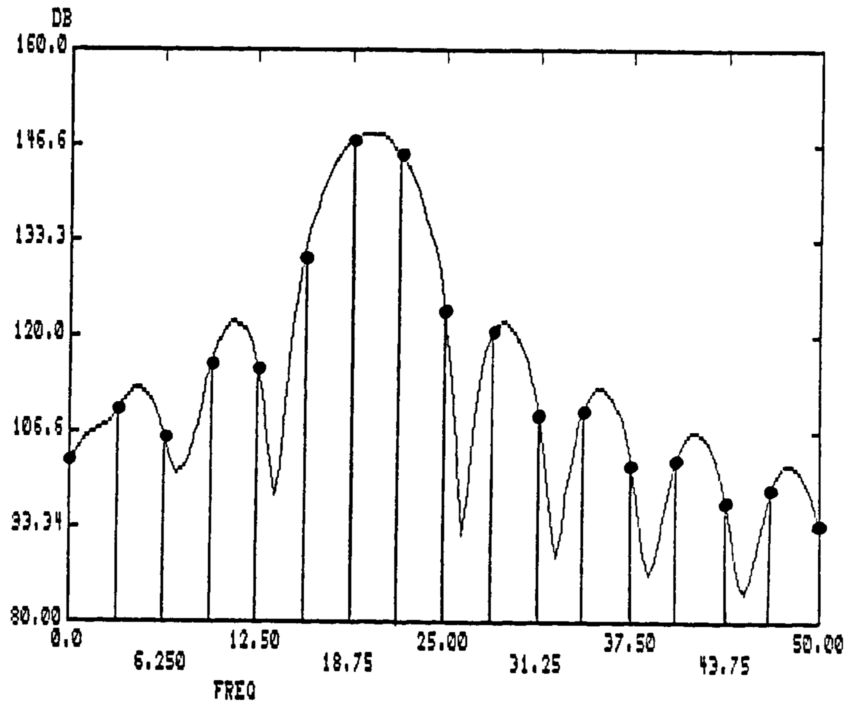

Figure III-6. (Continued).

functions involve a trade-off between the width of the main lobe and the reduction in the side lobes or leakage.

Over 200 window variations have been developed in the search of the ideal window function. Each window was developed to provide features that are desirable for different types of input functions and for extracting different types of information from the Fourier transform (Kaiser, 1966). All windows have a Fourier transform that consists of a main lobe at the origin and side lobes at both sides (Geckinil, 1983). The rectangular window produces the smallest main lobe at the expense of large side lobes. As seen from Figure III-5, the triangular window has smaller side lobes, but a wider main lobe then the rectangular window. The width of the main lobe is responsible for a broadening or "smearing" of the features of the DFT. Therefore, the main lobe is largely responsible for the broadening of the resolution of the DFT, while the side lobes give rise to ripples in the transformation. Thus, there is a trade-off between the width of the transition region and the magnitude of the side lobes. Both cause distortion in the DFT (Kaiser, 1966). The Hanning, Hamming and Blackman windows are common windowing functions used with digital data acquisition. Each represent a trade-off in the three main window characteristics -- resolution degradation due to the main lobe, leakage due to the near side lobes, and leakage due to the far side lobes (Geckinli, 1983). The window functions for the three windows are given below.

Hanning: $(0 <= n <= N-1)$

$$w(n)=1/2\ [1-\cos(2\Pi n)/(N-1)]$$

Hamming: $(0 <= n <= N-1)$

$$w(n)=0.54-0.46\cos(2\Pi n)/(N-1)$$

Blackman: $(0 <= n <= N-1)$

$$w(n)=0.42-0.5\cos(2\Pi n)/(N-1)+0.08\cos(4\Pi n)/(N-1)$$

where n is the nth point in the window, and N is the total number of points. The windows and their transforms are shown in Figures III-7, III-8, and III-9. As a comparasion of the windows the 3 dB bandwidth of the main lobe, peak ripple value of the side lobes, and the asymptotic decay rate of the side lobe envelope are tabulated in Table I for each of the window functions previously discussed.

As can be seen from Table I, the rectangular window does have the narrowest main lobe and the largest side lobes with only a 6 dB/octave rolloff. The triangular

(a)

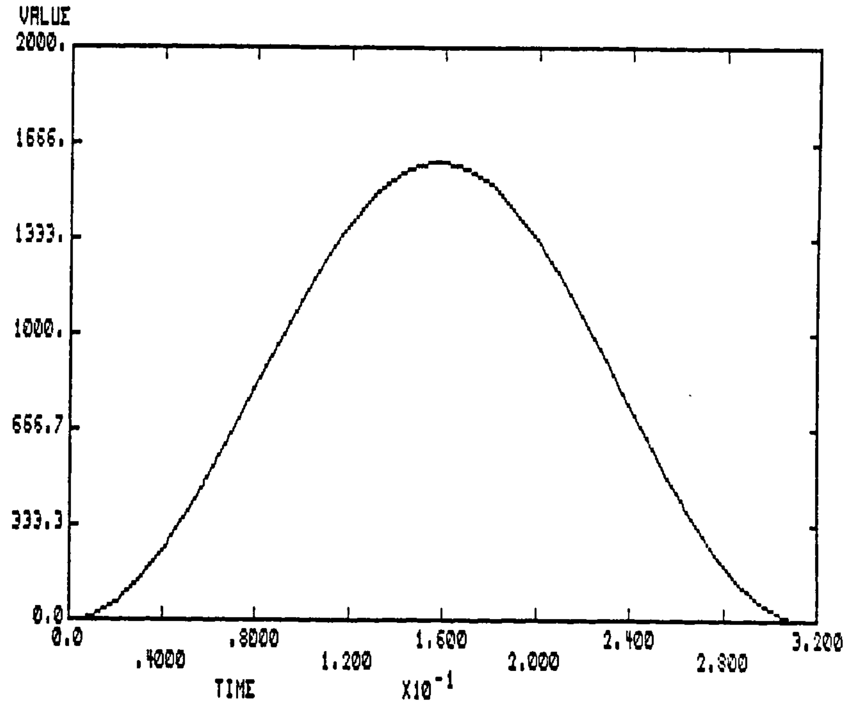

(b)

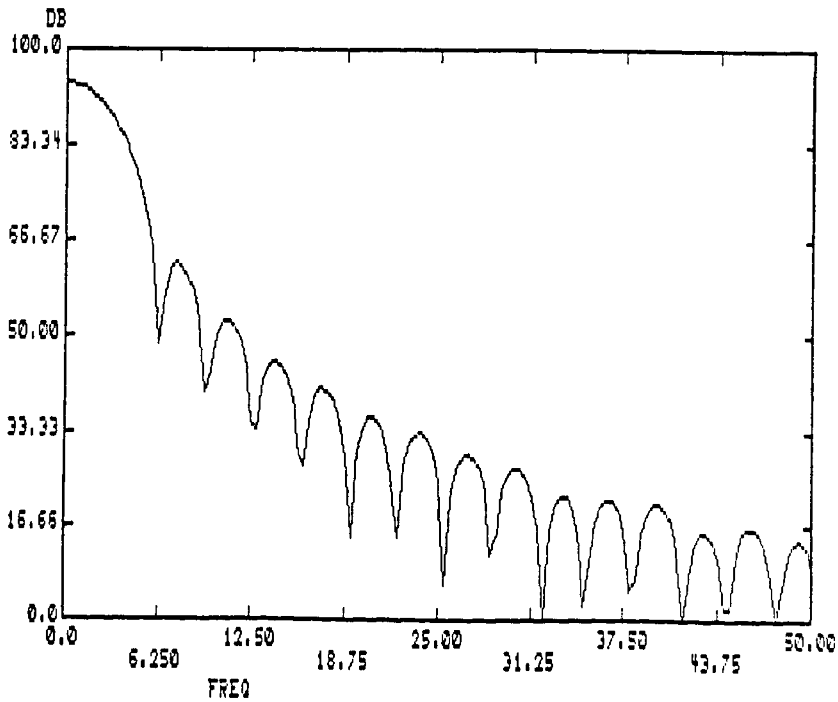

Figure III-7. The Hanning window (a) along with its Fourier transform (b).

(a)

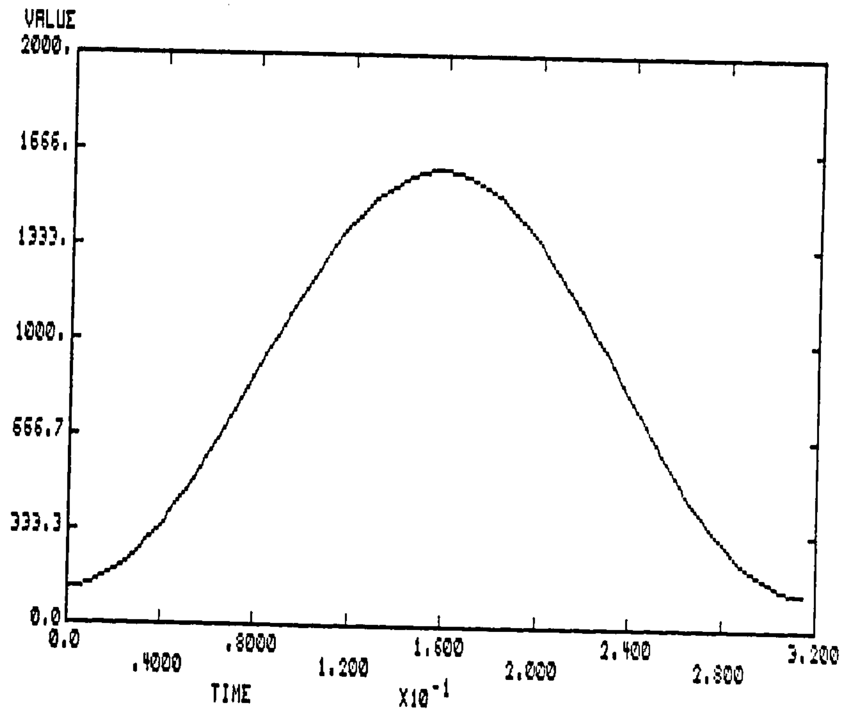

(b)

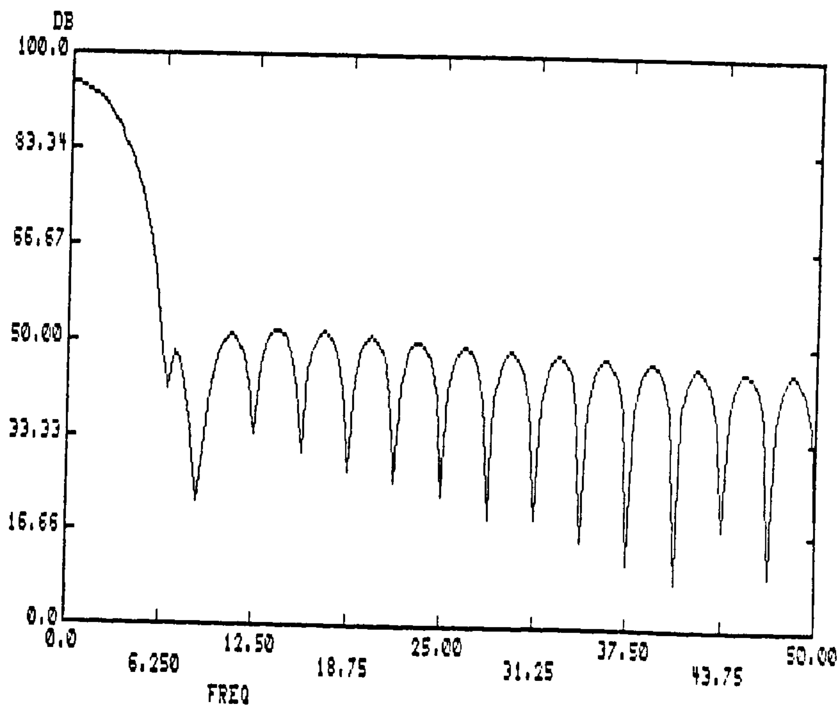

Figure III-8. The Hamming window (a) along with its Fourier transform (b).

(a)

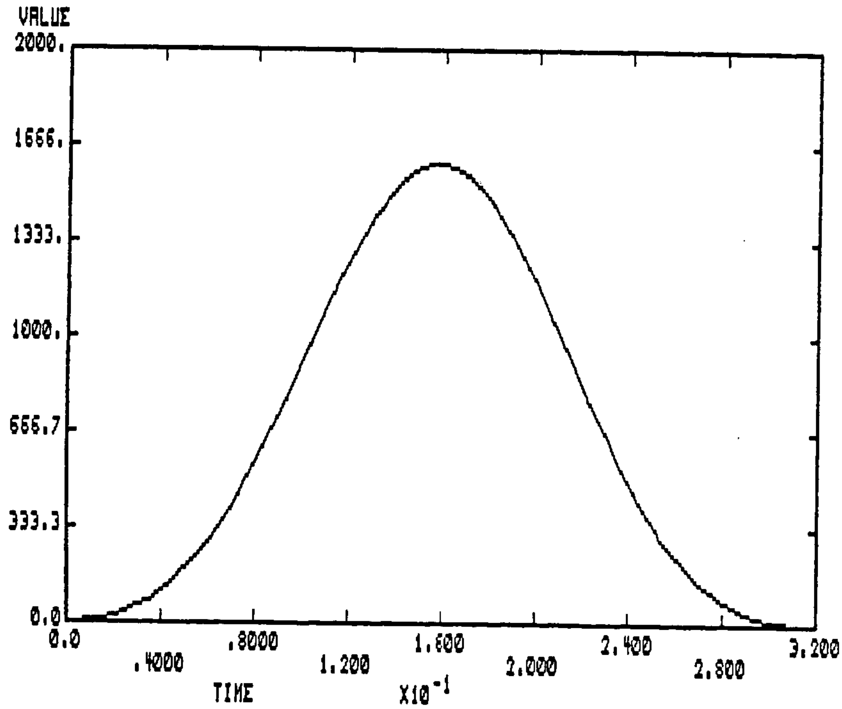

(b)

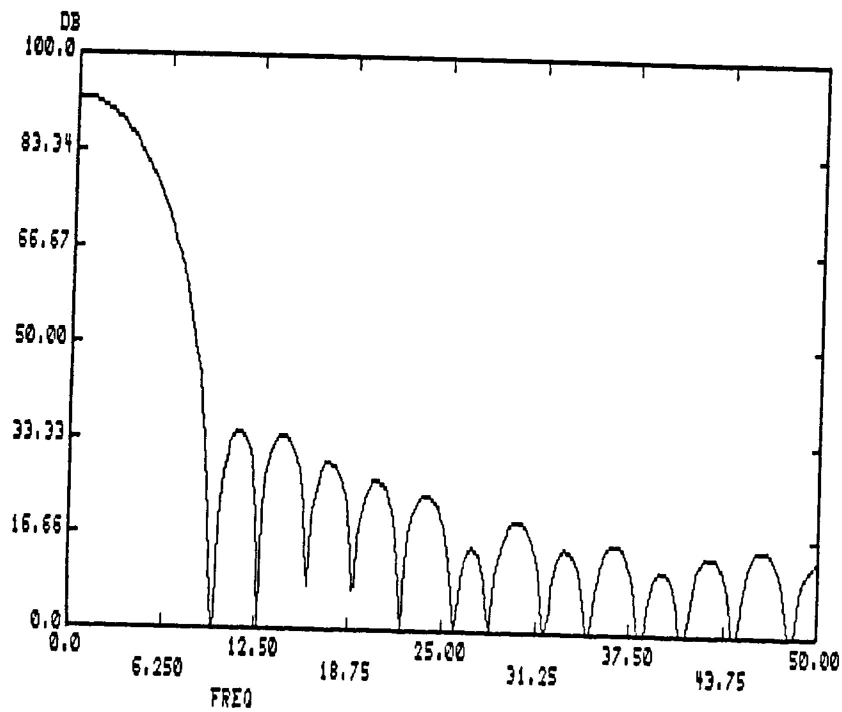

Figure III-9. The Blackman window (a) along with its Fourier transform (b).

Table I. Characteristics of some common symmetric windows.

Window Function	3 dB Bandwidth	Peak Ripple	Asymptotic Decay
Rectangular (Box-car)	0.85 1/T	-13 dB	6 dB/oct.
Bartlett (Triangular)	1.25 1/T	-26 dB	12 dB/oct.
Hanning (Raised-cosine)	1.40 1/T	-32 dB	18 dB/oct.
Hamming	1.30 1/T	-43 dB	6 dB/oct.
Blackman	1.68 1/T	-58 dB	18 dB/oct.

Note: T is the length of the time window.

window offers some improvement over the rectangular window in reduction of the side lobes in terms of absolute reduction (down 13 more db) and in terms of rolloff (12 db/octave versus 6 db/octave). However, the main lobe is approximately fifty percent wider. The Hanning window produces a still lower side lobe level (-32 db) than the triangular window and offers a greater side lobe rolloff rate (18 db/octave) at the expense of a slightly wider main lobe (12.8%). Finally, the Hamming (see Figure III-8) and Blackman (see Figure III-9) windows offer additional variations in the trade-offs between the width of the main lobe, side lobe magnitude and side lobe rolloff. Therefore, the amount of leakage present in the Fourier transform is dependent on which window function is applied to the input signal (Ramirez, 1985).

By choosing the proper function, windowing reduces leakage (energy leaking out of one resolution line of the DFT into all other lines). Choosing this window function, however, depends on the type of data that is being observed, and since one cannot define an optimum window for all digital signal acquisition applications, the window should be selected on the basis of which window produces the best results for a given application.

CHAPTER IV

INVESTIGATION OF EXPONENTIAL WINDOWS

All the windows presented thus far have been symmetric windows. That is, all of the windows exactly match if folded about their center point. These windows were designed to reduce the leakage effects of data that is present throughout the time window. However, many data signals are transient in nature and die out before the end of the time window. In addition, if the input data has a large damping constant, many of the symmetric windows greatly reduce the amount of data and therefore energy that is available to analyze as shown in Figure IV-1. Furthermore, if the signal is in the presence of noise, not only is much of the input signal blocked, but much of the noise is allowed to pass when the signal-to-noise ratio is very low. To decrease the effects of noise on transient data, non-symmetric windows offer an advantage over symmetric windows.

A common window used for transient data is the exponential window shown in Figure IV-2. The exponential window allows most of the data to pass at the beginning of the time window, but blocks the signal at the end of the time window. However, the exponential window allows for a possibly large transition to be present if the input signal does not have zero amplitude at the beginning of

(a)

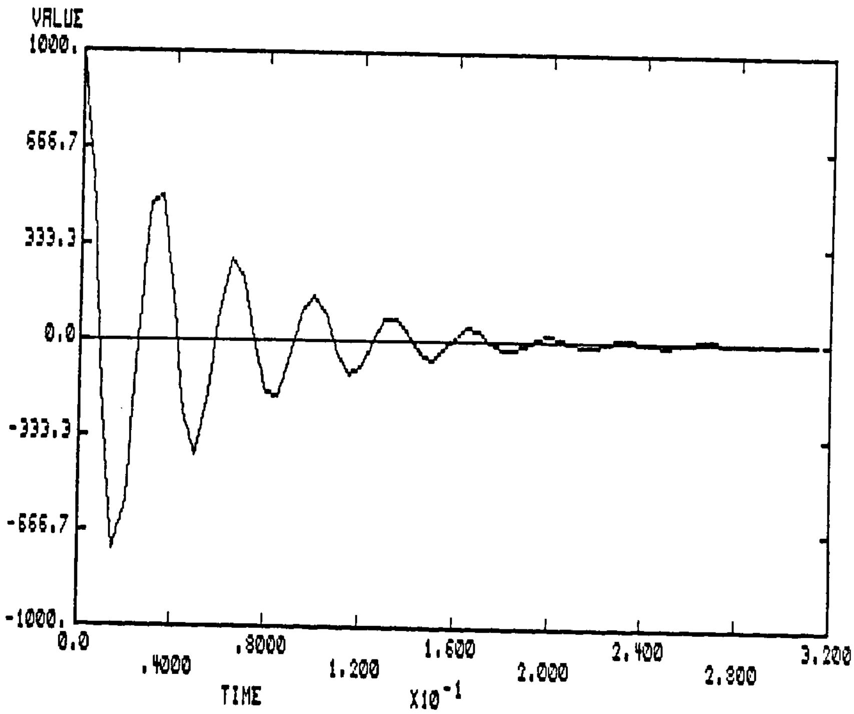

(b)

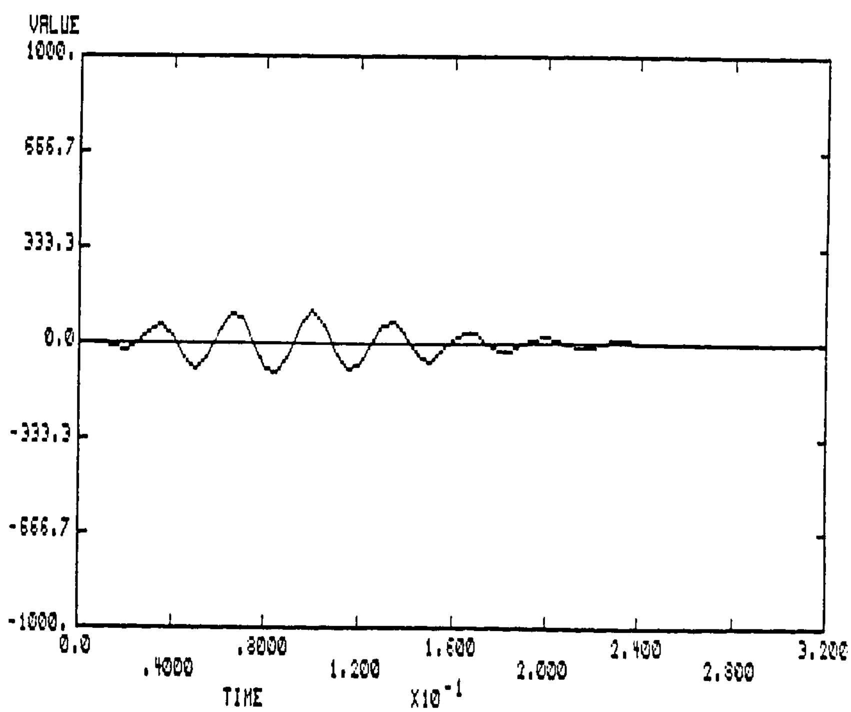

Figure IV-1. Transient wave form, f(t), (a) and the resultant wave form obtained by applying the Hanning window [$f(t)=1000\cos(30t+90^0)\ e^{-2t}$].

(a)

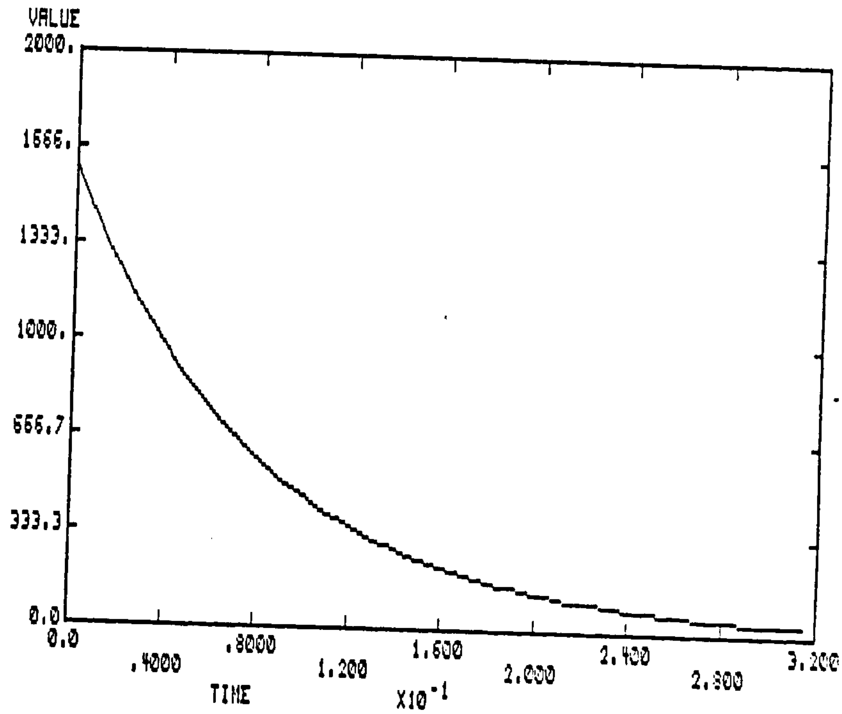

(b)

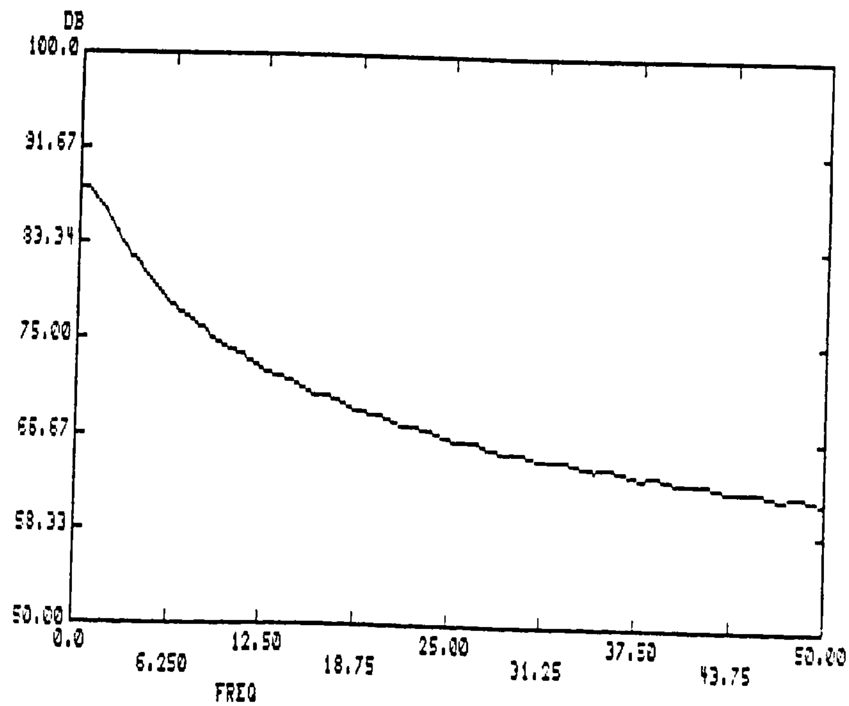

Figure IV-2. Exponential window (a) along with its Fourier transform (b).

the time window. That is, a large discontinuity may be produced when the input signal is assumed to be periodic by the DFT as shown in Figure IV-3. Therefore, exponentially damped windows were developed which have an initial value of zero, exponentially increase and then exponentially decrease such that most of a transient input is allowed to pass the window while any noise that is present at the end of the time window is blocked. One such window which has the same form as the Rayliegh distribution is expressed by the equation

$$w(n) = (n-1)\ \exp[-A(n-B)^2] \tag{1}$$

where A is the damping constant and B is an offset value. The Rayliegh window along with its Fourier transform is shown in Figure IV-4.

A second exponential window was developed from the Rayliegh window such that the slope of the window near the beginning of the time window is zero and then increased in an exponential manner as the Rayliegh window. This window along with its transform is shown in Figure IV-5 and will be referred to as the modified Rayliegh window. The modified Rayliegh window is expressed by the equation

$$w(n) = (n-1)^2\ \exp[-A(n-B)^2] \tag{2}$$

(a)

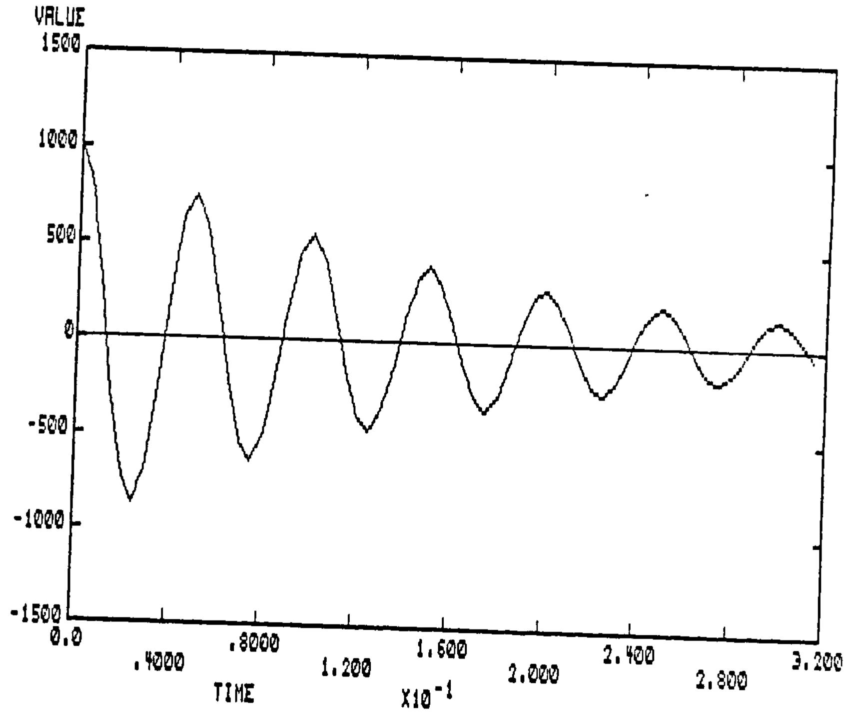

(b)

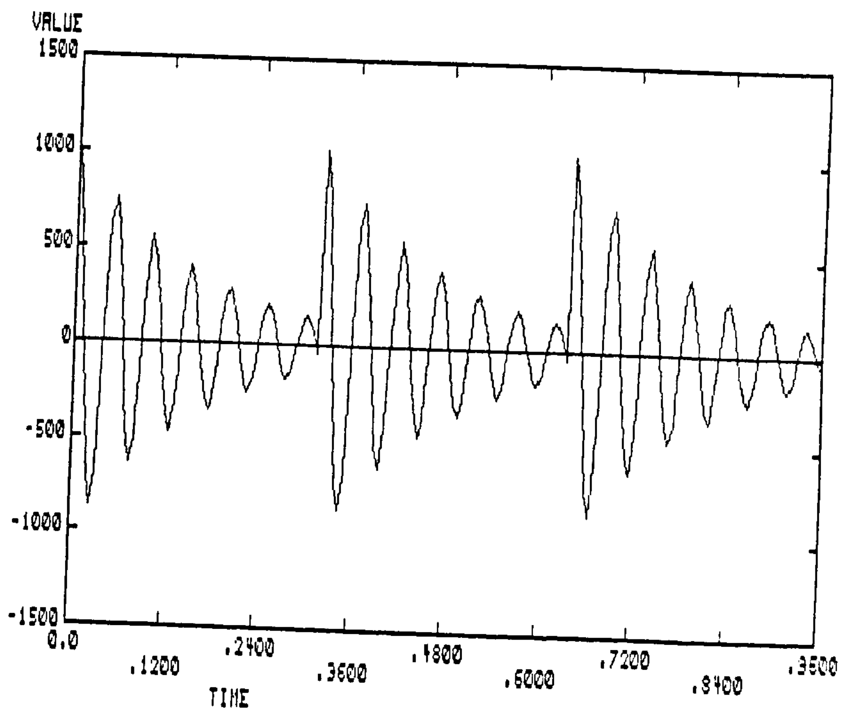

Figure IV-3. Transient signal (a) and the periodic extension of the wave form (b) along with the Fourier transform of the signal (c).

(c)

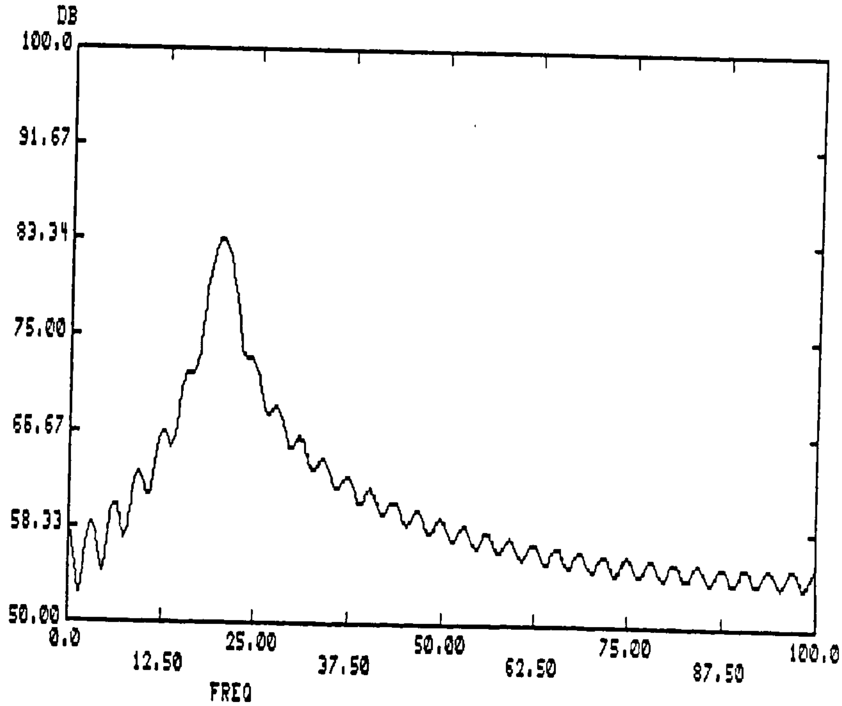

Figure IV-3. (Continued).

(a)

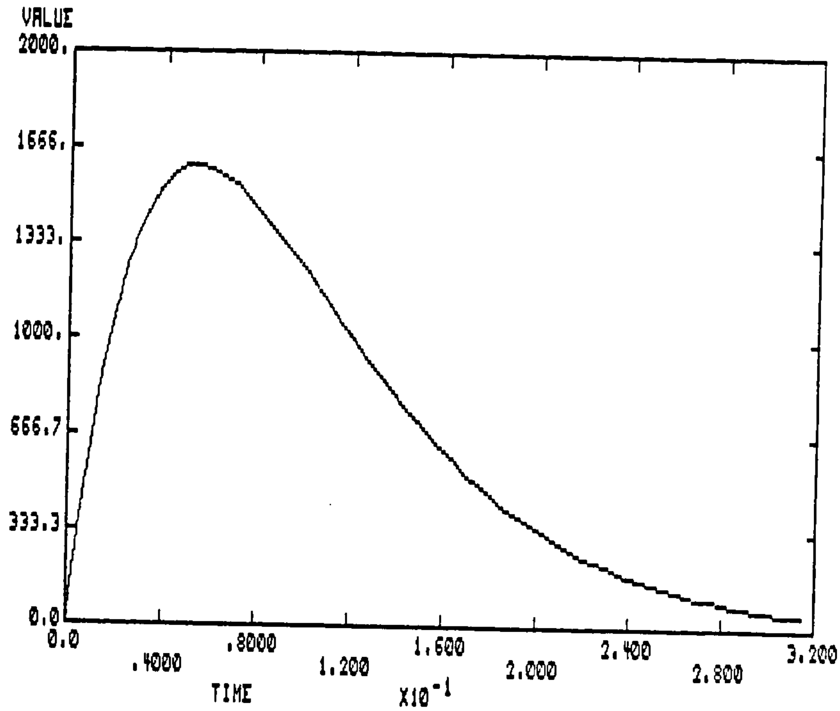

(b)

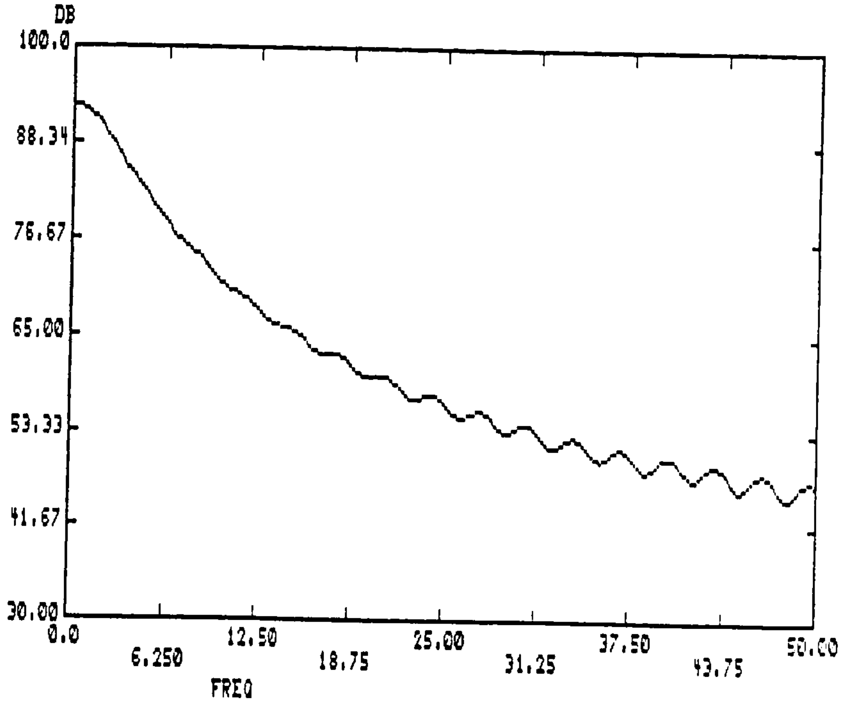

Figure IV-4. Rayliegh window (a) with its Fourier transform (b) (A=0.00015, B=-300).

(a)

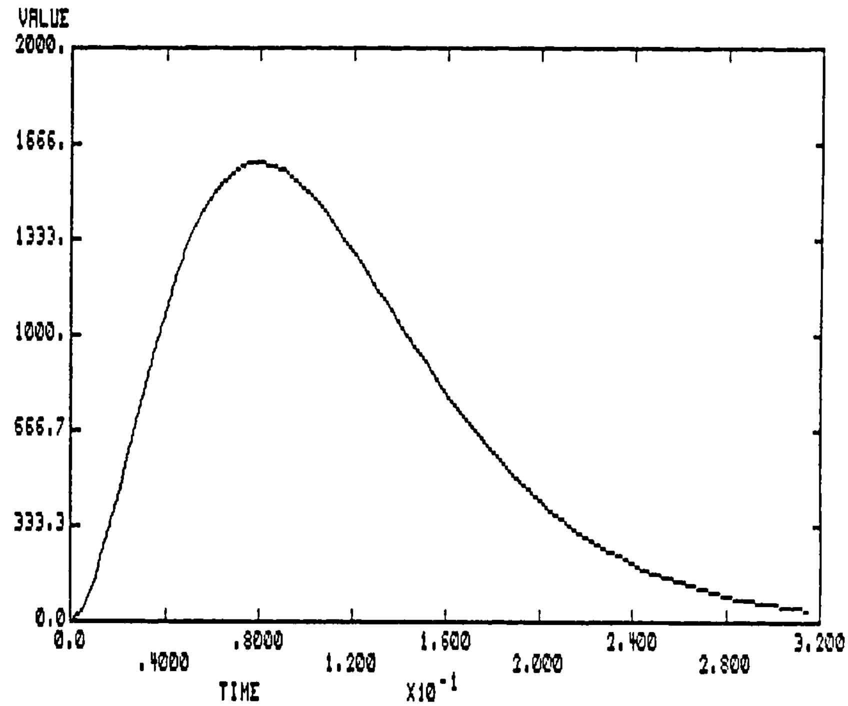

(b)

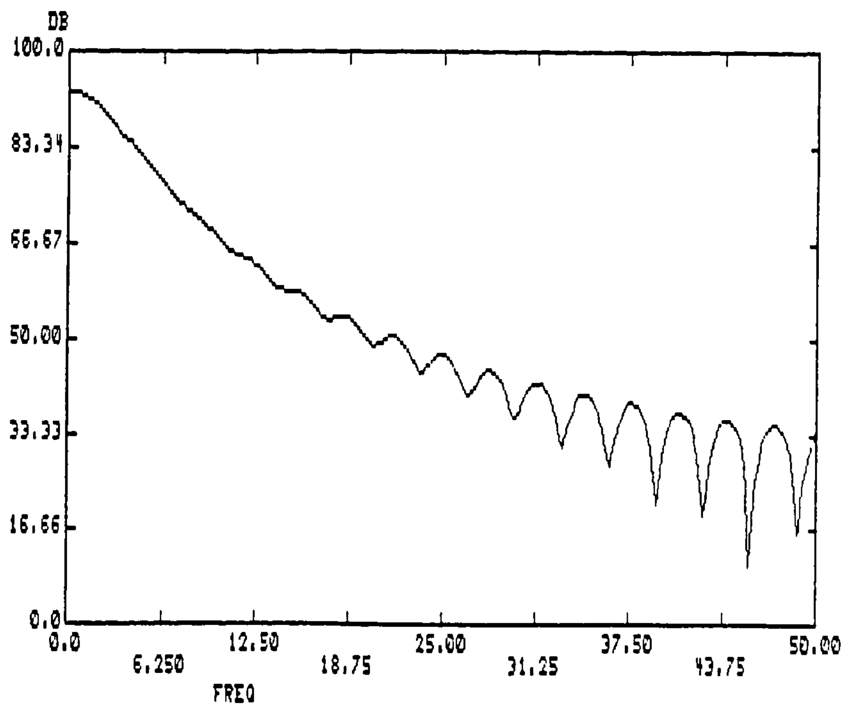

Figure IV-5. Modified Rayliegh window (a) with its Fourier transform (b) (A=0.0002, B=-300).

where A is again the damping constant and B is an offset.

The exponential windows (i.e. the Rayliegh and Modified Rayliegh) tend to have greater main lobes in the DFT due to the limiting of the time record by the windows. That is, the windows limit the time records to a greater extent then the symmetric windows which causes the frequency spectrum to spread-out. In addition, the exponential windows do not truncate the Fourier coefficients at the beginning of the time record as smoothly as many of the symmetric windows to reduce the side lobes in the transform.

In the presence of noise, the exponential windows allow more of the signal to pass at the beginning of the time window and block-out the noise when the signal has damped-out. The symmetric windows give the same weight to data at the beginning of the time record as to data at the end. With exponentially damped data, the input signal may only be distinguishable from the noise at the beginning of the time record. Thus, the symmetric windows do not effectively attenuate the noise at the end of a time record when the data signal is highly damped. The exponential windows allow more of the signal to pass at the beginning of the time record and attenuate the noise at the end of the time window in order to decrease the effects of the noise in the DFT.

From observing the effects of symmetric windows on transient signals, the resultant wave form used in the DFT calculation has much less amplitude than when using an exponential window (especially when the data is heavily damped). Since the input data losses a lot of its amplitude, noise effects the DFT to a much greater extent. When not in the presence of noise, the exponential windows allow for a DFT of greater magnitude, but less frequency resolution. The side lobes of the exponential windows are greater than those of most of the symmetric windows.

The Fourier transforms of the exponential window with different damping constants was also investigated. A very lightly damped exponential has very much the same frequency characteristics as a rectangular window (see Figure IV-6). As the damping constant is increased, the frequency response spreads out over a larger range of frequencies. The exponential window has side lobes much like the rectangular window which are present until the exponential window becomes critically damped (i.e. the window just goes to zero at the end of the time window). For a critically damped exponential window, the frequency response of the window has spread to a point that the side lobes are "buried" and are not visible in the transform as shown in Figure IV-7. As the damping constant is increased past the critically damped point, the frequency response of the window continues to spread out (without rippling) (see Figure IV-8). Taking the damping constant

(a)

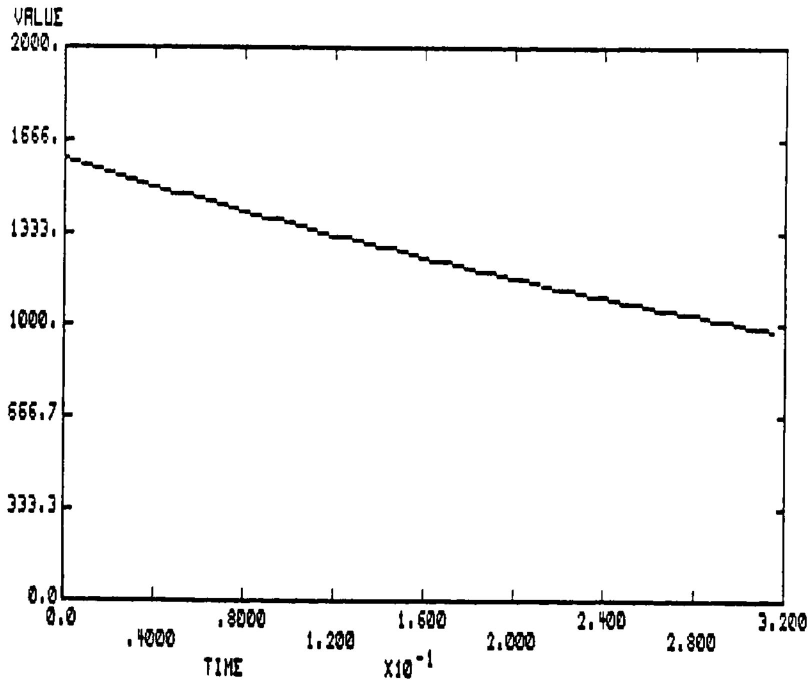

(b)

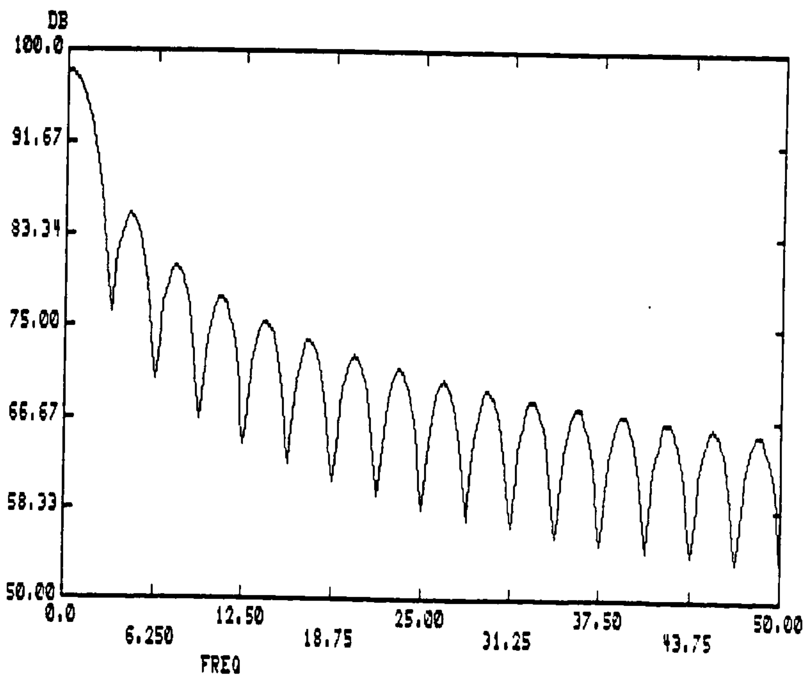

Figure IV-6. Lightly damped exponential window (a) with its Fourier transform (b).

(a)

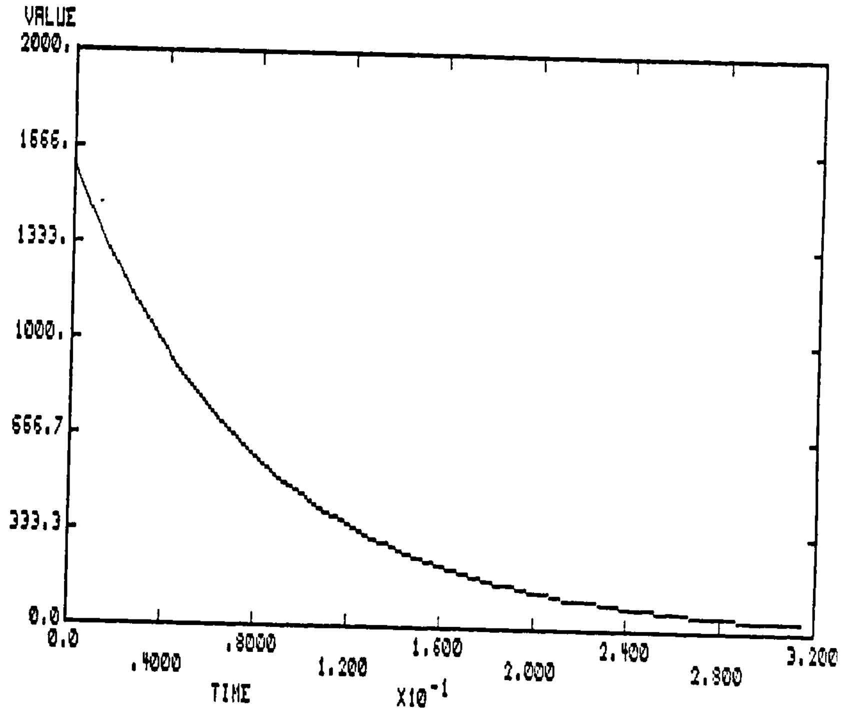

(b)

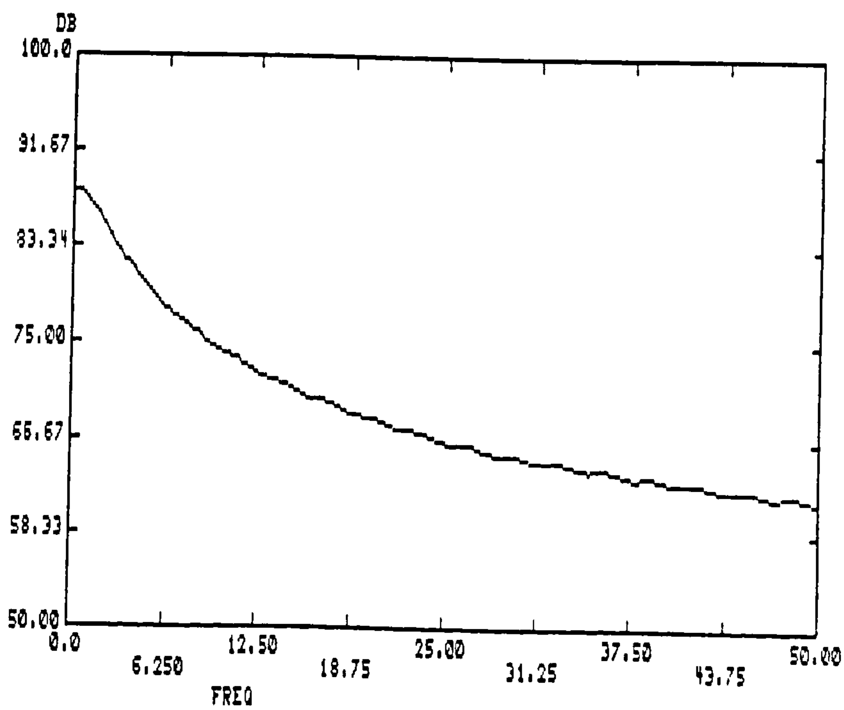

Figure IV-7. Critically damped exponential window (a) with its Fourier transform (b).

(a)

(b)

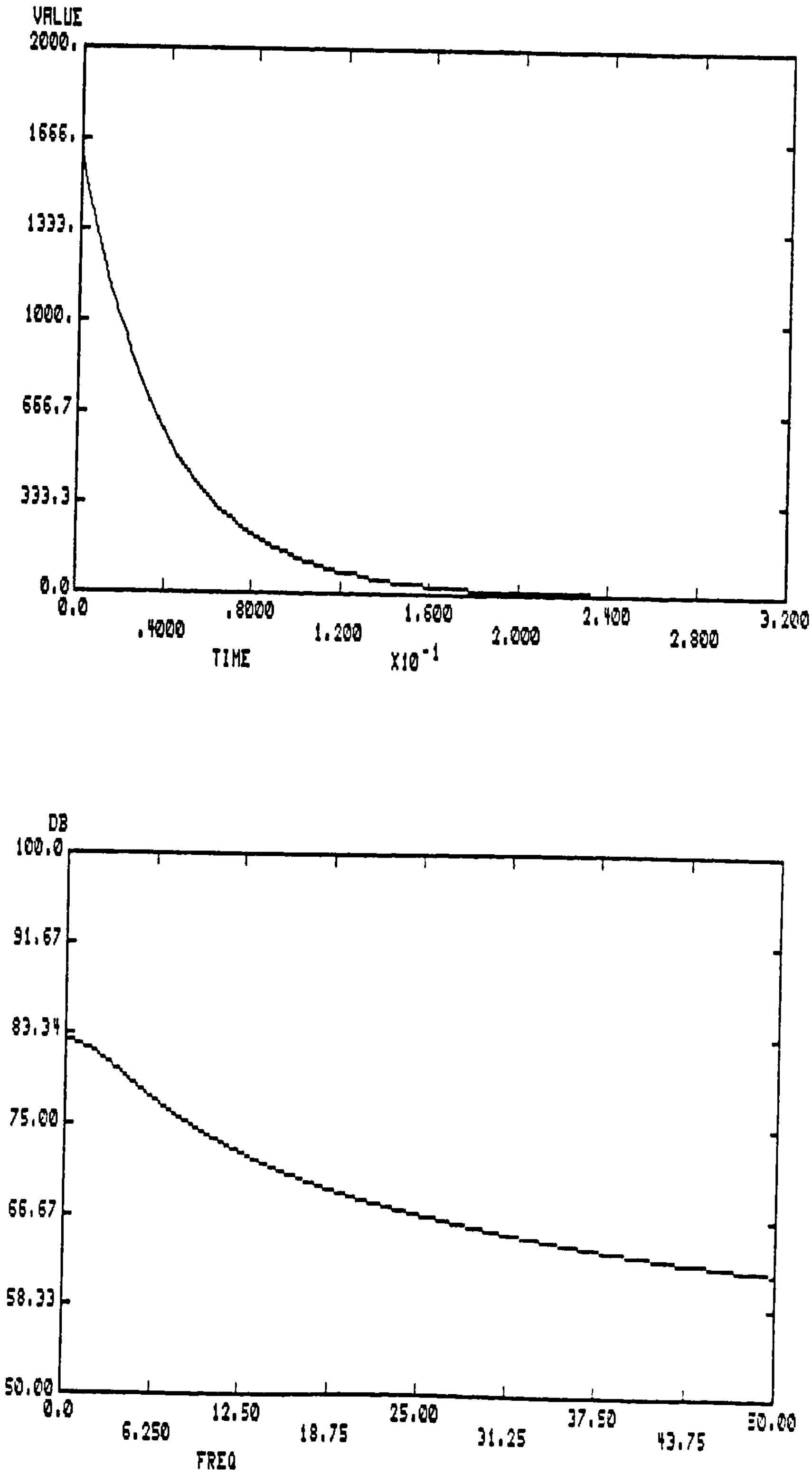

Figure IV-8. Heavily damped exponential window (a) with its Fourier transform (b).

increasingly larger causes the exponential to look more and more like an impulse in the time domain which corresponds to a flat frequency spectrum.

The window characteristics of the critically damped exponential, Rayliegh and modified Rayliegh windows are shown in Table II. Since these windows do not have large side lobes, the peak ripple values are not given.

Table II. Characteristics of the critically damped, exponential, Rayliegh and modified Rayliegh windows.

Window Function	3 dB Bandwidth	Asymptotic decay
Critically damped exponential	1.16 1/T	6 dB/oct.
Rayliegh	1.65 1/T	12 dB/oct.
Modified Rayliegh	1.41 1/T	12 dB/oct.

Note: T is the length of the time window.

CHAPTER V

TRANSMITTING TWO FREQUENCIES USING WINDOWING

Once the properties of windowing are understood, windows can be used for additional applications other than enhancing the frequency spectrum of input data. One may wish to use windowing to transmit a signal consisting mainly of two frequencies of a known separaton using a single oscillator. The transmitted frequencies are known precisely and are very stable.

Windowing an infinite sine or cosine wave form distorts its frequency spectrum -- a single impulse. By selecting the proper window function, the sine wave can be altered to consist of two frequency components of equal amplitude and with low side lobe levels. By using a bipolar rectangular window (see Figure V-1) to create a phase shift in the transmitting (or modulating) frequency, the transmitted signal and the Fourier transform of the signal has a DFT as shown in Figure V-2. The Fourier transform shows the energy of the transmitted signal concentrated at two frequencies close to each other.

The spacing of the two frequencies is determined by the length of the time window. For a time window of length T_W, the spacing of the main frequency components is given by

(a)

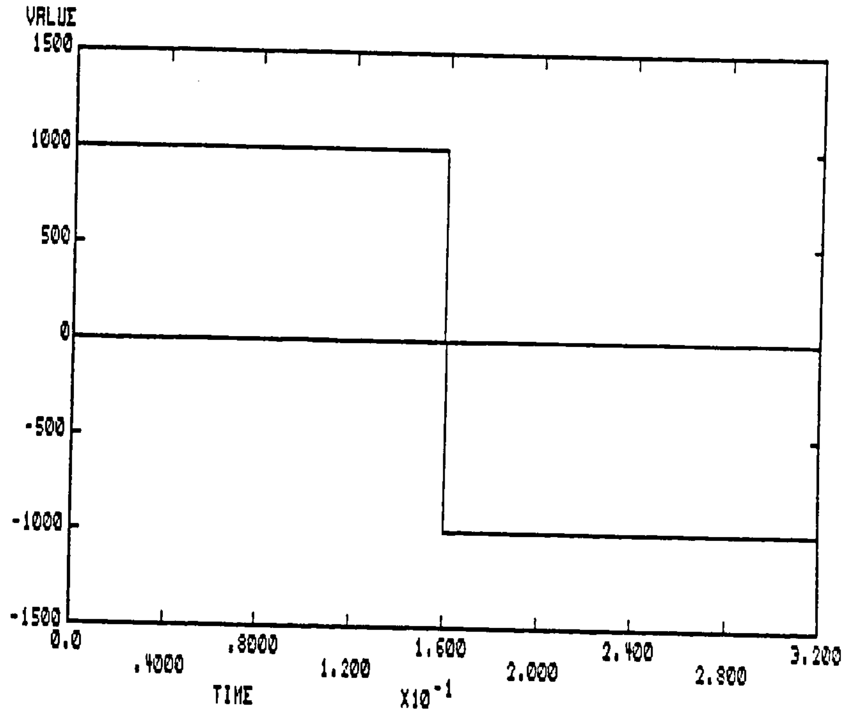

(b)

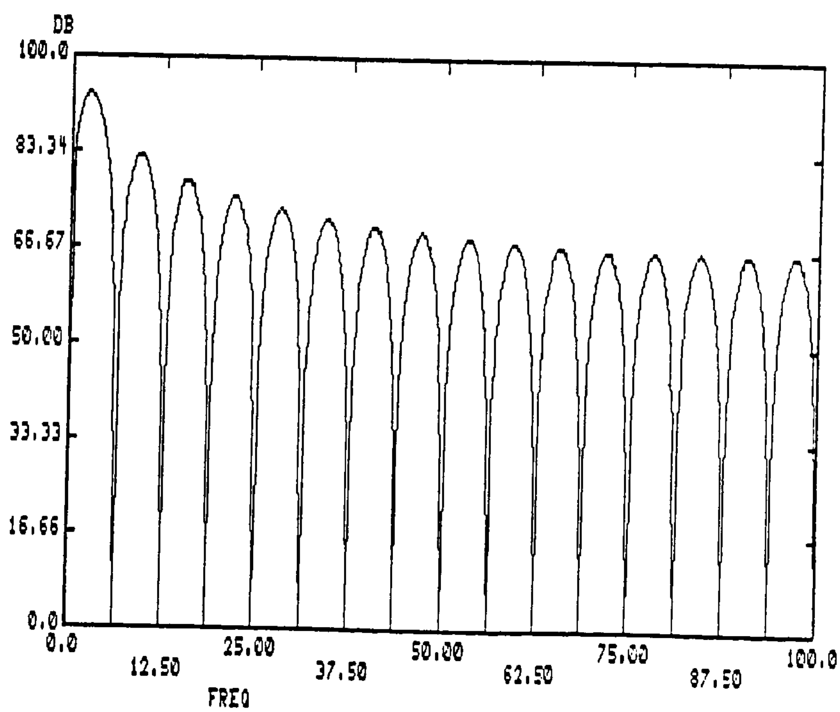

Figure V-1. Bipolar rectangular window (a) with its Fourier transform (b).

(a)

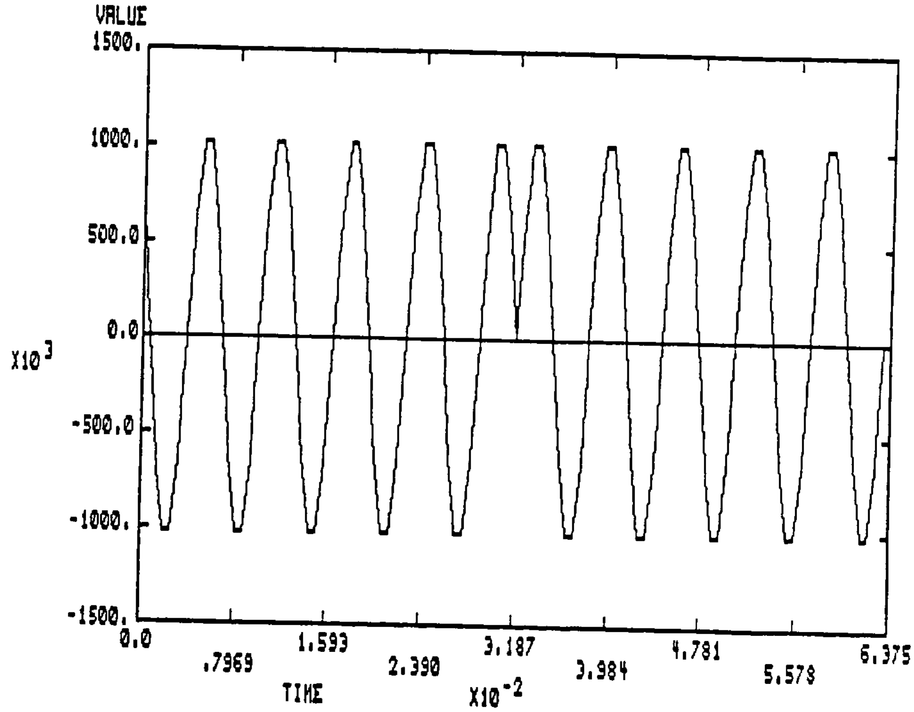

(b)

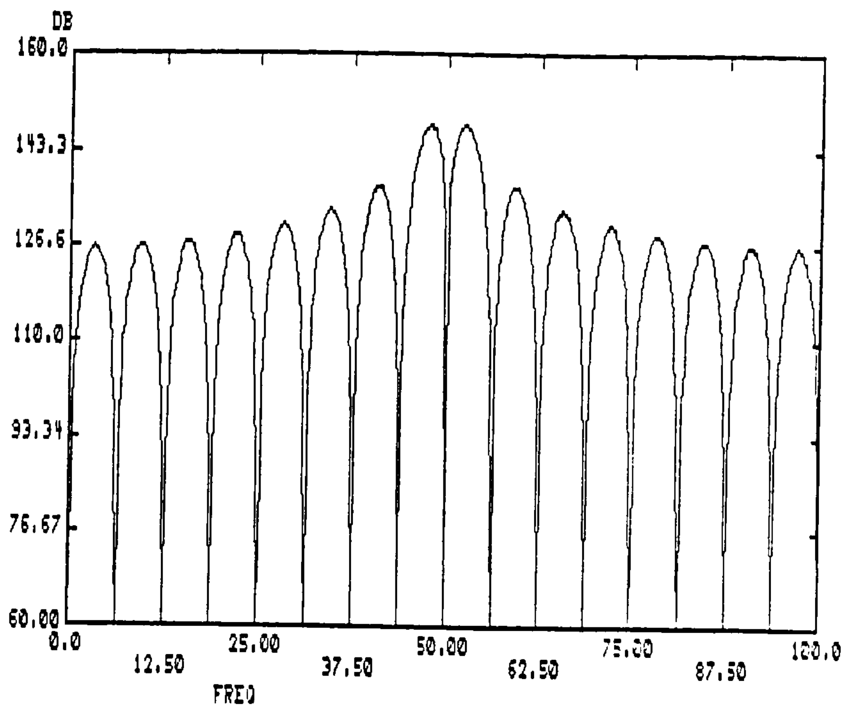

Figure V-2. Modulated bipolar rectangular window (a) with its Fourier transform (b).

$$F_{spacing} = 2/T_w$$

The two main frequencies are centered about the modulating frequency.

When generating the window by a digital system the frequency of the two main lobes is determined as follows. The length of the time window is

$$T_w = N/F_s$$

where N is the number of points in the window and F_s is the sampling frequency. Therefore, the spacing of the two main frequency components is given by

$$F_{spacing} = 2F_s/N$$

The Fourier transform of the bipolar rectangular window also shows large side lobes which represent additional frequency components which may not be desirable to transmit. To reduce these side lobes, the bipolar rectangular pulse window can be modified to truncate the Fourier coefficients in a smoother manner. By multiplying each rectangle by a Hanning window, the side lobes of the DFT of this window can be reduced considerabily as shown in Figure V-3. Additional reduction can be obtained by removing window points from the center of the window while keeping the window symmetric about the center point.

(a)

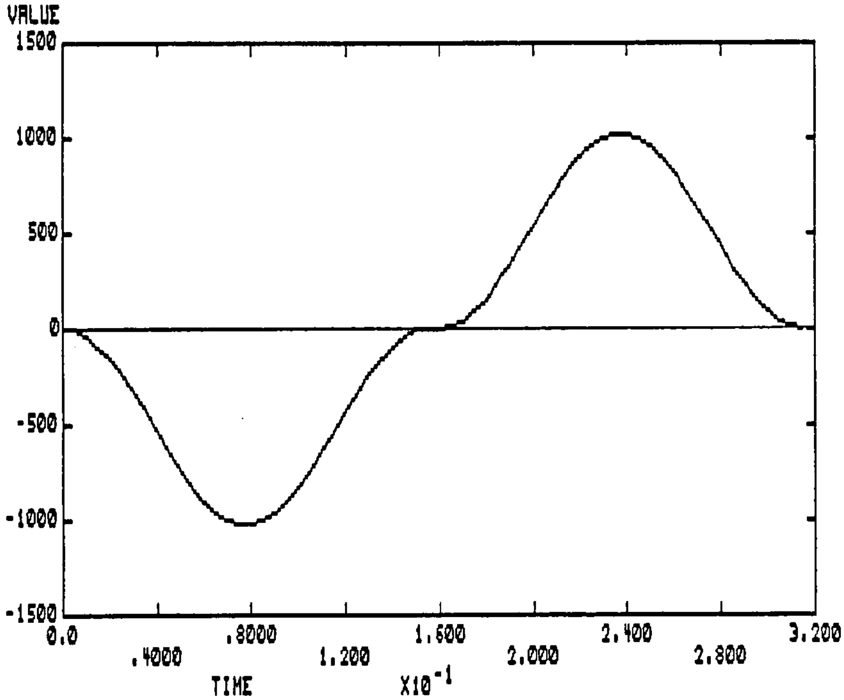

(b)

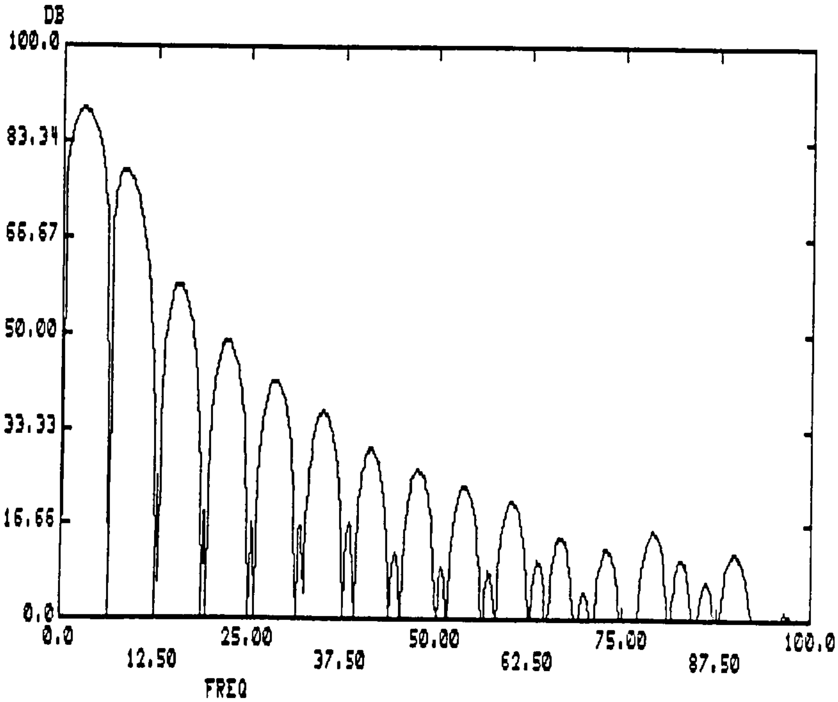

Figure V-3. Bipolar Hanning window (a) with its Fourier transform (b).

Removing these points creates an abrupt phase shift which generates additional side lobes of the opposite polarity than the original side lobes so the overall DFT contains smaller side lobes (see Figure V-4). However, the sharp transition introduced in the new window, causes a small increase in the power of frequencies far away from the main frequency.

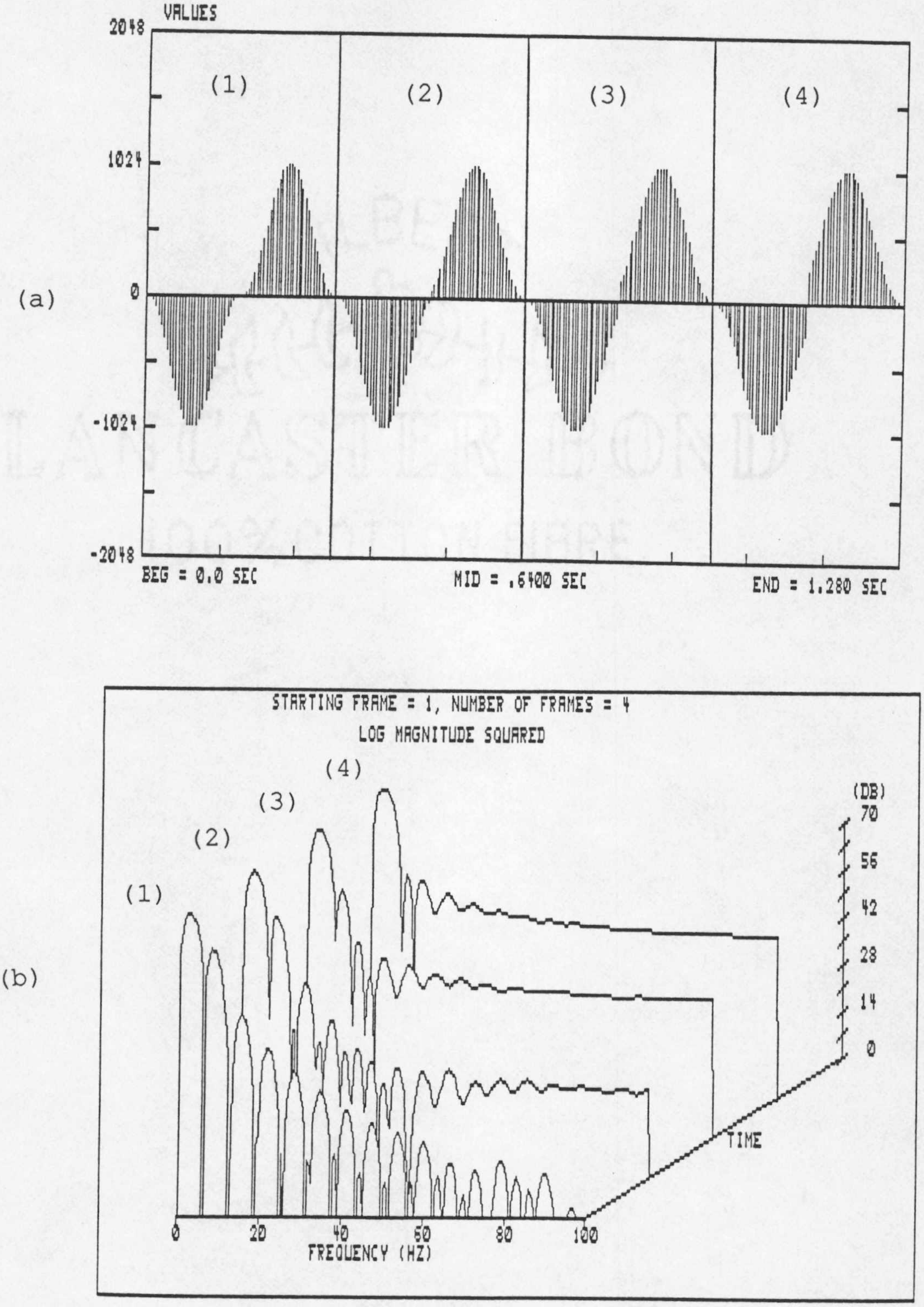

Figure V-4. Bipolar Hanning windows with center points removed (a) along with their Fourier transforms (b).

CHAPTER VI

EXPERIMENTAL RESULTS

To show the effects of leakage on a sinusoidal signal, a sine wave with a frequency of 50.75 KHz was sampled with a HP-3561A Dynamic Signal Analyzer. The sampling rate of the signal analyzer is 256 KHz and 1024 points were sampled. Therefore, the frequency resolution, Δf, of the discrete Fourier transform is

$$\Delta f = 1/N\Delta t = f_s/N = 256{,}000/1024 = 250 \text{ Hz}$$

The sine wave frequency was chosen to correspond to one of the frequency bins of the discrete Fourier transform (that is, exactly an even number of cycles of the sine wave in the time window). Therefore, leakage is not observed in the Fourier transform as shown in Figure VI-1. However, a second sine wave with a frequency of 50.70 KHz was also sampled by the HP-3561A under the same conditions. The frequency of the second sine wave does not correspond to one of the bins of the discrete Fourier transform so leakage in the Fourier transform is easily seen as shown in Figure VI-2. To show how windowing effects the Fourier transforms of the sine waves, the wave forms of Figures VI-1 and VI-2 were both windowed using the Hanning window and the windowed sine waves are shown along with their

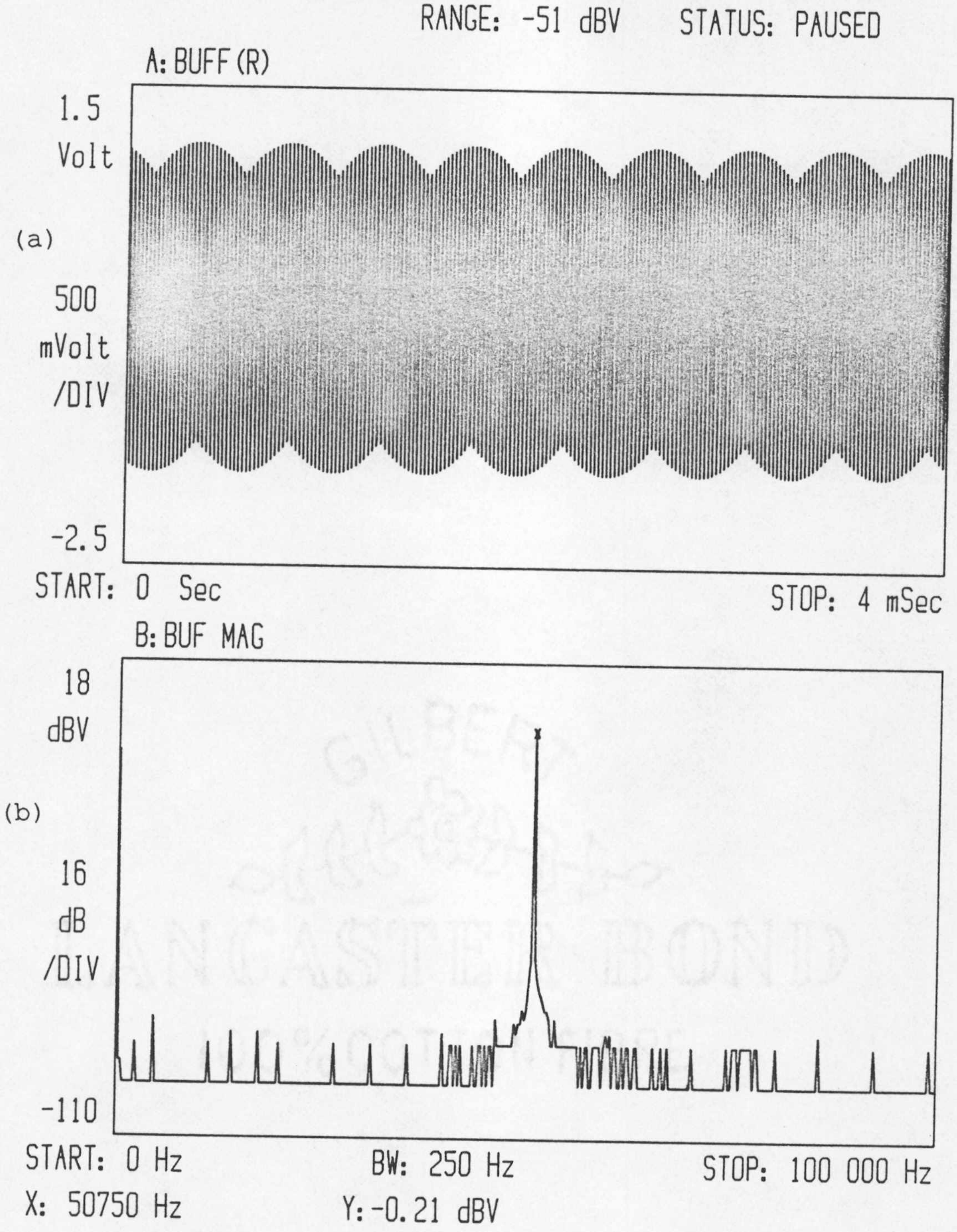

Figure VI-1. Sampled sine wave with a frequency of 50.75 KHz (a) (Sampling frequency=256 KHz, number of points=1024) along with its discrete Fourier transform (b).

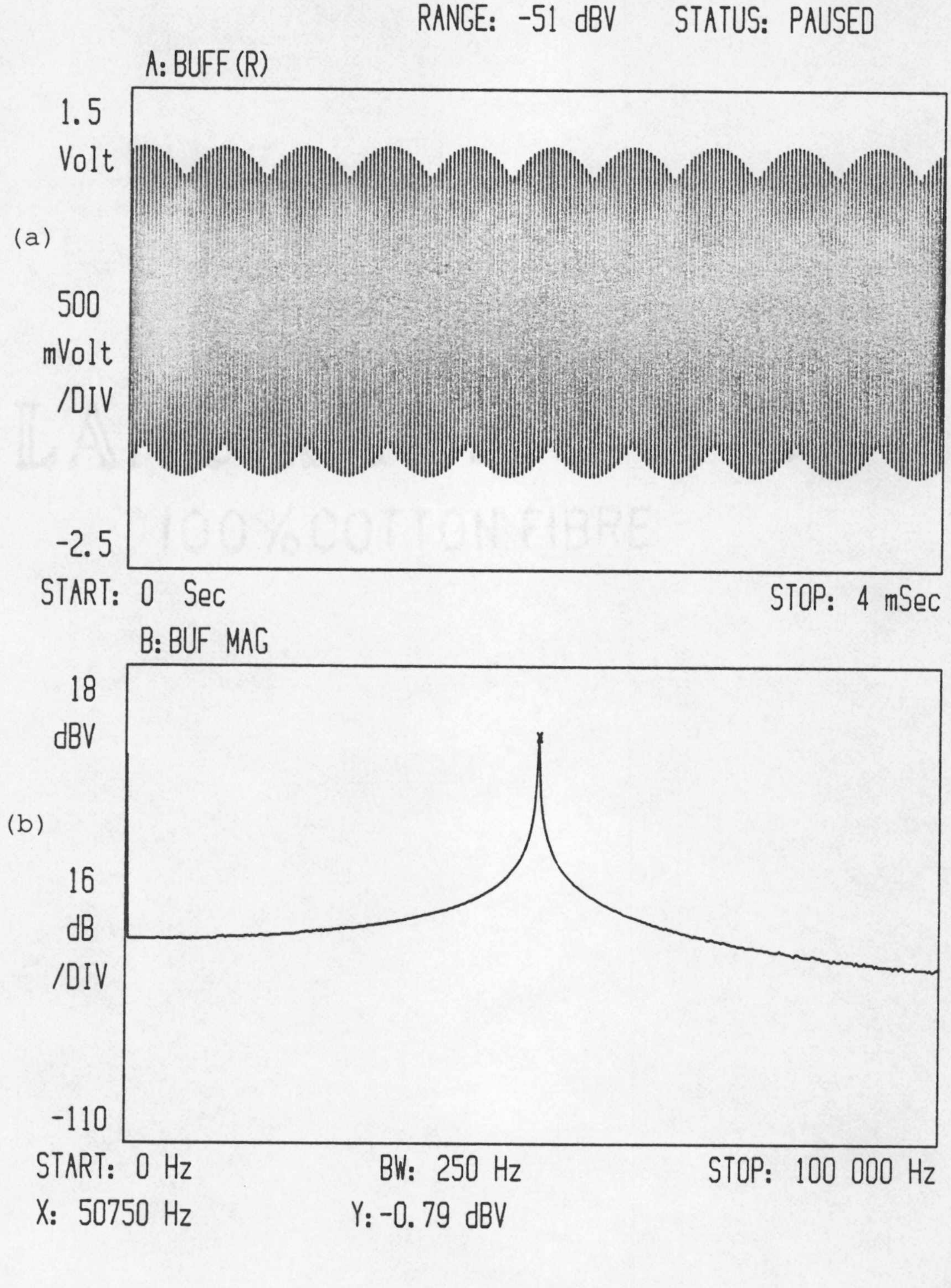

Figure VI-2. Sampled sine wave with a frequency of 50.70 KHz (a) (Sampling frequency=256 KHz, number of points=1024) along with its discrete Fourier transform (b).

discrete Fourier transforms in Figures VI-3 and VI-4. As expected, the windowing increased the width of the main lobe in the Fourier transform of the 50.75 KHz frequency sine wave, but had little effect on the rest of the transform as shown in Figure VI-3. However, as can be seen in Figure VI-4, the windowing of the 50.70 KHz sine wave greatly reduces the leakage effects due to the side lobes of the rectangular window (that is, no windowing).

In order to show the effects of different windows on transient data, several wave forms were "captured" by the HP-3561A Dynamic Signal Analyzer. The damped sinusoidal data was generated by observing the resonance frequencies of a 3/4 inch long cylinder (inside diameter = 1/4 inch, outside diameter = 1/2 inch). The cylinder was excited by dropping bee bees on it, and the resonance frequencies were determined using a Poloriod ultrasonic transducer to convert the sound waves produced by the vibrating cylinder to an electric signal. The HP-3561A signal analyzer was used to sample the electric signals and to store the signals in memory. The wave forms were then read out of the analyzer's memory using a Texas Instruments Business-Pro computer. Finally, the signals were windowed with several different windows, and the discrete Fourier transforms of the wave forms were calculated. The wave forms were windowed using software called Interactive Laboratory System Simulation (ILS-IEEE).

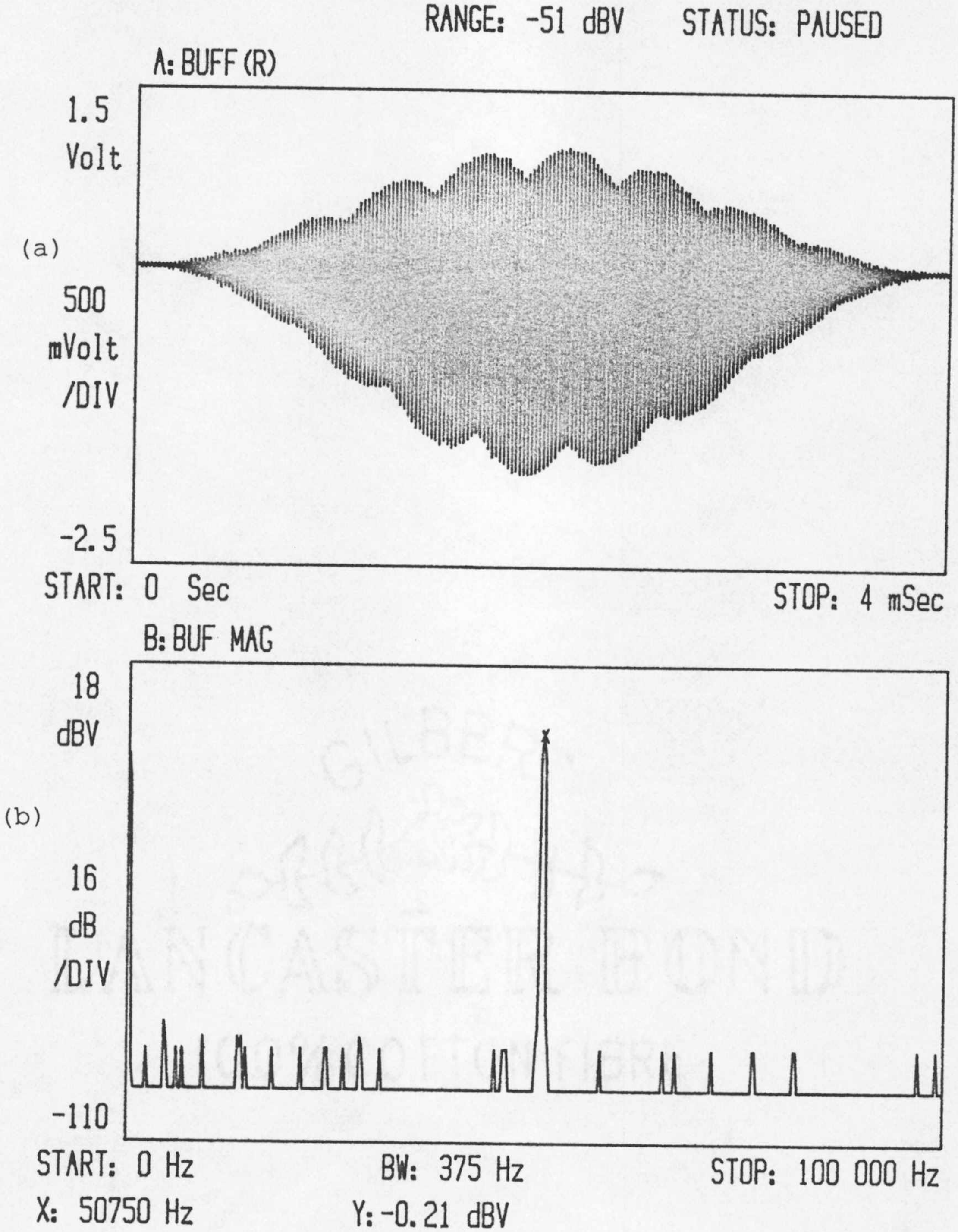

Figure VI-3. Hanning windowed Figure VI-1 (a) along with the windowed signal's discrete Fourier transform (b).

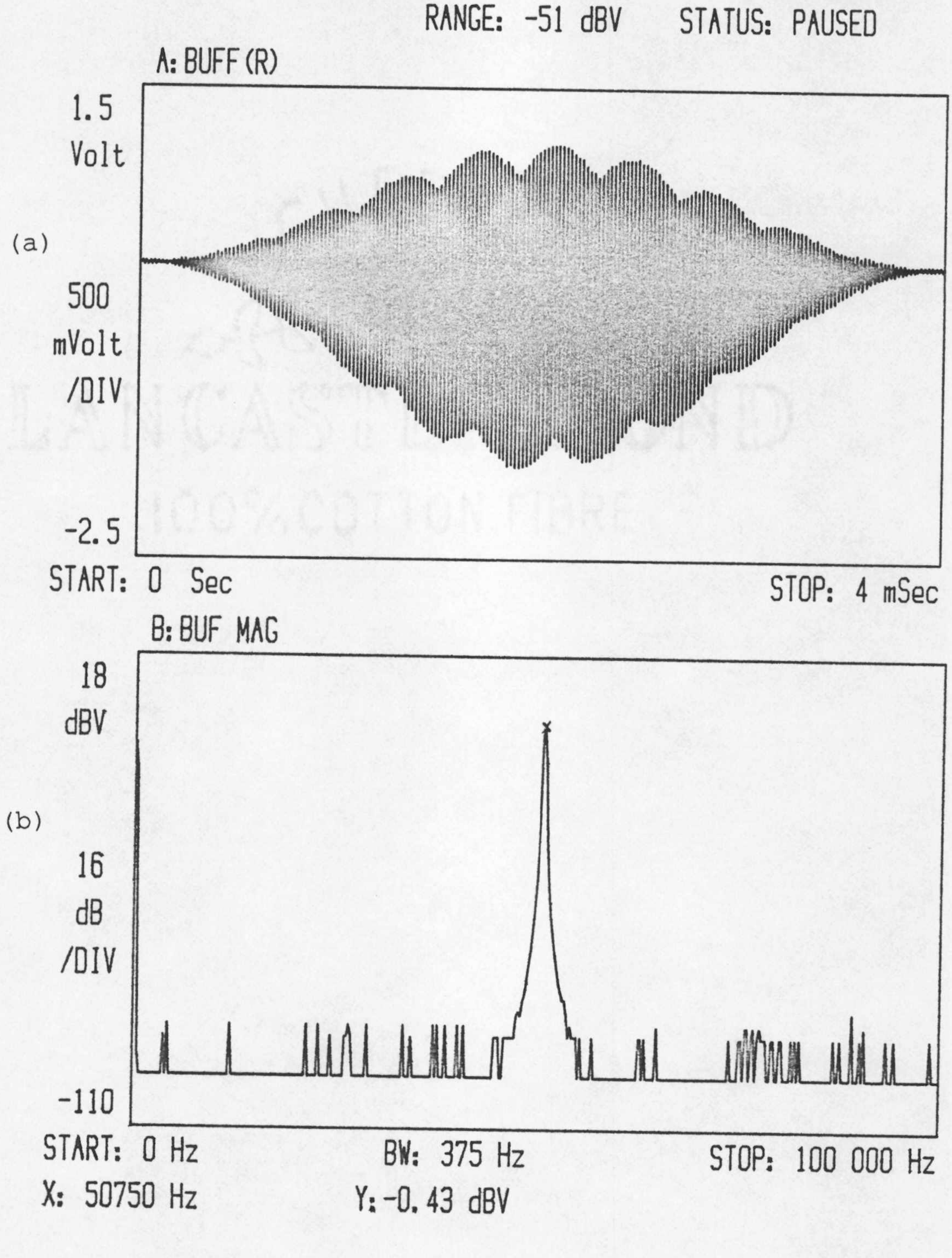

Figure VI-4. Hanning windowed Figure VI-2 (a) along with the windowed signal's discrete Fourier transform (b).

A typical signal obtained from the excitation of the cylinder is shown in Figure VI-5. As can be seen from this figure, the vibration modes of the cylinder are highly damped. Also, from the discrete Fourier transform, the two main resonance frequencies of the cylinder are at 38.75 KHz and at 91.00 KHz. However, since this data has been windowed using the rectangular window (recall that observing a signal for a finite amount of time corresponds to windowing the data with a rectangular pulse equal to the time that the signal is observed), the effects of leakage may be significant in the discrete Fourier transform, and the transform may not give an accurate picture of all the resonance frequencies present in the clyinder.

In order to reduce the leakage effects of the rectangular window, the data was windowed with the triangular window as shown in Figure VI-6. As can be seen from the Fourier transform of the triangular windowed data, the leakage effects in the frequency spectrum have been reduced (especially around the frequency component at 38.75 KHz). By windowing the signal with the triangular window, an additional frequency component at 37.0 KHz can be seen much clearer due to the reduction of the leakage from the 38.75 KHz component. Note, however, that the magnitude of the main frequency components is reduced by approximately 5 dB while the signal to noise ratio remains

(a)

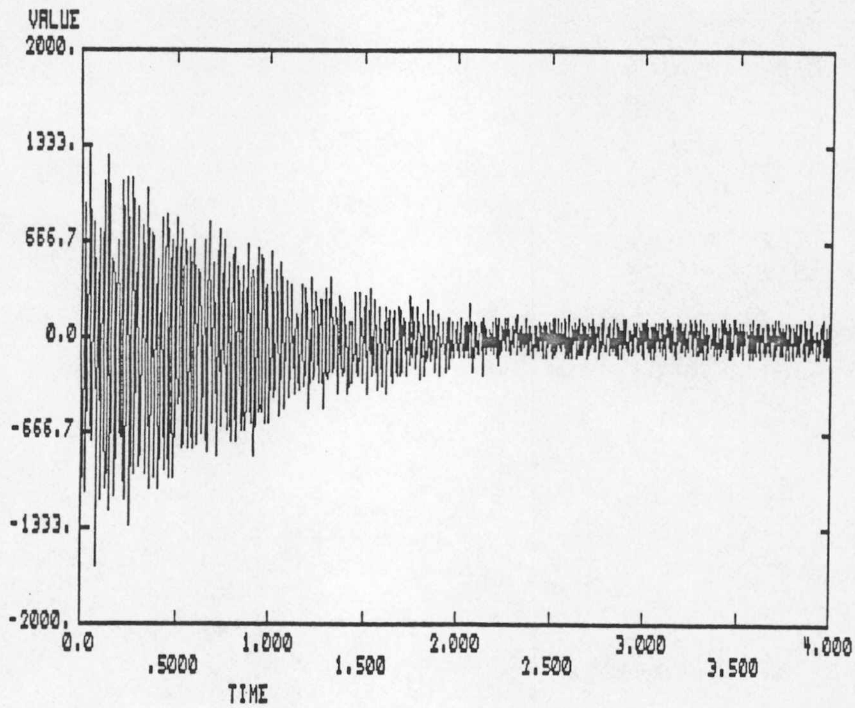

(b)

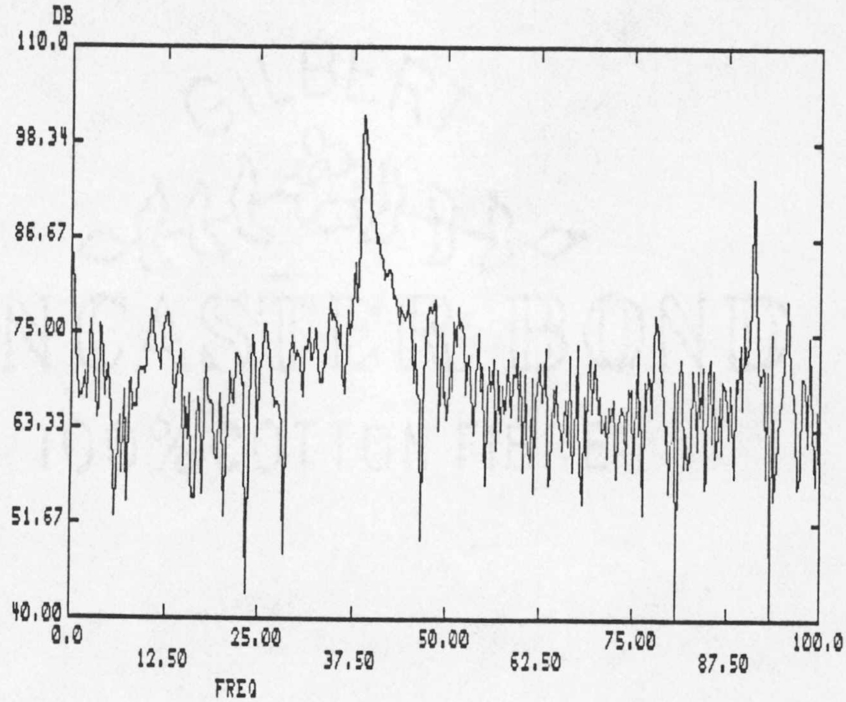

Figure VI-5. Received signal from excitation of the cylinder (a) and the discrete Fourier transform of the signal (b) (Time is in mili-seconds and frequency is in kilohertz).

(a)

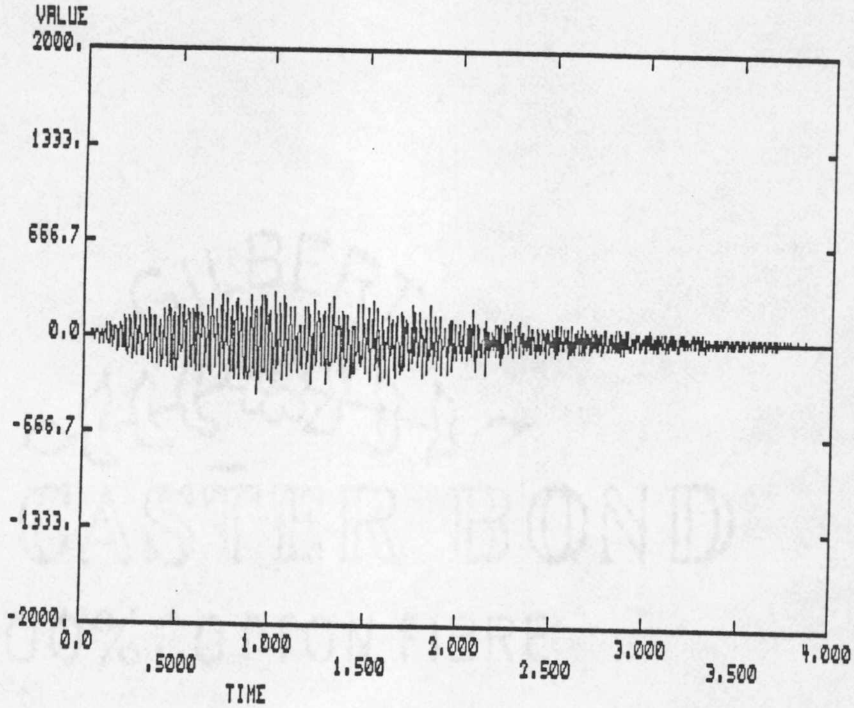

(b)

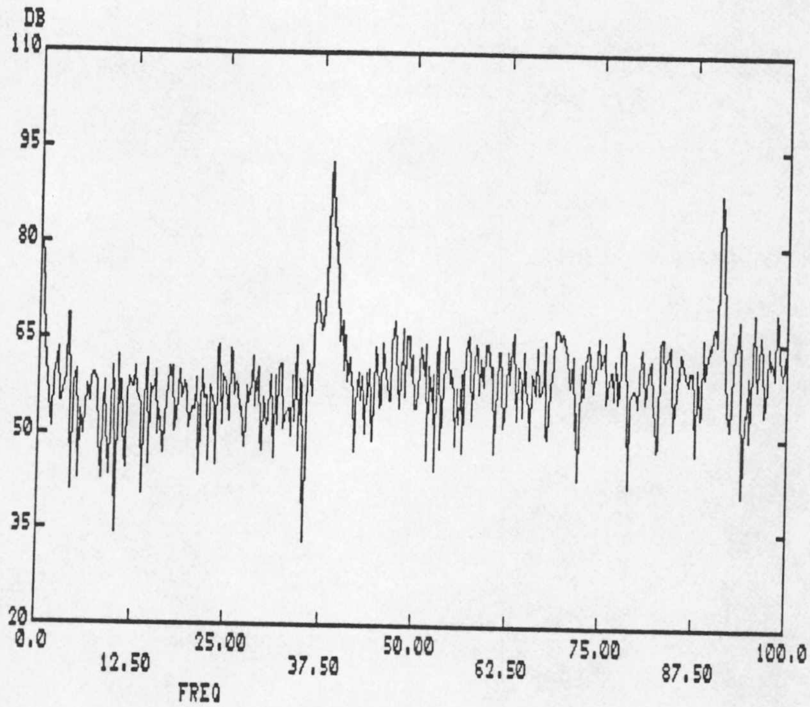

Figure VI-6. Time trace (a) and discrete Fourier transform (b) of the received signal of Figure VI-5 multiplied by a triangular window [Time (ms), Frequency (KHz)].

virtually unchanged with a slight improvement using the triangular window.

The most common window used in digital signal acquisition is the Hanning window due to its balance in the trade-offs of main lobe width and magnitude of the side lobes of the window function. The input signal of Figure VI-5 was windowed using the Hanning window and the time wave form and the resultant discrete Fourier transform are shown in Figure VI-7. The Hanning window has much the same effects as the triangular window in the reduction of leakage, but the Hanning window has a narrower main lobe so the Fourier transform shows slightly better resolution of the frequency components. The finer resolution of the Fourier transform can again be seen by noticing the greater separation of the two frequency components around 37.0 KHz. Again the signal to noise ratio is virtually unchanged.

As a final example of windowing transient data with symmetric windows, the wave form of Figure VI-5 was windowed with the Hamming window as shown in Figure VI-8. The discrete Fourier transform of the windowed data shows much the same characteristics as the triangular and Hanning windows. The Hamming window does show a slight decrease in the resolution in the Fourier transform compared to the Hanning window as expected from the Hamming windows wider main lobe. The Hamming window has

(a)

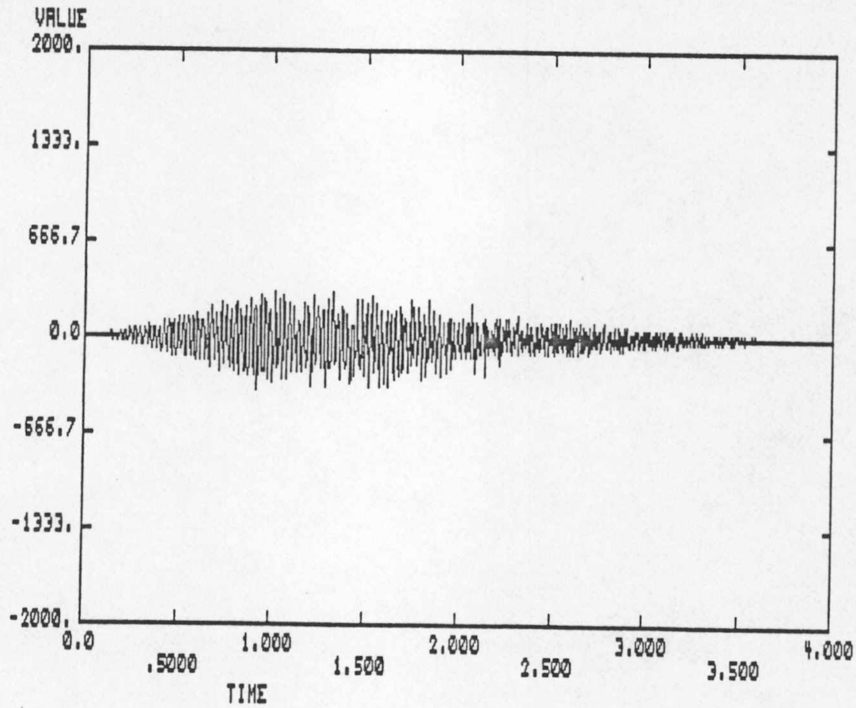

(b)

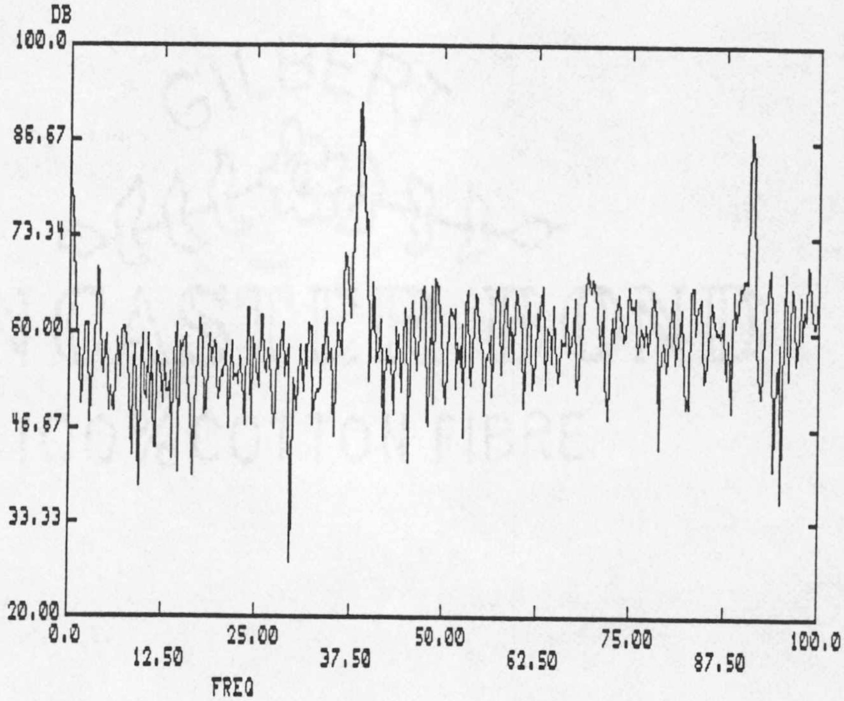

Figure VI-7. Time trace (a) and discrete Fourier transform (b) of the received signal of Figure VI-5 multiplied by a Hanning window [Time (ms), Frequency (KHz)].

(a)

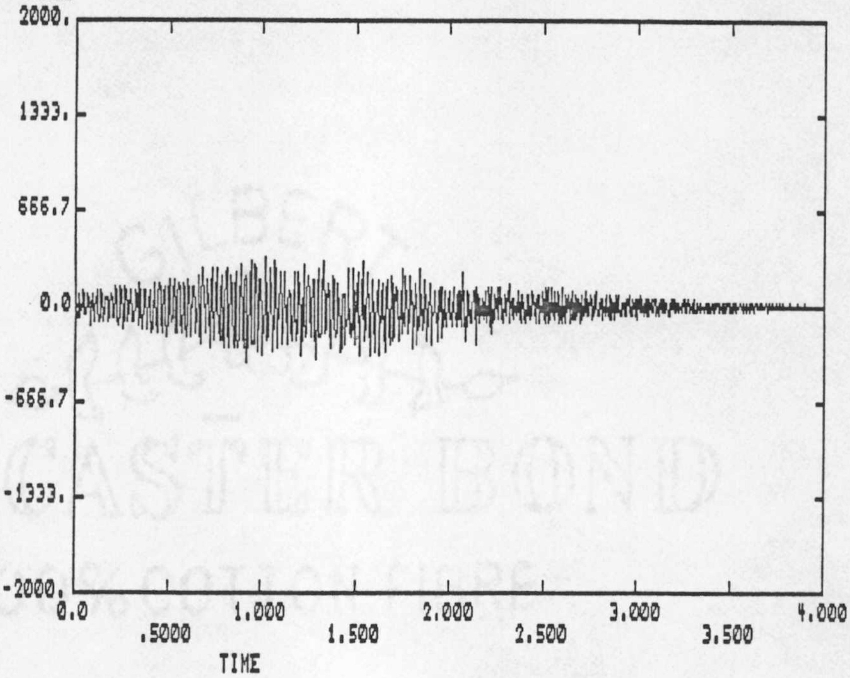

(b)

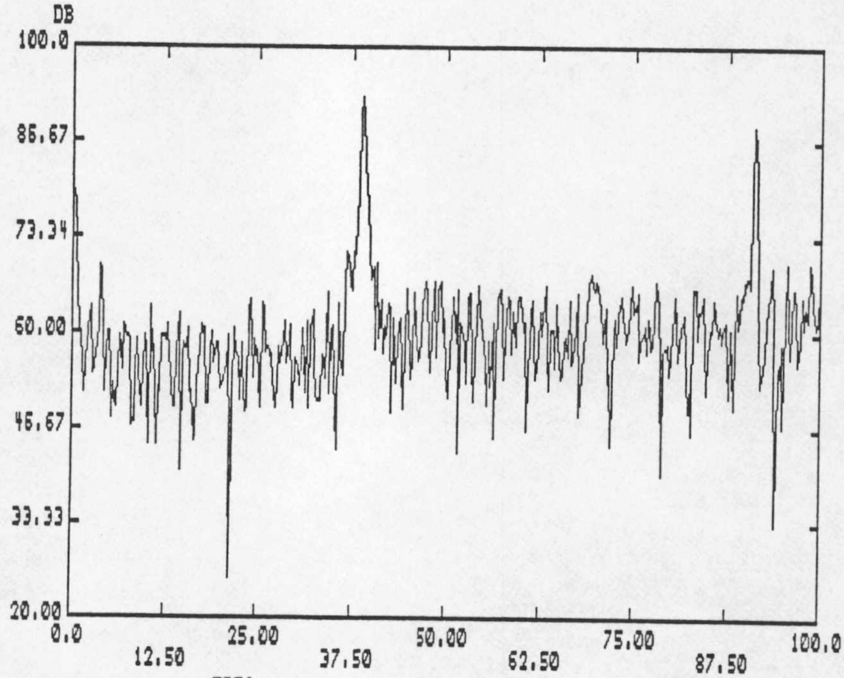

Figure VI-8. Time trace (a) and discrete Fourier transform (b) of the received signal of Figure VI-5 multiplied by a Hamming window [Time (ms), Frequency (KHz)].

much the same characteristics as the triangular window as can be seen by comparing the Fourier transforms of Figures VI-6 and VI-8.

The input signal was then analyzed using the critically damped exponential window. Figure VI-9 shows the input signal of Figure VI-5 windowed by a critically damped exponential window and the resultant discrete Fourier transform. The exponential window significantly reduces the resolution in the Fourier transform due to the wide main lobe and high side lobe levels of the exponential window. As can be seen from the Fourier transform of the exponential windowed signal, the frequency component at 37.0 KHz is "buried" in the main lobe of the frequency component at 38.75 KHz. However, the magnitude of the frequency component at 38.75 KHz is approximately 3.75 dB greater than the same component in the Hanning window. On the other hand, the magnitude of the frequency component at 91.0 KHz is approximately 3.3 dB down in the exponential windowed signal from the Hanning windowed signal.

The reason that the magnitude of the 91.0 KHz frequency component decreased is due to the time constant of this frequency component. Refering back to Figure VI-5, the frequency spread of the 91.0 KHz component is less than the frequency spread of the 38.75 KHz component. The greater spread of the 38.75 KHz frequency suggest that

(a)

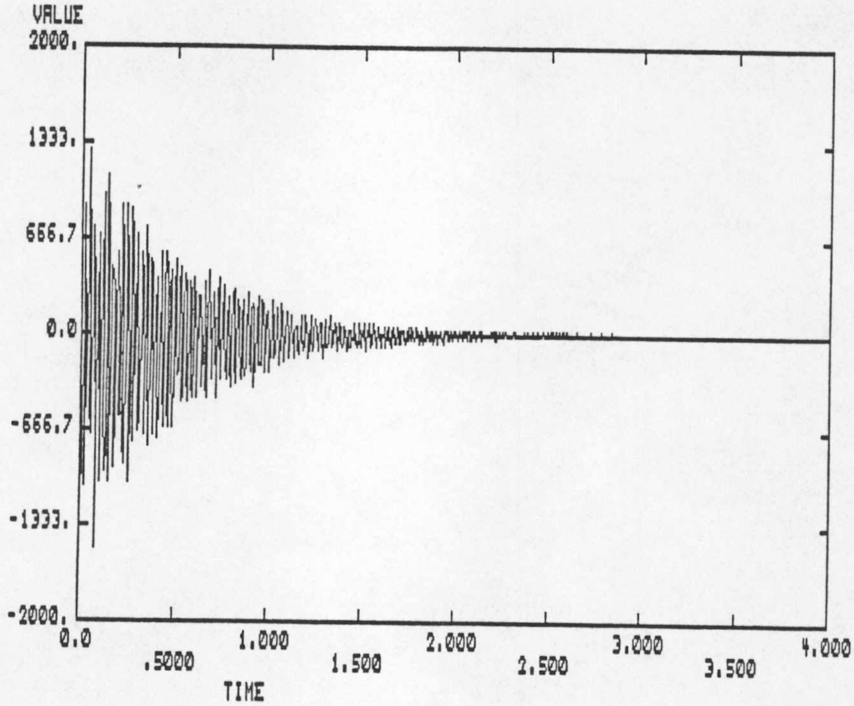

(b)

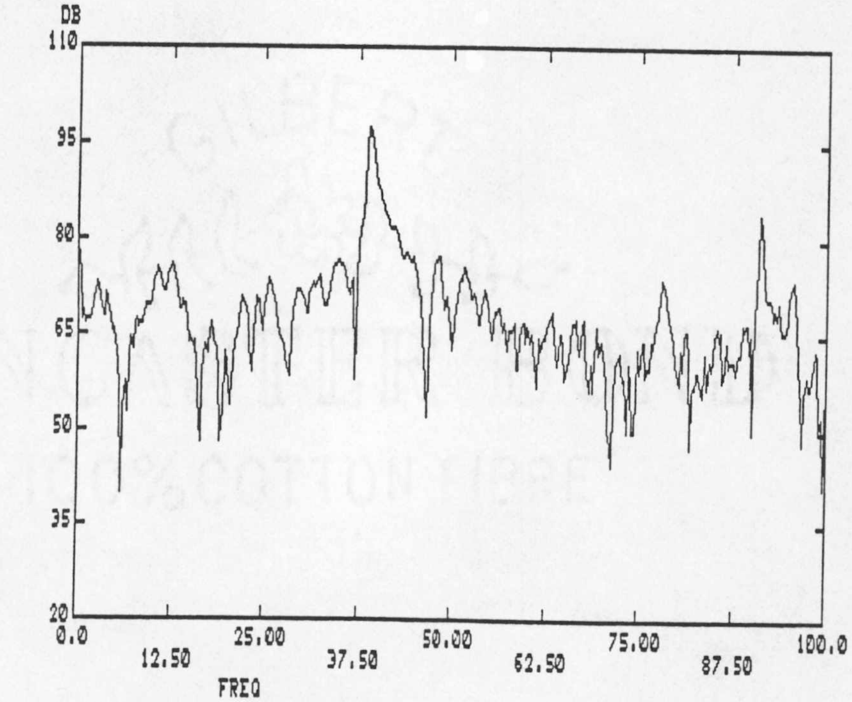

Figure VI-9. Time trace (a) and discrete Fourier transform (b) of the received signal of Figure VI-5 multiplied by a critically damped exponential window [Time (ms), Frequency (KHz)].

this component has a smaller time constant than the 91.0 KHz frequency. Therefore, the exponential window actually decreases the amount of the 91.0 KHz frequency signal that is allowed to pass through the exponential window. On the other hand, several frequency components that were apparent in the rectangular windowed signal and are not noticable when the symmetric windows are used appear when the exponential window is applied to the received signal.

As an example of the different effects of the symmetric windows verses the exponential window consider the frequency components at 10.75 KHz and 10.50 KHz. These frequencies can be easily seen in the Fourier transform of both the rectangular and exponential window, but cannot be seen in the transforms of any of the symmetric windows. As can be seen from the Fourier transform of Figure VI-5 (p.74.), the frequency components at 10.75 KHz and 12.50 KHz are spread out in the frequency spectrum suggesting that these frequencies are highly damped.

Since these frequencies are highly damped, the symmetric windows do not allow much of the signal at these frequencies to pass while the exponential window allows almost all of the signal to pass the windowing process thus allowing these frequencies to have a greater magnitude in the frequency spectrum. However, the frequency resolution is greatly decreased when the exponential window is used due to the wide main lobe of the exponential window's frequency transform. The wide main lobe gives the Fourier transform of the received signal a smoothing effect since the main lobe of each of the frequency components of the signal are spread over a range of frequencies.

Next the Rayliegh and modified Rayliegh windows were used to window the received signal. The Fourier transforms of both of these windows are very similiar as can be seen in Figures VI-10 and VI-11. The frequency resolution of these windows is considerably improved from the exponential window. The Fourier transforms of the Rayliegh and modified Rayliegh windows do not have as great a smoothing effect as the exponential window. Also notice the frequency components are better separated and the frequency at 37.0 KHz is again noticable in both the Fourier transforms using the Rayliegh and modified Rayliegh windows. The modified Rayliegh window has slightly better resolution than the Rayliegh window, but both transforms show approximately the same frequency components present in the received signal. The only variation in the two transforms appears at the frequencies at 10.75 KHz and 12.50 KHz.

Since these frequencies are highly damped as previously determined, the modified Rayliegh window blocks much of these components through the windowing process and

(a)

(b)

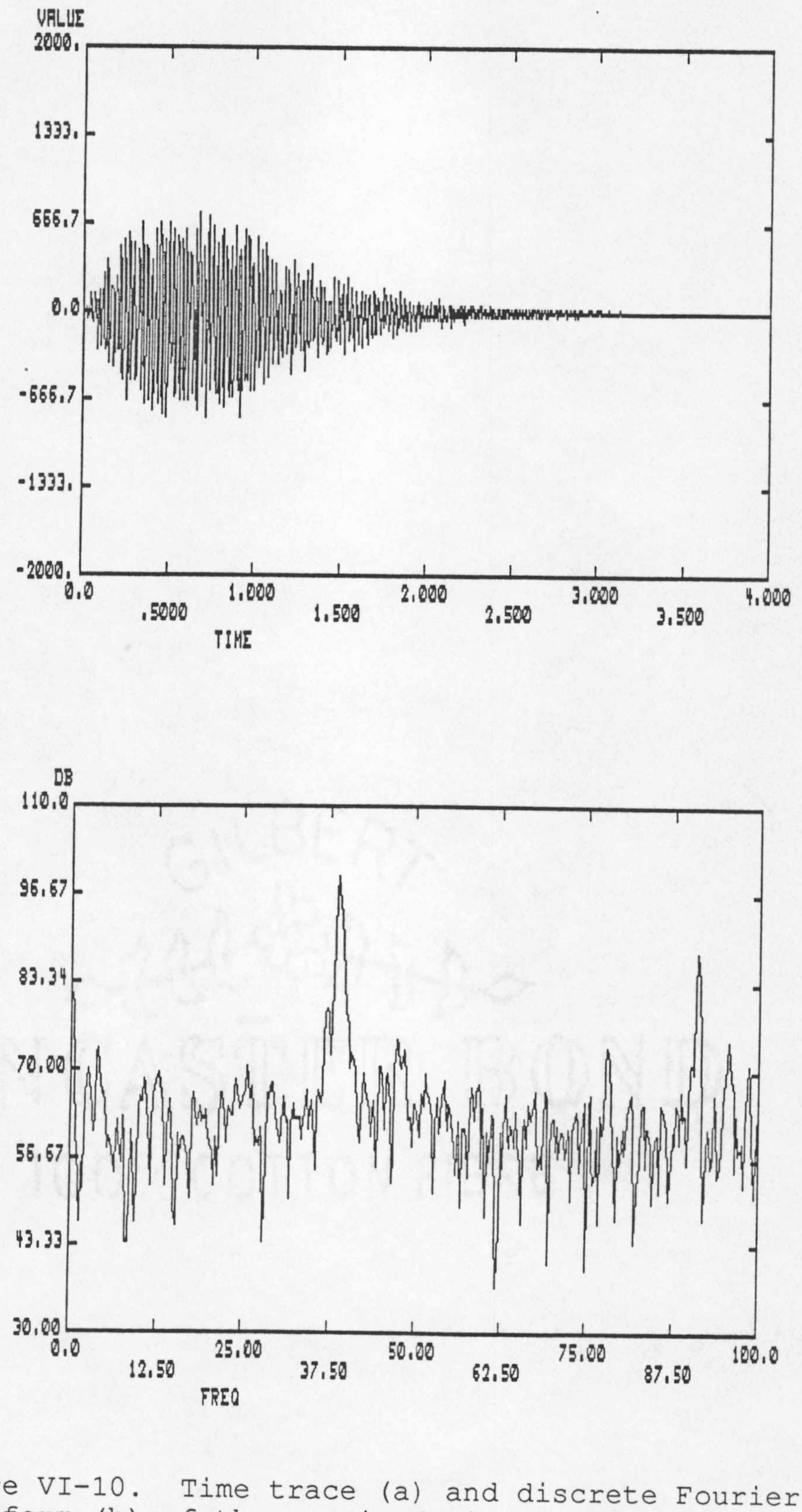

Figure VI-10. Time trace (a) and discrete Fourier transform (b) of the received signal of Figure VI-5 multiplied by a Rayliegh window [Time (ms), Frequency (KHz)].

(a)

(b)

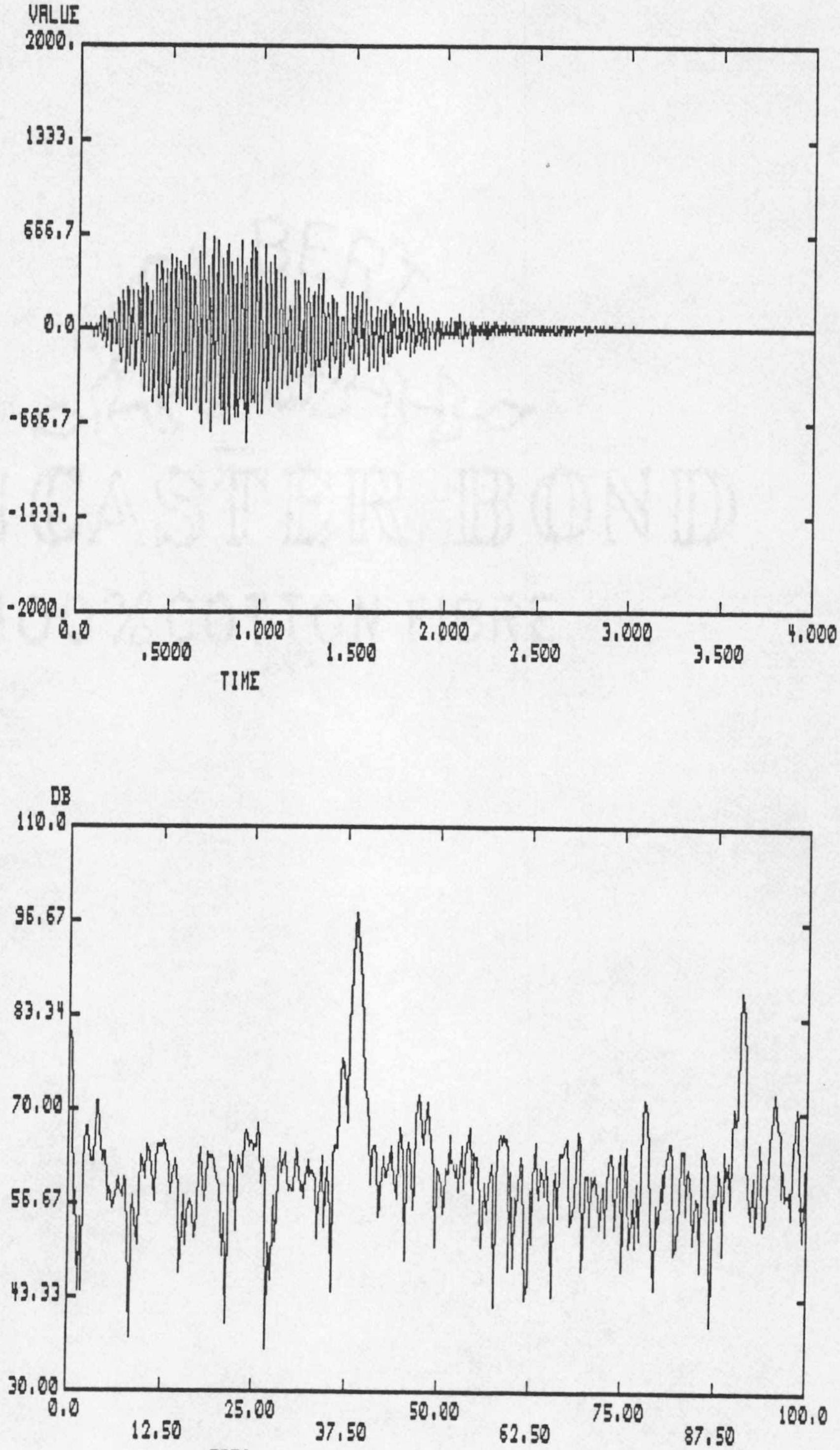

Figure VI-11. Time trace (a) and discrete Fourier transform (b) of the received signal of Figure VI-5 multiplied by a modified Rayliegh window [Time (ms), Frequency (KHz)].

the magnitude of these frequencies is slightly less (3 dB) in the modified Rayliegh window's transform compared to the Rayliegh window's transform. Also of interest is the frequency component at 78.0 KHz which can be seen when the received signal is windowed with the rectangular window (see Figure VI-5, p. 74.) and in all three of the exponential windowed signals (that is, critically damped exponential, Rayliegh and modified Rayliegh windows) but is not clearly present in any of the symmetric windows. Again, since this frequency component is relatively spread when the rectangular window is used, this component has a small time constant and decays rapidly. Therefore, the symmetric windows do not allow much of the signal at this frequency to pass and the frequency component at 78.0 KHz does not appear in the transforms of the symmetric windows.

To show the effects of noise present in the received signal, the ILS noise generation function was used to add noise to the received signal of Figure VI-5 (p. 74.). The noise signal is shown in Figure VI-12 along with the discrete Fourier transform of the noise. As can be seen from the Fourier spectrum of the noise signal, the noise is pretty much white. The maximum amplitude of the noise is approximately twenty percent of the signal amplitude at the beginning of the time window and the magnitude of the noise is twice as large as the signal near the end of the

(a)

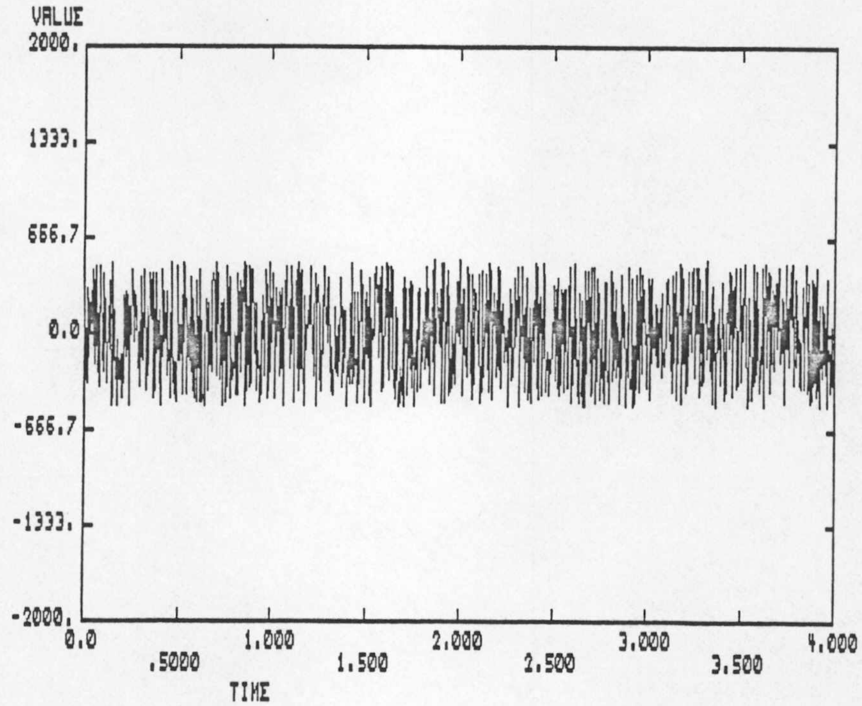

(b)

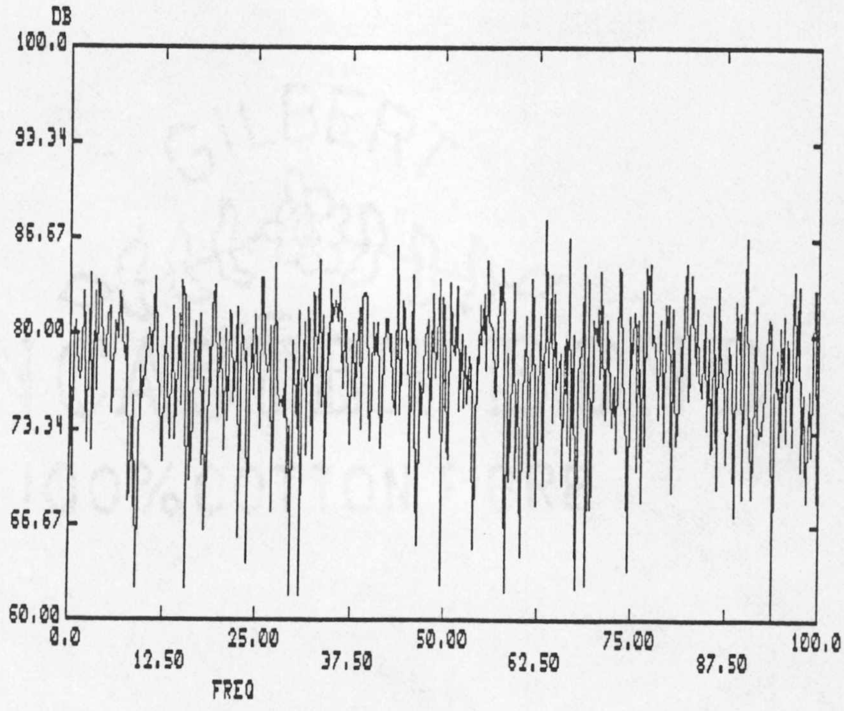

Figure VI-12. Noise signal (a) along with the discrete Fourier transform (b) of the noise [Time (ms), Frequency (KHz)].

time window. The received signal from the vibrating cylinder with the added noise along with the discrete Fourier transform of the noisy signal is shown in Figure VI-13. The Fourier transform of the noisy signal shows that the signal to noise ratio of the signal has been decreased by approximately twelve percent. The only two distinguishable frequencies in the Fourier transform are the frequency components of the received signal at 38.75 KHz and 91.0 KHz. However, much of the magnitude at 91.0 KHz comes from the noise since the frequency component at this frequency has very little spread associated with it. Since it was previously determined that the frequency component at 91.0 KHz is at least lightly damped, this component should have some spreading due to the Fourier transform of a damped sinusoidal signal.

The noisy signal of Figure VI-13 was windowed using the Hanning window and the time wave form and the discrete Fourier transform are shown in Figure VI-14. As can be seen from the Fourier transform of the windowed signal, the signal to noise ratio is approximately the same as the signal to noise ratio of the rectangular windowed signal (Note the change of scale on the vertical axis of the Fourier spectrum). A better signal to noise ratio is obtained when the critically damped exponential window is used to window the signal as shown in Figure VI-15. The two main frequency components of the vibrating cylinder

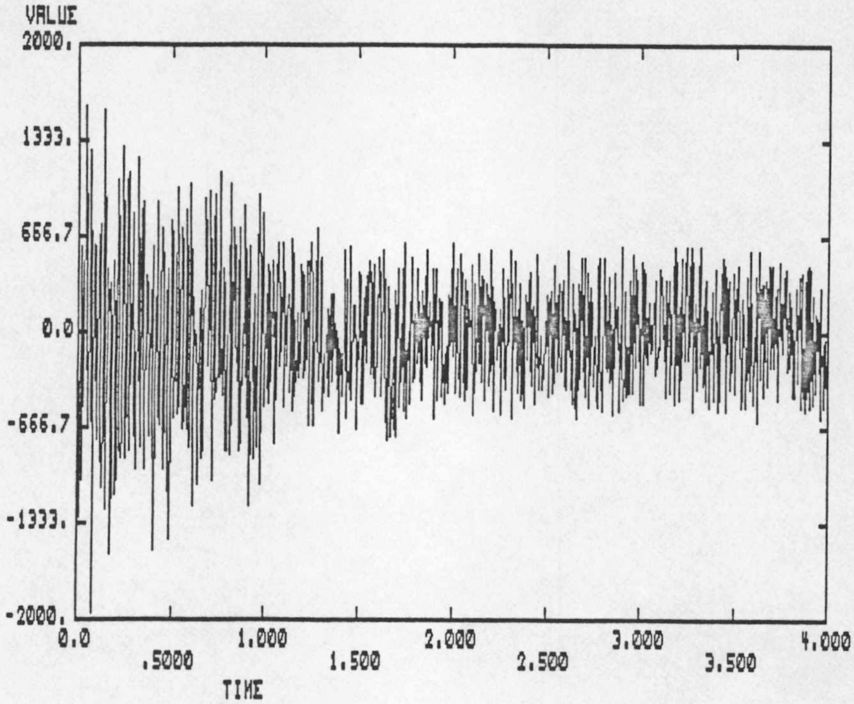

(a)

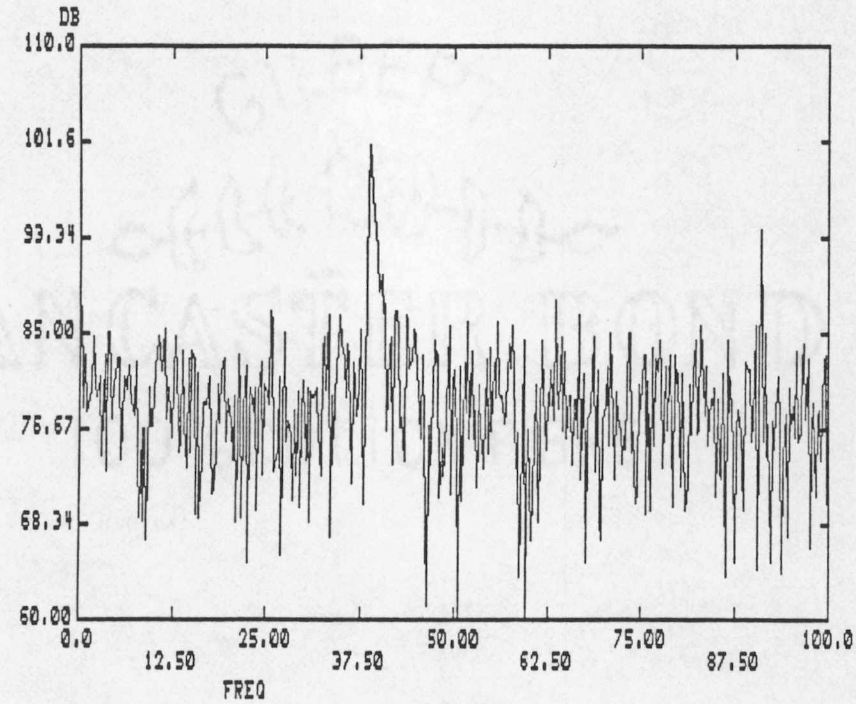

(b)

Figure VI-13. Received signal of Figure VI-5 with the noise signal of Figure VI-12 added to it (a) along with the discrete Fourier transform of the noisy signal (b) [Time (ms), Frequency (KHz)].

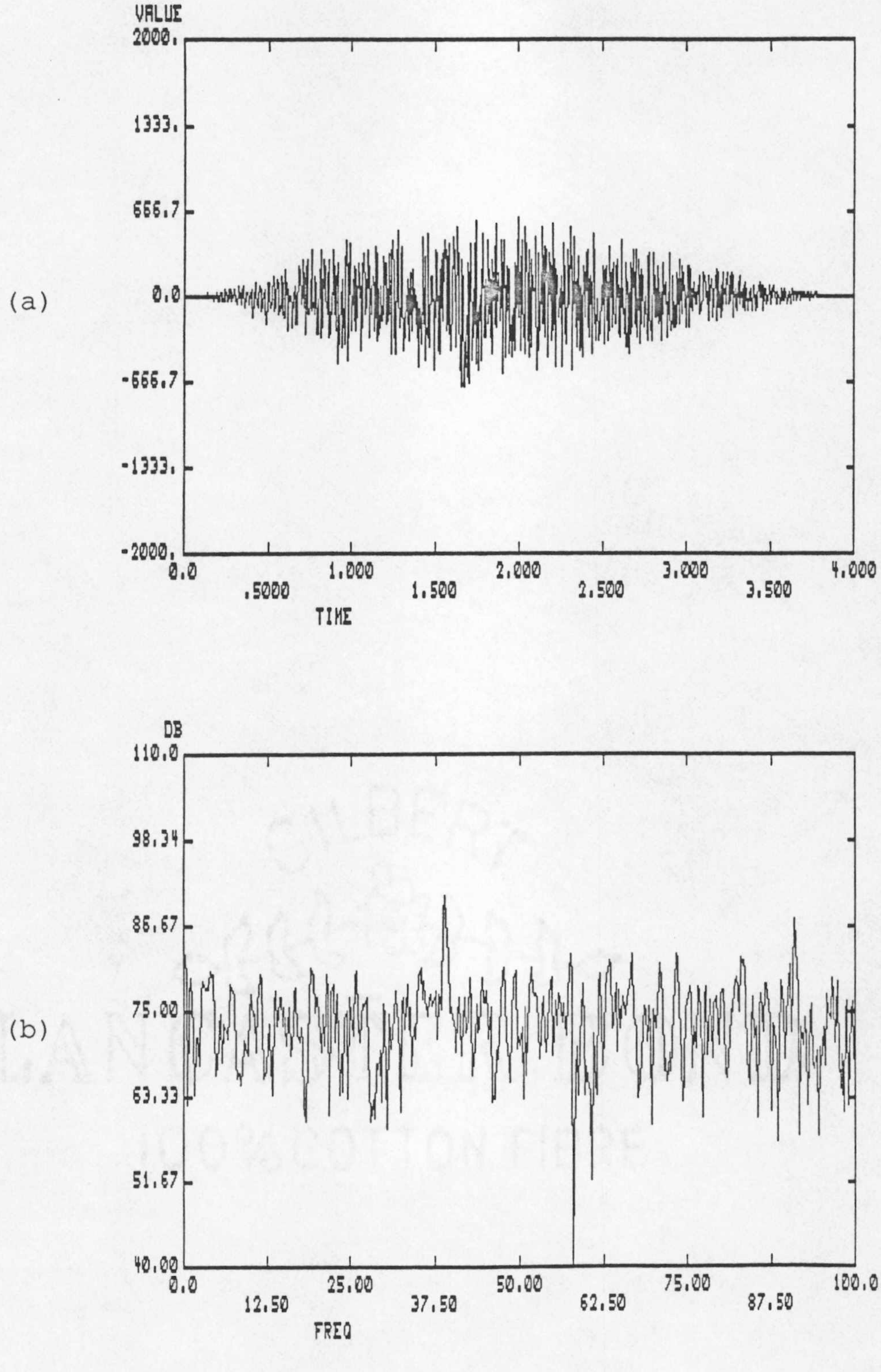

Figure VI-14. Time trace (a) and discrete Fourier transform (b) of the noisy signal of Figure VI-13 multiplied by the Hanning window [Time (ms), Frequency (KHz)].

(a)

(b)

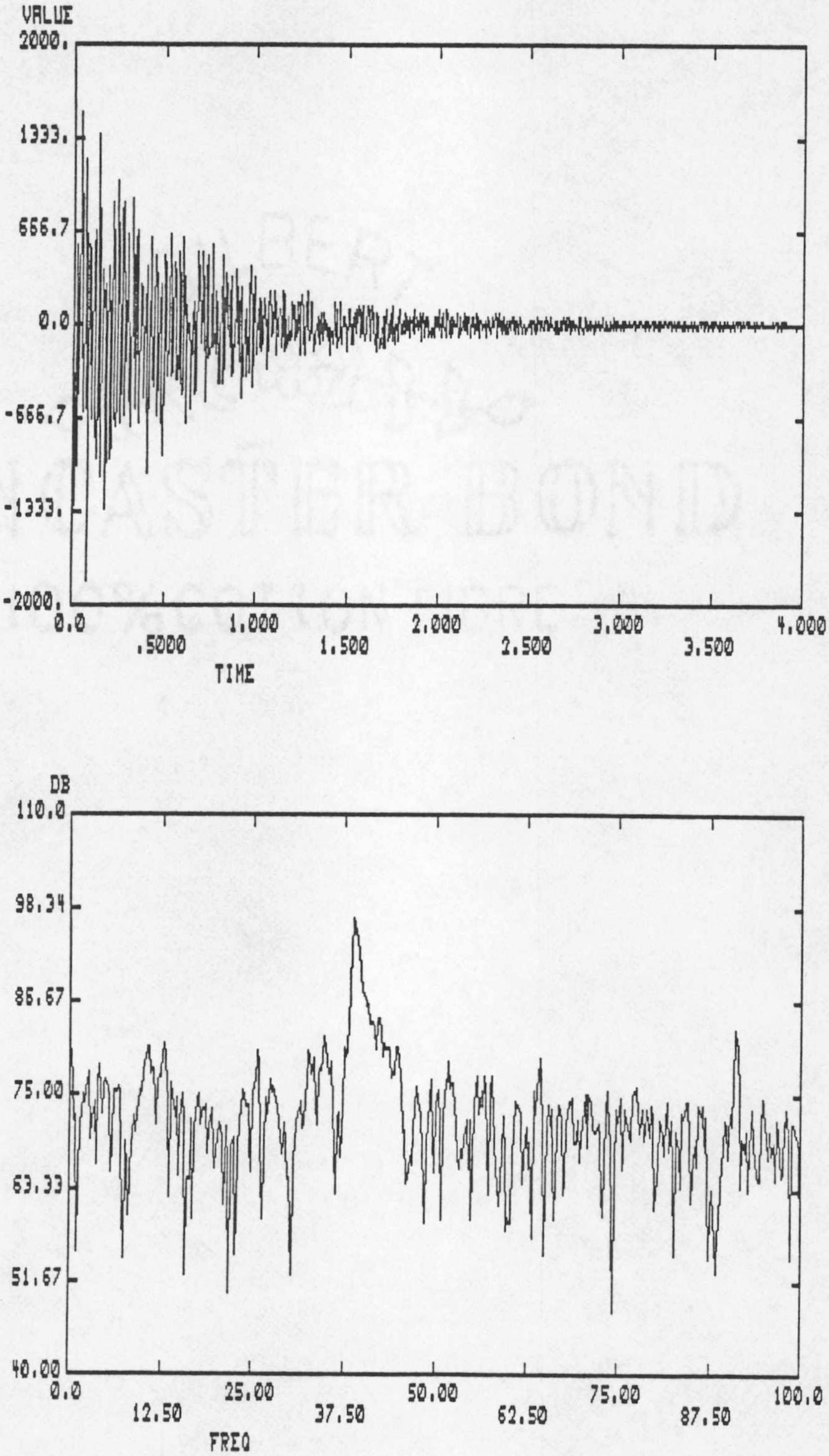

Figure VI-15. Time trace (a) and discrete Fourier transform (b) of the noisy signal of Figure VI-13 multiplied by the critically damped exponential window [Time (ms), Frequency (KHz)].

are easily visible in the Fourier transform and the signal to noise ratio is increased by approximately ten percent. Note, however, that the frequency spectrum has been smoothed by the wide main lobe of the exponential window.

Using the critically damped exponential window, the Fourier spectrum shows more of the resonance frequencies of the vibrating cylinder. For example, the frequency components at 10.50 KHz and 10.75 KHz are again distinguishable in the Fourier trasform of the exponential windowed signal. These frequencies were determined to be present and highly damped from the received signal without added noise. When noise was added to the received signal, the frequency components at 10.50 KHz and 10.75 KHz were no longer distinguishable due to the increased noise floor (refer to Figure VI-13).

Finally, the Rayliegh and modified Rayliegh windows were applied to the received signal. Again the discrete Fourier transforms of the windowed signal are very similiar as seen in Figures VI-16 and VI-17. The Fourier transforms of the windowed signal reveal only about as much information about the resonance frequencies of the cylinder as the rectangular windowed signal. The two main resonance frequencies at 38.75 KHz and 91.0 KHz are easily distinguished, but most of the other resonance frequencies are buried in the noise.

Additional noise was added to the received signal to

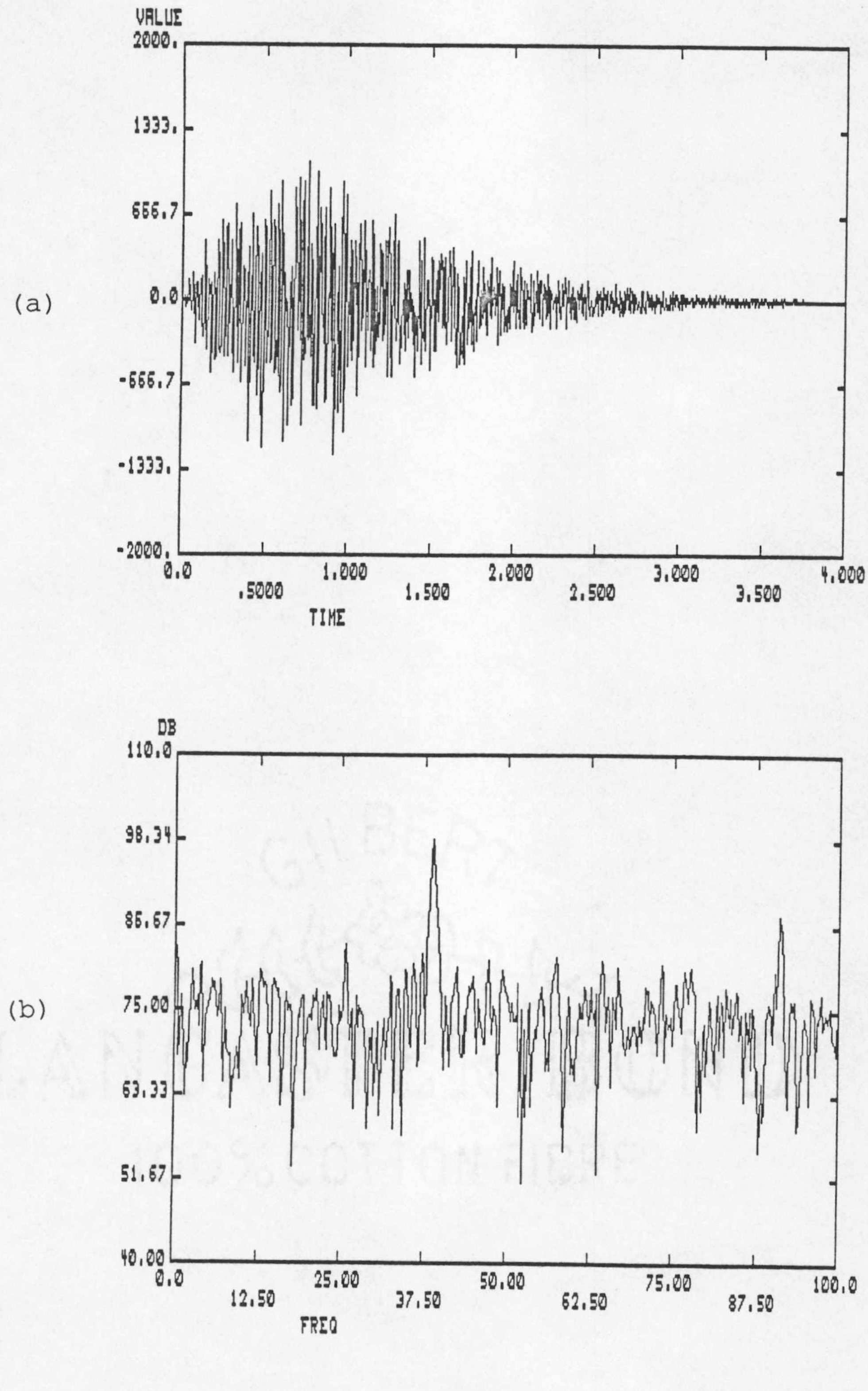

Figure VI-16. Time trace (a) and discrete Fourier transform (b) of the noisy signal of Figure VI-13 multiplied by a Rayliegh window [Time (ms), Frequency (KHz)].

(a)

(b)

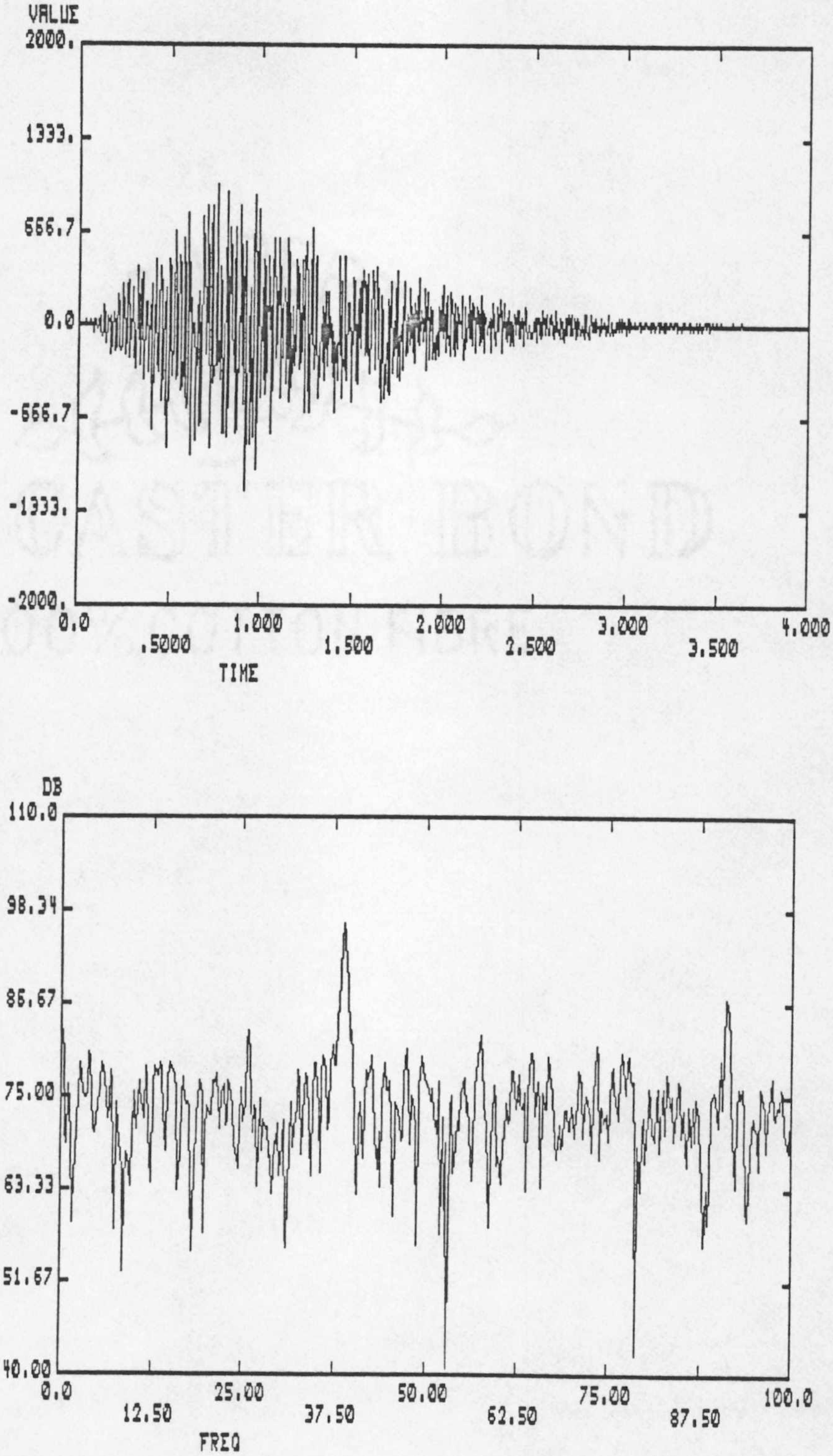

Figure VI-17. Time trace (a) and discrete Fourier transform (b) of the noisy signal of Figure VI-13 multiplied by a modified Rayliegh window [Time (ms), Frequency (KHz)].

see the effects of the received signal completely buried in noise and how windowing the signal could help separate the resonance frequencies from the noise signal. As expected, windowing a very noisy transient signal with the symmetric windows is not effective in determining the vibration modes of the cylinder. The resonance frequency components are buried in the noise floor of the discrete Fourier transform and are not distinguishable from the noise. However, the critically damped exponential, Rayliegh and modified Rayliegh windows are much more effective in separating the signal from the noise and several of the resonance frequencies are still distinguishable in the discrete Fourier transforms even when the received signal is completely buried in noise. Since the critically damped exponential window is very effective in separating the signal from the noise, differently damped exponential windows were used to window damped data with and without added noise. In the absence of noise the lightly damped exponential window has the best frequency response as expected (that is, the narrowest frequency spread, greatest amplitude of the input frequency and greatest attenuation of frequencies away form the input frequency). As the damping was increased, the main lobe of the input frequency spread to adjacent frequencies and there is less resolution in the frequency spectrum.

When adding noise to damped data, the higher damped exponential windows show better noise rejection than the lighter damped exponential windows. The lightly damped exponential windows still have the same characteristics (that is, narrow main lobe, greater main lobe amplitude and greater attenuation of adjacent frequencies), but allow noise to pass after the input signal has damped to a small amplitude compared to the noise. Therefore, the lightly damped window allows the input signal (damped sine wave with noise) to pass with only light attenuation even when the signal to noise ratio has decreased significantly compared to the beginning of the time window. As the damping constant is increased, the exponential window attenuates the input data to a greater extent when the signal to noise ratio decreases at the end of the time window. Therefore, the frequency spectrum shows a greater signal to noise ratio at the expense of a greater main lobe spread. As the damping constant is continually increased, however, the noise rejection effect of the exponential window is over taken by the spreading effects of the highly damped exponential. Therefore, there is an optimum damping constant for a given damped input signal. (As the exponential is increased, the noise in the frequency spectrum is smoothed due to the leakage characteristics of the higher damped exponential windows). The best window appears to be a window that matches the general shape of the input data (i.e. the same damping constant of an exponential window as the damped input data) for the maximum noise rejection and best spectral estimation.

CHAPTER VII

DISCUSSION OF RESULTS

In experimenting with transient signals, the results show that the best window is one that has the same characteristics as the input data (that is, the same general shape). Without noise added to the input signal, the Hanning window produces a Fourier spectrum with the least leakage compared to the other windows presented in the thesis. The Rayliegh and modified Rayliegh windows produce transforms that have slightly more spread than the Hanning window (30% and 17.7%, respectively). The exponential window's spectrum has the greatest spread as expected due to the low roll-off rate of its Fourier transform. The greater the damping constant used in either the exponential, Rayliegh, or modified Rayliegh windows, the greater the spread in the Fourier transform.

For higher damped signals especially in the presence of noise, the signal blocking effects of the symmetric windows becomes more significant and the ability to detect the resonance frequencies of the signal decreases. Therefore, the critically damped exponential, Rayliegh and modified Rayliegh windows are needed to separate the signal from the noise. In the presence of noise, the exponential window has the best spectrum for exponentially damped data using the Fourier Transform. The Hanning window attenuates the data at the beginning and the end of the time window, thus blocking much of the input signal at the beginning of the time window while allowing the noise to pass in the middle of the time window when the signal-to-noise ratio of the input data is less. The Rayliegh and modified Rayliegh windows have the same type of effect on the input data, but to a lesser extent than the symmetric windows. Therefore, the Rayliegh and modified Rayliegh windows show improvement over the Hanning window. The exponential window, however, allows all the input signal to pass at the beginning of the time window when the signal to noise ratio is greatest and attenuates the data to a greater extent as the signal to noise ratio decreases. Therefore, even though the exponential window has the greatest spread in the Fourier transform, it also has the best noise rejection characteristics for exponentially damped data.

BIBLIOGRAPHY

BIBLIOGRAPHY

Bracewell, Ronald N. The Fourier Transform and its Application: Second Edition. McGraw-Hill, Inc., 1986.

Chen, Chi-Tsong. One Dimensional Digita Signal Processing. Marcel Dekker, Inc., 1979.

Cheng, David K. Analysis of Linear Systems. Reading Massachusetts: Addison-Wesley Publishing Company, Inc., 1959.

Childers, Donald and Allen Durling. Digital Filtering and Signal Processing. West Publishing Company, 1975.

Geckinli, Nezih C. and Davras Yavuz. Studies in Electrical and Electronic Engineering 8: Discrete Fourier Transformation and its Application to Power Spectra Estimation. New York, New York: Elsevier Scientific Publishing Company, Inc., 1983.

Gold, Bernard and Charles M. Rader. Digital Processing of Signals. McGraw-Hill, Inc., 1969.

Harris, F. J. "On the use of windows for harminic analysis with the DFT", PROC IEEE, vol. 66, pp. 51-83, Jan. 1978.

Jackson, Leland B. Digital Filters and Signal Processing. Kluwer Academic Publishers, 1986.

Kaiser, J. F. "Digital Filters" in System Analysis by Digital Computer. New York: Wiley and Sons, 1966.

Kreyszig, Erwin. Advanced Engineering Mathematics: Fifth Edition. New York: John Wiley and Sons, Inc., 1983.

Oppenheim, Alan V. and Ronald W. Schafer. Digital Signal Processing. Englewood Cliffs, New Jersey: Prentice-Hall, Inc., 1975.

Oppenheim, Alan v. and Alan S Willsky. Signals and Systems. Englewook Cliffs, New Jersey: Prentice-Hall, Inc., 1983.

Peled, Abraham and Bede Liu. Digital Signal Processing: Theory, Design, and Implementation. John Wiley & Sons, Inc., 1976.

Ramirez, Robert W. The FFT: Fundamentals and Concepts. Englewook Cliffs, New Jersey: Prentice-Hall, Inc., 1985.

Stearns, Samuel D. Digital Signal Analysis. Hayden Book Company, Inc., 1975.

Widrow, Bernard and Samuel D. Stearns. Adaptive Signal Processing. New Jersey: Prentice-Hill, Inc., 1985.

Williams, Charles S. Designing Digital Filters. Englewood Cliffs, New Jersey: Prentice-Hall, Inc.

VITA

John Young was born in Manchester, Tennessee on October 21, 1962. He attended elementary schools in that city and graduated as Valedictorian form Central High School in June 1981. The following September he entered the University of Tennessee where he graduated at the top of his class with a Bachelor of Science Degree in March of 1986. He then continued his education at the University of Tennessee with a research assistantship and received a Master of Engineering Degree in Electrical Engineering in March 1987. During his college career, he competed in Cross Country, Indoor and Outdoor Track for the University of Tennessee and received the Cross Country Captain Award in 1985 and the Southeastern Conference Male Athlete Scholar Award that same year.

He is a member of the Order of the Engineer, Institute of Electrical and Electronic Engineers, Phi Eta Sigma, and the Eta Kappa Nu.